An investigation of the spatial distribution and inference of dispersal method in the semi-aquatic lichenised green alga *Diplosphaera chodatii* around Payuk Lake, Manitoba

by

Jennifer A. Doering

A Thesis submitted to the Faculty of Graduate Studies of
The University of Manitoba
in partial fulfilment of the requirements of the degree of

MASTER OF SCIENCE

Department of Biological Sciences
University of Manitoba
Winnipeg, Manitoba, Canada

ABSTRACT

The spatial distribution of haplotypes within the lichenised green alga *Diplosphaera chodatii* was investigated by collecting specimens from the inflows, lake, and outflow of Payuk Lake, Manitoba. Rock scrapings were cultured showing the presence of free-living *Di. chodatii* and seven additional algal taxa on rocks near the lichen thallus. The Internal Transcribed Spacer of ribosomal DNA (ITS rDNA) and β-actin genes were sequenced for phylogenetic and haplotype network analyses showing similarity to one another, but neither corresponded to geographic location suggesting high levels of gene flow. Haplotype variation was investigated with respect to four landscape hypotheses to infer the mode of dispersal, which supported the Wind (ITS) and Hydrology (β-actin) hypotheses. This is the first study to provide evidence that *Di. chodatii* is dispersed by wind and water, and free-living *Di. chodatii* may aid in the potential establishment of the lichen, *Dermatocarpon luridum*, and other semi-aquatic lichens within this ecosystem.

ACKNOWLEDGMENTS

I would like to thank my advisor, Dr. Michele Piercey-Normore, for her many years of guidance and mentorship throughout this project and the many years spent in her lab. I also thank my committee members, Drs. Jim Roth and Georg Hausner, for their constructive feedback of both the project and thesis. Special thanks is given to Kyle Fontaine, whose previous research and enthusiasm fuelled the motivation of this project, and for assistance with the microscopy.

I would like to give special thanks to Dr. Yolanda Wiersma and the Landscape Ecology and Spatial Analysis lab (Emma LeClerc, Emilie Kissler, Matt McWilliams, Andrew Roberts, Rachel Winsor) at Memorial University for their invaluable mentorship of advanced GIS analyses and techniques. Furthermore, thank you to Mr. Mac Pitcher for an exhilarating excursion along Salmonier Line to experience the beauty and mystique of coastal Newfoundland lichens. Thank you to the staff at the Roses Heritage Inn for their hospitality during my stay.

Many thanks are given to Mohanad Zraik, Dr. Tom Booth, and Kam Chhokker for their valuable assistance in both the field and lab. Thank you to Mr. Andre Dufresne for additional help with the microscopy. I would also like to acknowledge the assistance of Dr. David Walker and Mr. Jason Northage for the use of the GIS software at the University of Manitoba. Thank you to Mr. Garry Lux (Government of Manitoba) for providing the digital elevation data of Payuk Lake/Cranberry Portage. Many thanks are given to my lab mates, both past and present, for their companionship. Thank you also to my family for their endless support.

Funding was provided by Natural Science and Engineering Research Council of Canada (NSERC CGS-M), The University of Manitoba (TSMA, Dalgarno Award), and Nature Manitoba through scholarships, and through a NSERC Discovery Grant award to Dr. Piercey-Normore.

DEDICATION

Maria, a child is one of the most beautiful gifts the world has to give. You have filled my life with happiness and my heart with love; to you I dedicate this thesis.

"There is a low mist in the woods –
It is a good day to study lichens."

~ Henry David Thoreau, 1851

TABLE OF CONTENTS

LIST OF TABLES

LIST OF FIGURES

CHAPTER 1 : INTRODUCTION

1.1 Overview

1.1.1 Significance

Aquatic ecosystems are unusual due to their fragmentation (such as separate river systems, watersheds or lakes) and their ability to support aquatic microbial populations, which include algae, fungi, bacteria and protists. High occurrences of human activities from boating, logging, and fishing, runoff from agricultural land, pollution etc., as well as the increasing consequence of climate change can have a detrimental (or beneficial) effect on the microbes in these sensitive ecosystems (Woodward et al. 2010). Aquatic eukaryotic microbial populations have been previously studied but little is known about their biology, gene flow, and dispersal patterns making the changes in population biology and their effect on the surrounding environment difficult to predict. It is generally assumed that aquatic algae may be dispersed by water currents and terrestrial algae may be dispersed by wind currents. The single-celled green alga, *Diplosphaera chodatii* Bialosuknia, grows on rock at the interface between the water and the terrestrial environment around rivers and lakes. *Diplosphaera chodatii* can form a free-living component in the environment (Flechtner et al. 1998; Lukešová and Hoffmann 1996) and form a symbiosis with a lichen-forming fungus, *Dermatocarpon luridum* (With.) Laundon (Fontaine et al. 2013). The study of the dispersal vector, the level of photobiont gene flow, and the potential for contribution from a free-living algal counterpart would provide significant insights into lichenisation (formation of a lichen thallus) and survival strategies of this semi-aquatic lichen, which forms a significant biotic component of lake margins in northern Manitoba. This study will also improve our understanding of population structure and dispersal of *Di. chodatii* in a northern lake in Manitoba, which may also be important as an indicator of change for less

sensitive species, endangered or threatened species, and the microbial populations that occur in the area.

1.1.2 Background and Rationale

Lichens are the result of unique symbioses between fungi (mycobionts) and photosynthetic green algae or cyanobacteria (photobionts). Lichens are mostly terrestrial (Aptroot and Seaward 2003); however, aquatic lichens exist, where the entire thallus is submerged for part or all of the year (Thüs 2002). Some freshwater lichens that are submerged for part of the year are termed "semi-aquatic" lichens (Aptroot and Seaward 2003). Most semi-aquatic lichens belong to the Verrucariaceae, which most commonly contain coccoid, unicellular green algae (Aptroot and Seaward 2003; Thüs et al. 2011). They occur most commonly along lake shores (Gilbert 2000) and along the margins of streams (Aptroot and Seaward 2003; Gilbert and Giavarini 1997; Gilbert 1996). Due to the requirement of a stable substrate, semi-aquatic lichens occur on rock or concrete (Aptroot and Seaward 2003; Keller 2005; Nascimbene et al. 2009).

One semi-aquatic lichen common to boreal lakes in Manitoba is *Dermatocarpon luridum* (Verrucariales; Fontaine et al. 2013). This foliose lichen occurs along the acidic granitic shores of northern lakes (Fontaine et al. 2012), near flowing water (Amtoft et al. 2008). It is considered to be obligately saxicolous, and attaches to the substrate via many small holdfasts along a single thallus lobe (Amtoft et al. 2008), making it difficult to be dislodged from the rock surface. *De. luridum* is considered shade-intolerant and prefers to inhabit areas of open exposure near flowing water (Amtoft et al. 2008). This lichen has been studied for its copper tolerance due to its ability to absorb ionic metals into its thallus and its possible use as a bioindicator of pollution in streams (Monnet et al. 2005). Furthermore, it often co-occurs with several other lichens such as

Staurothele fissa (Taylor) Zwackh, *Rhizocarpon geminatum* Korber, and *Lecanora muralis* (Schreber) Rabenh (Fontaine et al. 2014), as well as *Leptogium rivulare* (Ach.) Mont. (Fontaine et al. 2014), which is a threatened species as listed by COSEWIC (COSEWIC 2004). *Dermatocarpon luridum*, which is both the lichen and the fungal partner, associates with the unicellular green alga *Diplosphaera chodatii* (Fontaine et al. 2013) and turns a grass green colour when wet (Heiđmarsson 2000).

Diplosphaera chodatii is a unicellular, rod-shaped green alga (Fontaine et al. 2012) and is closely related to members of *Stichococcus* Nägeli (Thüs et al. 2011). *Diplosphaera chodatii* has high desiccation tolerance and can survive up to two months of desiccation (Zhang and Wei 2011), which could help the lichen adapt to fluctuating water levels and contribute to the success of the semi-aquatic nature of *De. luridum*.

Lichen algae have become the subject of population genetic studies (Dal Grande et al. 2010; Doering and Piercey-Normore 2009; Fontaine et al. 2012; Fontaine et al. 2013; Piercey-Normore and DePriest 2001; Werth 2011) showing that genetic diversity can be high in local populations, with several haplotypes occurring in the same area. Population structure is the spatial distribution and amount of genetic variation within and among populations and individuals of the same species (Templeton 2006). Population studies in lichens have been complicated by the fungal requirement to associate with a suitable photobiont and the combinations of symbionts have also been examined. Werth (2012) found that juvenile *Ramalina menziesii* Taylor thalli shared the same photobiont haplotype with each other, but the same algal haplotype was not found in mature *R. menziesii* thalli or in neighbouring lichens of different species. The association of algae and lichenised fungi produce a complex symbiont structure superimposed on the symbiont population genetic structure within a lichen community, where

multiple haplotypes of the photobiont may be present within the lichen population (Doering and Piercey-Normore 2009; Nyati et al. 2013) or associated with a single lichen-forming fungal species (Piercey-Normore 2006). Furthermore the photobiont may be found free-living until it forms an association with a compatible fungus (Mukhtar et al. 1994). Algal switching may also occur between nearby thalli of the same lichen species, resulting in horizontal transfer of algae between thalli (Piercey-Normore and DePriest 2001; Piercey-Normore 2009), changing the algal population structure if different genotypes were transferred.

The population structure of photobionts within a population of lichen thalli can be affected by several factors such as method of reproduction, dispersal vector, and geographic distance between populations. Population structure of the photobiont in vegetatively reproducing lichens may be affected by co-dispersal of both symbionts from the thallus via soredia or other vegetative/thallus propagules (Fernández-Mendoza et al. 2011) where both symbionts remain together. Co-dispersal might result in localised areas where the population structure of the photobiont would remain the same as that of the parent population structure due to the physical weight, shape, presence of a cortex, hydrophobicity, or ecological niche of larger propagules preventing widespread wind dispersal. Population structure may also be affected by the dispersal of free-living algae by wind (Tormo et al. 2001) and water currents (Rout and Gaur 1994), where the alga is dispersed separately from the fungus. Since free-living algae would lack surrounding fungal tissue and therefore be lighter, they may be able to travel farther than they could as co-dispersed propagules, which could potentially introduce algal haplotypes from free-living algae to new lichen populations if they are genetically compatible and establish new photobiont population structures relative to the structure already present. Dal Grande et al. (2014b) found that lichenisation of the photobiont *Dictyochloropsis* Geitler spp. was strain specific and free-

living photobionts were genetically separated from lichenised counterparts. Wind dispersal would potentially result in longer distance dispersal than water and perhaps landing in many unsuitable habitats, but water dispersal may limit dispersal to suitable habitats and within the watershed and cause differences in the distribution of population structures due to the direction of water flow or wind. Derycke et al. (2006) found that the numbers of haplotypes of nematodes were fewer upstream compared to downstream, which were thought to increase as a result of the additional tributaries entering the stream system, adding additional haplotypes to the system. Additional haplotypes can then be incorporated into the community, increasing the genetic variation within the population or by replacing haplotypes over time and causing turnover in the population structure.

Geographic distance between populations may also cause the population structure to differ (Slatkin 1993). Fernández-Mendoza et al. (2011) found that isolation by distance from temperate to Polar Regions can cause different population structures in the same species of lichens. It was also found that there was separation of populations in *Lobaria pulmonaria* (L.) Hoffm. due to glacial and postglacial histories among geographic locations, suggesting that local landscapes and regional scales are also needed to understand dispersal (Walsner et al. 2005). In contrast, population structure in localised studies may not correspond to geographical regions, indicating that the photobiont is more widely dispersed and that other mechanisms such as fungal and algal genetic compatibility or environmental features may be influencing algal population structure (Franscisco de Oliveira et al. 2012). A lack of population structure at a local level may indicate high levels of gene flow (Werth and Sork 2008) or influences from genetic drift, sexual reproduction, historical processes, or dispersal vectors, such as water, wind, or animal dispersal.

While studies of photobiont populations on gene flow for *De. luridum* have been done between large geographic areas of different continents (Fontaine et al. 2013) showing that gene flow occurred mainly within continents, the study could not distinguish between water and wind vectored gene flow within a single lake relative to hydrology and water flow. Payuk Lake is a boreal lake in northern Manitoba, surrounded by a variety of granitic acidic substrata that is fed by two boreal creeks: Mistik Creek and Twin Creek (McLeod 1943). If the lichen alga *Diplosphaera chodatii* is dispersed by water, the direction of gene flow would be expected to be same as the direction of water flow in the lake, though it may also be affected by the inflowing streams as shown in nematodes (Derycke et al. 2006). Larger source streams with more tributaries, such as the Mistik Creek, may yield higher numbers of haplotypes than smaller streams, such as Twin Creek, because of the greater potential for rock substrata around the larger streams, resulting in differences in the spatial and genetic variation of *Di. chodatii* within Payuk Lake, where larger numbers of haplotypes may occur on the Mistik Creek side of the lake (northwest) compared to the Twin Creek side (southeast). Understanding how the alga may be dispersed within a single lake can help to assess how similar lichens within the aquatic system may also disperse.

An understanding of the population structure of the photobiont of a semi-aquatic lichen, *Dermatocarpon luridum* within Payuk Lake has many implications. Knowledge of photobiont population structure would reveal the level of gene flow among photobionts and an indication of the dispersal mechanism: water or wind. The photobiont in this lake system has been studied previously between continents, providing a unique opportunity now to compare spatial scales. Differences in photobiont haplotypes throughout the lake may also identify unique populations of *De. luridum* within the lake, which would have implications for conservation around the lake

and raise questions about the possibility of free-living *Di. chodatii* contributing to the lichenised population. Other organisms such as invertebrates, aquatic plants, and other lichens, including the endangered *Leptogium rivulare* (COSEWIC 2004), may be studied to incorporate a broader context for conservation. Lastly, an extensive study of the genetic variability of lichenised *Diplosphaera chodatii* has never been done on a single lake using local spatial scales to better understand gene flow and potential dispersal.

1.1.3 Objectives

The general goal of this thesis was to gain insights into dispersal by better understanding the spatial and genetic variation in the haplotypes of lichenised *Diplosphaera chodatii* around Payuk Lake, Manitoba. The objectives of this research were to: 1) assess the spatial distribution of genetic variation in *Diplosphaera chodatii*, in which it is predicted that populations closer together will be genetically more similar than populations further apart; 2) compare hydrological movement and other models with haplotype variation in *Di. chodatii* since haplotype numbers around Payuk Lake will correspond with net hydrological flow or inflow sources if the alga is dispersed by water currents; and 3) isolate and culture the lichen alga and the algae in the immediate vicinity on rocks to determine whether *Di. chodatii* is available in a free-living form for potential switching. Since *Di. chodatii* is known to be a terrestrial species (Flechtner et al. 1998; Lukešová and Hoffmann 1996), it is expected that the alga will be found in free-living form.

1.2 Literature Review

1.2.1 The Lichen Symbiosis

Lichens are the result of symbiotic associations between lichenised ascomycetes or basidiomycetes (mycobionts) and photosynthetic green algae (phycobionts) or cyanbacteria

(cyanobionts) (Ahmadjian 1993). Collectively, the phycobiont and cyanobiont are called photobionts (Friedl and Büdel 2008). Even though a lichen association contains both a fungus and alga/cyanobacterium, lichens are classified based on the mycobiont taxonomy and there are approximately 13500 – 17000 species of lichens worldwide (Hawksworth and Hill 1984; Hale 1974). Terrestrial lichens can be epiphytic or terricolous, occurring on tree bark, leaves, rock, dirt, and many other substrata. Lichens are poikilohydric and maintain the same level of moisture in the thallus as the relative humidity of the surrounding environment (Hale 1974; Nash 2008).

While many researchers describe lichens as a symbiotic association, others consider lichens to be a controlled parasitism between the photobiont and the mycobiont. The fungus in the lichen association may control the production of carbohydrates in the photobiont and their transfer to the fungus (Wang et al. 2014). The photobiont supplies mobile carbohydrates for the fungus, which are converted into mannitol (which cannot be used by the algae; Hill and Ahmadjian 1972). The mannitol, and other sugars, are then used by the mycobiont for growth as well as to produce secondary compounds that allow the lichen to survive in some of the most extreme habitats on Earth (Deduke et al. 2012; Millot et al. 2012), such as deserts, tundra, exposed alpine hillsides, and near fluctuating water bodies.

Lichens reproduce and disperse both sexually and asexually. Asexual reproduction and subsequent dispersal can involve both symbionts together, such as in soredia or isidia, or from thallus fragmentation (Honegger and Scherrer 2008). Mycobiont asexual reproduction also includes conidia, which are usually wind dispersed. Symbiotic propagules can be dispersed by wind or water, but animal vectors such as snails or mites can disperse the propagules through fecal matter left behind in new locations (Honegger and Scherrer 2008; McCarthy and Healey 1978; Fröberg et al. 2001; Meier et al. 2002). Thallus fragments can be dispersed via wind

(Robertson and Piercey-Normore 2007), animals, or water. Sexual reproduction results in the production of fungal ascospores in asci. The asci have a hymenium that is filled with a hydrophilic mucilage to protect the vulnerable spores from desiccation (Honegger and Scherrer 2008). The asci are contained in two types of sexual structures: apothecia (discs) and perithecia (sunken flasks). When the ascospores are mature, they are released into the environment and likely dispersed by wind (Honegger and Scherrer 2008). The photobiont has not been observed to undergo sexual reproduction within the thallus (Friedl and Büdel 2008) and requires a free-living state for sexual reproduction.

1.2.2 Aquatic and Semi-Aquatic Lichens

Aquatic habitats can be subdivided into four main zones (Aptroot and Seaward 2003; Gilbert 1996; Gilbert and Giavarini 1997; Hawksworth 2000). The upper terrestrial zone is not affected by running water but influenced by high humidity. The fluvial xeric zone follows below the terrestrial zone closer to the body of water and is an irregularly sprayed terrestrial zone (Aptroot and Seaward 2003). Next is the fluvial mesic zone, which is immediately above the submerged zone. Lastly, the submerged zone is the lowermost zone and is inundated for most of the year. Aquatic (or amphibious) lichens are those where the entire thallus is submerged for part or all of the year (Thüs 2002; Hachułka 2011). Marine lichens inhabit the intertidal zones, as well as fluvial xeric and mesic zones, and exhibit distinct zonation patterns based on their tolerance of desiccation (Brodo and Sloan 2004; Fletcher 1973). Freshwater lichens also show zonation patterns within these zones (Gilbert and Giavarini 1997; Ryan 1998a, b; Rosentreter 1984). Ephemeral pools can support water dependant species, which are mostly cyanolichens, but these species are not considered truly aquatic lichens (Aptroot and Seaward 2003).

About 200 freshwater lichen species are known to exist (Santesson 1939). Most aquatic lichens are crustose species within the Verrucariales (Nascimbene and Nimis 2006), though some foliose lichens do occur, such as *Peltigera hydrotheria* Miadlikowska & Lutzoni (Davis et al. 2000; Davis et al. 2003) and species of *Dermatocarpon* Eschw. Due to the nature of flowing debris, most aquatic lichens occur on rock or rock-like materials, such as cements (Aptroot and Seaward 2003; Keller 2005; Nascimbene et al. 2009), which provide a stable substratum for growing. Some aquatic lichens have been found on submerged alder roots (Hachułka 2011).

Like terrestrial lichens, aquatic lichens have habitat requirements in order to thrive. Some important characteristics of aquatic habitats include fluctuation in pH levels, copper concentration, and different degrees of shade (Pentecost 1977). For example, aquatic lichens such as some species from the genera *Staurothele* Norman, *Verrucaria* Shrad., and *Thelidium* A. Massal. prefer basic streams surrounded by limestones (Gilbert 1996). In contrast, *Hydrothyria venosa* Russell. prefers acidic waters (Denis et al. 1981), as with the lichens *Dermatocarpon luridum* (With.) Laundon, some species of *Verrucaria*, and *Staurothele fissa* (Taylor) Zwackh. (Gilbert and Giavarini 1997). Glavich (2009) found that growth of *Dermatocarpon meiophyllizum* Vainio, *Leptogium rivulare*, and *Peltigera hydrothyria* was also influenced by stream width and depth, and stream elevation, suggesting that the chemical nature of the substratum is not the only factor affecting lichen growth.

Aquatic lichens weather rock just like terrestrial lichens and help release elements into the water body (Kulikova et al. 2011). Many aquatic lichenised fungi are hypothesised to use thigmotropism to form associations with compatible algae (Stocker-Wörgötter and Turk 1988), which may help contribute to their ability to colonise new substrata quickly due to the movement of water and algae in suitable habitats. For example, *Verrucaria aquatilis* Mudd is a rapid

coloniser, invading the substratum by several small-sized and thin thalli (Nascimbene et al. 2009). These thalli then support a large number of small perithecia whose development begins in the earlier phase of thallus formation. However, not all aquatic lichens are fast colonisers. *Verrucaria elaeomelaena* (A. Massal.) Arnold develops according to a different strategy, establishing a thick thallus on which relatively large perithecia are formed, much later than in *V. aquatilis* (Nascimbene et al. 2009), suggesting that the rate of colonisation and establishment are not the only things controlling reproductive development and success.

Some freshwater lichens that are submerged for part of the year are termed "semi-aquatic" lichens (Aptroot and Seaward 2003). Most semi-aquatic lichens belong to the Verrucariaceae or Collemataceae, which most commonly contain coccoid, unicellular green algae (Aptroot and Seaward 2003; Thüs et al. 2011). They occur most commonly along lake shores (Gilbert 2000; Gilbert and Giavarini 1997) and along the margins of streams having only been found in water areas that have some sort of flow or current/wave action (i.e. not ponds or standing water; Aptroot and Seaward 2003). Most semi-aquatic lichens occur in the fluvial mesic zone or the submerged zone and included species of *Verrucaria, Staurothele, Dermatocarpon,* and *Thelidium* (Thüs and Nascimbene 2008). Some semi-aquatic lichens, such as *Verrucaria elaeomelaena* and *V. funckii* (Sprengel) Zahlbr, are indicator species of calcareous and siliceous springs (Nascimbene et al. 2007), as well as water quality (Monnet et al. 2005).

Semi-aquatic lichens have unique adaptations to survive in both extreme environments of full submersion and high desiccation. Some species develop air bubbles internally during submersion to provide oxygen to the photobiont and internal hyphae (Aptroot and Seaward 2003). Some semi-aquatic and aquatic lichens, such as *H. venosa*, lack ellipsoidal bodies in the

mycobiont, which are usually present in terrestrial lichens and hypothesised to aid in desiccation tolerance (Jacobs and Ahmadjian 1973).

Most semi-aquatic lichens reproduce via perithecia (and are called pyrenocarpous) since the hymenium is protected from water flow and eroding particles from sediments (Aptroot and Seaward 2003). Perithecia also require forceful ejection of the ascospores from the enclosed hymenium, which may assist in wind dispersal of these lichens. Asexual reproduction occurs in the form of diaspores and fragmentation, which allows for long distance dispersal in water (Aptroot and Seaward 2003). While the habitat of semi-aquatic lichens can be extreme and highly variable, these lichens are able to thrive and successfully inhabit these unique niches.

1.2.3 Dermatocarpon luridum

The lichen genus *Dermatocarpon* Eschw. is a solely foliose genus found within the Verrucariales (Heiđmarsson 2003), a lichen order composed mostly of crustose species (Nascimbene and Nimis 2006). Species of *Dermatocarpon* are globally distributed: North America has 19 to 24 species (Esslinger 2011), Nordic countries have about 10 species (Heiđmarsson 2000), and South Korea has about three species (Hur et al. 2004), with occurrences in New Zealand, Central America, Africa, Asia, and Antarctica (Heiđmarsson 2000). Within the Verrucariales, *Dermatocarpon* forms a monophyletic clade (Gueidan et al. 2009), however the species within the genus are considered polyphyletic due to high occurrences of phenotypic plasticity and species-complexes (Heiđmarsson 2003), as well as high genetic variation within the internal transcribed spacer (ITS) region of the ribosomal DNA gene region (Heiđmarsson 2000). *Catapyrenium* Flotow is a sister group to *Dermatocarpon s. lat.* and was taxonomically removed from *Dermatocarpon* following molecular and morphological

investigations (Heiðmarrson 2003, Harada 1993). However, within the genus, *Dermatocarpon luridum* is considered to be monophyletic (Heiðmarsson 2003).

Dermatocarpon luridum (With.) Laundon is a semi-aquatic species that grows in the fluvial mesic zone along the granitic shores of boreal lakes and can be found in Manitoba, Canada (Fontaine et al. 2013). It is a typical foliose lichen (Gueidan et al. 2009; Figure 1.1). Due to the requirement of a stable substrate this lichen is obligately saxicolous and attaches to the substrata via many small holdfasts along a single thallus lobe, which are smaller and narrower than a typical umbilicus (Amtoft et al. 2008). The lower surface of *D. luridum* often is wrinkled and a pale tan color with a pink tinge (Amtoft et al. 2008). The upper cortex is usually scabrose (Harada 1993), and contains a characteristic epinecral layer composed of dead hyphal cells that were once thought to be pruina (Heiðmarrson 1996). The upper cortex turns vibrant green when wet (Heiðmarsson 2000; Figure 1.2). This species produces microsporine-like compounds that aid in photoprotection within its exposed habitats (Nguyen et al. 2015).

Sexual reproduction results in perithecia sunken within the lichen thallus with exserted brown ostioles revealing the opening of the perithecia. These perithecia are characterised by the absence of hymenial algae, which are commonly found in other members of the Verrucariaceae (Gueidan et al. 2009). Eight narrowly ellipsoidal spores produced within the asci of the perithecium are often surrounded by a gelatinous sheath when young (Amtoft et al. 2008). The spores are usually > 15 μm long, a characteristic shared among four other species of *Dermatocarpon*: *D. bachmannii* Anders; *D. deminuens* Vain.; *D. meiophyllizum* Vain.; and *D. rivulorum* (Arnold) (Heiðmarrson 1998). However, *D. luridum* can be distinguished from these four other species due to the presence of multiple thallus lobes rather than single thallus lobes

(Heiđmarrson 1998). Pycnidia, or asexual fungal conidiomata, may also be present and are hard to distinguish from perithecia (Heiđmarsson 2000).

Dermatocarpon luridum is considered to be a shade-intolerant species and prefers to inhabit areas of open exposure near flowing water (Amtoft et al. 2008). Like many freshwater macrophytes (Zuccarini and Kampuš 2011), many lichens including *De. luridum* can be used as a bioindicator of freshwater ecosystems (Nascimbene et al. 2013). It has high copper tolerance due to its ability to absorb ionic metals into its thallus and therefore it has a possible use as a bioindicator of pollution in streams by measuring the amount of copper in the thallus (Monnet et al. 2005). Lichen photobionts are sensitive to copper, but the mycobiont can regulate the thallus microhabitat to protect the photobiont (Braanquinho et al. 2011), allowing for the use of the lichen to measure copper levels in aquatic systems. Furthermore, it often co-occurs with several other lichens such as *Staurothele fissa, Rhizocarpon geminatum*, and *Lecanora muralis* (Fontaine et al. 2014), as well as *Leptogium rivulare* (Fontaine et al. 2014), which is a threatened species as listed by COSEWIC (COSEWIC 2004). Like *De. miniatum* (L.) W. Mann, *De. luridum* may produce tyrosinases following rehydration that aid in the production of melanins, which would protect the thallus from exposure to sunlight on the open rock faces (Beckett et al. 2012).

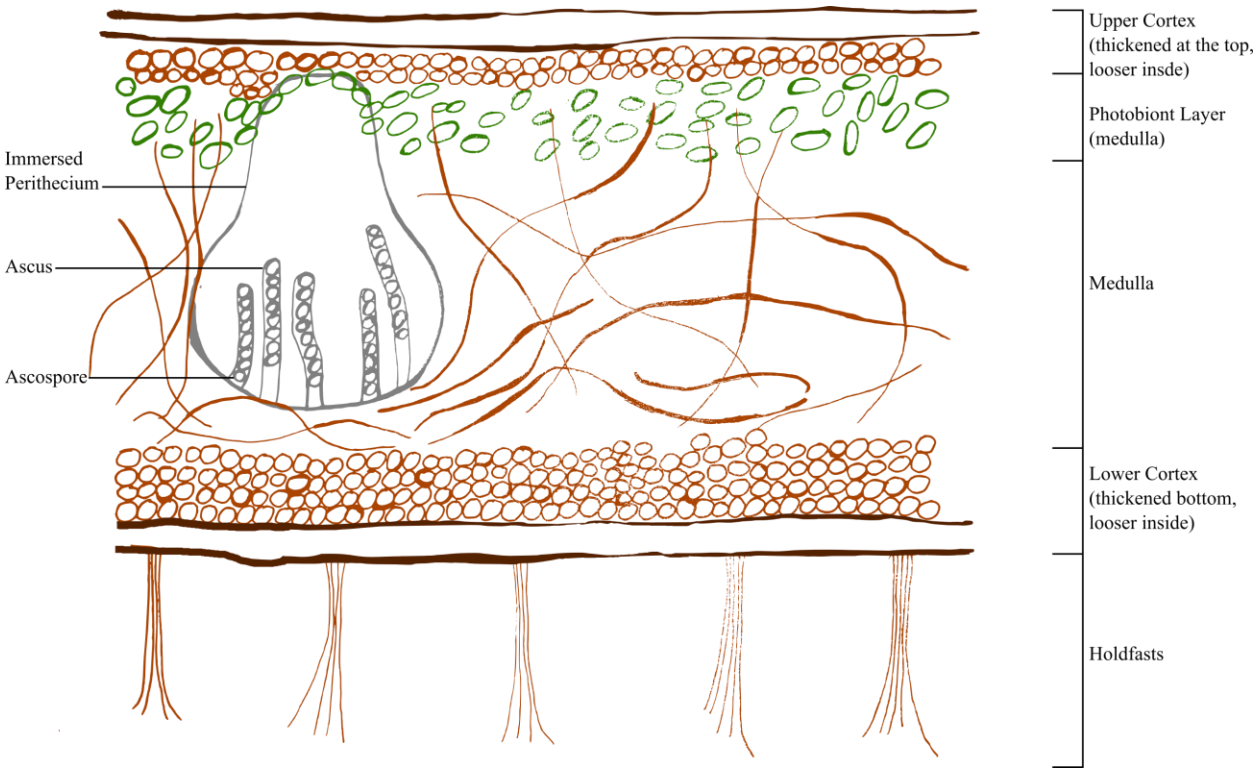

Figure 1.1. Schematic diagram of *Dermatocarpon luridum* in cross section. Schematic created by J. Doering (2017).

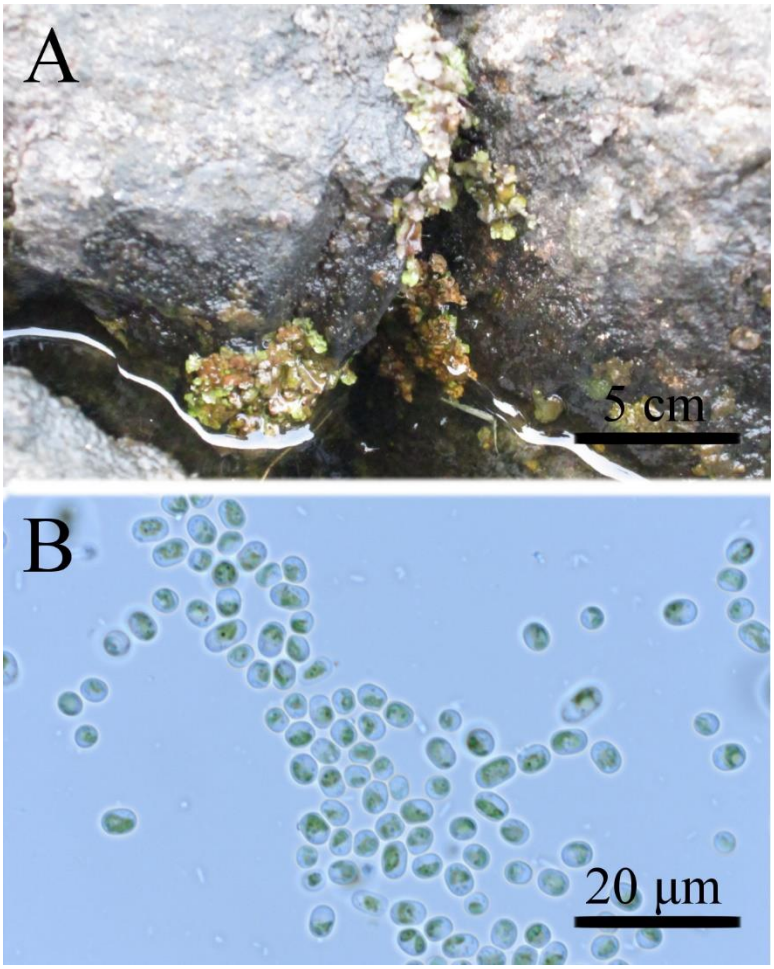

Figure 1.2. *Dermatocarpon luridum* and its photobiont partner. A) The grass green thallus of *D. luridum* growing on rock (photo: J. Doering). B) The photobiont *Diplosphaera chodatii* (photo: K. Fontaine).

1.2.4 Free-living Green Algae and Lichen Photobionts

Algae are simple, photosynthetic autotrophs found worldwide, across many Kingdoms and Domains (Guiry et al. 2012). They lack roots, vascular tissues, and complex tissues (van den Hoek et al. 1995), with mostly unicellular and some multicellular forms. Photosynthetic green algae belong to the Domain Eukaryota and cyanobacteria (or "blue-green algae") belong to the Domain Bacteria (Woese et al. 1990; van den Hoek et al. 1995). There are an estimated 72,536 free-living species of green algae and cyanobacteria, of which 43,918 are described and an estimated 28,618 are undescribed (Guiry 2012). In general, algae are a paraphyletic group of organisms, which includes representatives of four Kingdoms (Plantae, Chromista, Protozoa, and Eubacteria), 15 phyla, and 54 classes (Guiry 2012). There are an estimated 8000 species of lichenised cyanobacteria and 4500 species of lichenised green algae, but the number of species is underestimated due to cryptic species and discrepancies in species concepts (Guiry 2012).

Broadly, most green algae are in the phylum Chlorophyta, while some charophytic algae (related to land plants) are in the Streptophyta (Guiry 2012; Leliaert et al. 2012). Green algae are mostly aquatic but some terrestrial species exist (Holzinger 2009; Holzinger et al. 2011). Green aquatic algae are commonly abundant in freshwater ecosystems, with marine algae consisting of the Ulvophyceae less common. Species within the Trentipohliales are exclusively terrestrial (Leliaert et al. 2012). Cyanobacteria belong to Cyanophyta (Guiry 2012; van den Hoek et al. 1995).

Green algae are eukaryotic organisms and have plastids enveloped in a double-membrane, containing chlorophylls a and b, along with accessory pigments of carotenes and xanthophylls (van den Hoek et al. 1995). Pyrenoids are embedded in the chloroplast, surrounded by starch, and have firm cell walls with a cellulose cellular matrix (Leliaert et al. 2012).

Cyanobacteria, on the other hand, are prokaryotic organisms that usually occur either unicellularly, as a chain of cells, or as filaments and lack any membrane-bound organelles (Broady 1996; Lee 2008; van den Hoek et al. 1995). Chlorophyll b is absent, though photosynthesis occurs in unstacked thylakoids containing the pigment cyanophycin (Lee 2008; van den Hoek et al. 1995). Cell walls contain peptidoglycan instead of cellulose and are surrounded by mucilage (Lee 2008; van den Hoek et al. 1995). Like green algae, cyanobacteria occur worldwide in marine, freshwater, estuarine, and terrestrial habitats (Lee 2008; van den Hoek et al. 1995).

Reproduction in green algae is haplontic (with the exception of the Trentepohliophyceae, which has diplontic aspects), with the zygote being the only diploid stage in the life cycle (Lee 2008; van den Hoek et al. 1995). Sexual reproduction usually occurs with flagellated zoospores. Asexual reproduction can also occur via binary fission (Lee 2008; van den Hoek et al. 1995). Cyanobacteria do not undergo sexual reproduction due to their prokaryote nature and only reproduce asexually via binary fission (Lee 208; van den Hoek et al. 1995). Genetic variation is maintained through prokaryotic processes such as transformation and conjugation (Lee 2008; van den Hoek et al. 1995).

Green algae (phycobionts) and cyanobacteria (cyanobionts) commonly associate with lichenised ascomycetes to form lichen symbioses (Ahmadjian 1993). It is estimated that known photobionts do not exceed 148 species (Voytsekhovich et al. 2011a), from 22 – 48 genera (Ahmadjian 1993). Only two percent of lichen photobionts are known to the species level (Honegger 2008b), and ten percent of all lichen-forming fungal species associate with cyanobionts (which is approximately 100 species; Honegger 1997; Friedl & Büdel 2008). Most phycobionts from terrestrial lichens are from the Trebouxiales (Friedl and Büdel 2008), with the

most common algal species being members of *Trebouxia* Puymaly or *Trentepohlia* Mart. Semi-aquatic lichens and species from the Verrucariaceae associate with other green algal orders (Ulvales, Xanthophyceae, Trentipohliales, as well as Trebouxiophyceae; Thüs et al. 2011; Honegger 2008b), though rarely with the algal genera *Trebouxia* and *Trentepohlia* (Aptroot and Seaward 2003). Many lichen photobionts are also facultatively obligate to the symbiosis, meaning they are also found in a free-living state, such as *Trebouxia*, *Trentepohlia*, and *Diplosphaera*. Lüttge and Büdel (2010) found that many lichenised photobionts, including *Trebouxia*, exhibited high desiccation tolerance (30 – 40 days in the air), but green algae were more tolerant than cyanobionts.

Lichen phycobionts occur in three forms: coccoid, sarcinoid, or filamentous (Friedl and Büdel 2008). Cyanobionts occur in short filaments or chains (Friedl and Büdel 2008). They are arranged in a plane under the upper cortex in foliose and crustose lichens or in the periphery of the thallus in fruticose lichens (Honegger 2008a). The photobiont provides the fungus with carbohydrates, such as sorbitol (and mobile polyols in *Stichococcus* and related species), which the fungus uses to produce secondary compounds to aid in survival (Hill and Ahmadjian 1972). Some researchers consider the lichen to be a controlled parasitism rather than a symbiosis since the photobiont partner is thought to receive little benefit from the mycobiont partner (Nash 2008); however, the presence of the photobiont ensures the lichen can survive in its habitat and allows the photobiont to survive in habitats it could not normally tolerate.

1.2.5 Diplosphaera chodatii

Diplosphaera chodatii Bialosuknia (Bialosuknia 1909) is a uni-cellular green alga that is within the family Trebouxiophyceae of the order Prasiolales (Thüs et al. 2011), and is believed to be the photobiont partner of the lichenised ascomycete *Dermatocarpon luridum* (Reháková

1968; Fontaine 2013). Taxonomically, it is synonymous with *Stichococcus diplosphaera* (Bialosuknia) Heering (Heering 1914) and *Stichococcus chodatii* Chodat (Chodat 1913). Phylogenetically, it is also related to *Chlorella sphaerica* Tschermak-Woess (Karbovska and Kostikov 2012), a green alga once thought to be within the genus *Chlorella*. This alga was reassigned to another genus as *Di. sphaerica* due to the presence of external mucous structures, and the high similarity of the ITS1 and ITS2 rDNA sequences between it and other *Diplosphaera* species but not with that of *Chlorella* species.

Diplosphaera chodatii exhibits a wide variety of morphological shapes including micareoid and globose (Coppins 1983) as well as ovular/spherical and cylindrical (Fontaine et al. 2012; Stocker-Wörgötter and Turk 1989). Regardless of shape, cells are approximately 4 – 8 μm long by 3 – 5 μm wide (Coppins 1983; Fontaine et al. 2012; Yahr et al. 2006). It is a thin-walled alga and often occurs in groups of two to four cells, which may be surrounded by a gelatinous matrix (Stocker-Wörgötter and Turk 1989). *Diplosphaera chodatii* differs from *Stichococcus* due to its occurrence in two-celled to short-chain clusters (Ettl and Gärtner 1995) but *Stichococcus* has spherical to cylindrical cell shapes ranging from less than 10 μm – 15 μm (John 2003; Neustupa et al. 2007). *Diplosphaera chodatii* has a parietal chloroplast (Yahr et al. 2006; Fontaine et al. 2012), which is similar in appearance to the parietal, plate-like chromatophore found in *Hyalococcus dermatocarponis* H.Warén, the photobiont of *Dermatocarpon miniatum* (L.) W. Mann (Stocker-Wörgötter and Turk 1989), a lichen related to *De. luridum*. *Diplosphaera chodatii* is considered a relatively fast growing lichen photobiont, with an exponential growth rate of about 68 days (or 0.04/day; Elshobary et al. 2015). It also has a relatively high chloroplast biomass (0.90 mg), high pigment content (15.07 μg/mg chlorophyll a, 6.04 μg/mg carotenoids), and produces 34.84 μg/mg of carbohydrates (Elshobary et al. 2015). It may also produce sorbitol

for the fungus since *Stichococcus* (previously believed photobiont) produced sorbitol when it associates with *De. miniatum* (Hill and Ahmadjian 1972), which may be used to protect the lichen from extreme desiccation and damage from annual freeze-thaw cycles.

Diplosphaera chodatii is considered a terrestrial species, found in soil (Flechtner et al. 1998; Lukešová and Hoffmann 1996), wooden piers (Handa et al. 2001), and deserts (Fletchtner et al. 2008). It is a desiccation tolerant alga, but undergoes contortion and plasmolysis after one month (Zhang et al. 2011), making it very ideal for association with fungi in the Verrucariaceae in stressful habitats. *Diplosphaera chodatii* is found to be associated with a wide-variety of lichen-forming fungi in the Verrucariaceae including species of *Staurothele, Endocarpon* Hedw., *Dermatocarpon, Verrucaria, Normandina* Nyl., and is related to the green alga *Stichococcus* Nägeli (Thüs et al. 2011). Genetically, it shows high genetic variation within local populations but it has low gene flow in distant populations exhibiting isolation by distance (Fontaine et al. 2013), indicating that it may possibly be water dispersed. Within the lichen thallus, algal reproduction is limited to asexual sporulation or binary fission (Friedl and Büdel 2008). In a free-living state, the alga can reproduce both sexually via flagellated zoospores or asexually as above (Friedl and Büdel 2008).

1.2.6 Population Genetics and Structure

Population genetics is the study of the origin, amount, and distribution of genetic variation within a population (Templeton 2006) and is the basis for microevolution within a species. This field of research investigates the distribution of genetic variation between and within populations (Werth 2010). A haplotype is an alternative form of a specific nucleotide sequence (Templeton 2006), and is one of several types of variation examined when studying genetic variation. Population as a genetically isolated group of individuals, may be defined in at

least three ways: 1) a local breeding group of individuals found in close proximity; 2) a collection of breeding groups over a landscape where individuals only have access to individuals in their local group; 3) group of individuals continuously distributed over a broad geographical area such that individuals at the extremes of the distribution will not likely come into contact with each other (Templeton 2006). Populations may be affected by several factors, such as population structure, gene flow, and dispersal within the area of study.

Population structure can be defined as the presence, amount, and pattern of genetic variation within individuals in the same population (small scale) or as the spatial distribution and amount of genetic variation within and among populations and individuals of the same species (large scale; Templeton 2006). In lichens, population structure is a complicated concept due to the dual nature of the symbiosis. Haplotypes of individual genes exist in both the mycobiont and photobiont, and are further complicated by the specificity of the lichen association. Multiple haplotypes of the photobiont may be present within the population (Doering and Piercey-Normore 2009; Nyati et al. 2013) or within a single lichen species (Piercey-Normore 2006). For example, Piercey-Normore (2006) found that multiple haplotypes (also called strains) of photobiont occurred within a single thallus of *Evernia mesomorpha* Nyl. Guzow-Krzeminska (2006) also found multiple strains of photobionts within a single lichen thallus; however, some mycobionts are known to only associate with a specific strain of a single species of algae (Yahr et al. 2004). Beck et al. (2002) also found some lichen mycobionts associated with only one haplotype of a single photobiont species.

Photobiont specificity does not solely determine population structure. Environmental influence due to habitat characteristics and location are also known to affect population structure. For example, the substratum on which the lichen association occurs may affect photobiont

specificity. Beck (1999) found that lichens growing on iron-rich rocks only associated with one species of *Trebouxia* in the lichen thallus and the photobiont species were different among neighbouring lichen species. Yahr et al. (2006) found algal haplotype variation corresponded to habitats and not fungal genotypic variation, which was opposite of Yahr et al. (2004) in which the mycobiont haplotype was believed to cause photobiont specificity. Some lichens, such as *Ramalina menziesii* may also associate with photobionts due to the photobiont's ability to adapt to the habitat (Werth and Sork 2010). Location may also play a role in genetic variation. Beiggi and Piercey-Normore (2007) found that lichen haplotypes clustered based on location. The photobiont haplotypic variation can also vary between geographic sites (Piercey-Normore 2004). In this study fungal genetic variation did not vary based on sites, which indicated that some lichen fungi might preferentially select certain algal haplotypes, resulting in unique population structures among locations. Nyati et al. (2014) also found that there was a weak correlation between algal haplotypes and environmental or geographic location in the lichen family Teloschistaceae based on analysed internal transcribed spacer region (ITS) rDNA and large subunit of the *Rubisco-carboxylase* gene sequences.

Several lichens can share the same photobiont pool or haplotypes (Beck et al. 2002). Additionally, the photobiont may be found free-living until association with a compatible fungus (Mukhtar et al. 1994). These free-living haplotypes may be different than the haplotypes found in the photobiont (of the same algal species) within the thallus, and could potentially be incorporated into the thallus. Horizontal gene transfer (lateral gene transfer) is common in green algae and helps to rapidly spread evolutionary innovations across lineages (Leliaert et al. 2012). Horizontal gene transfer was supported by Piercey-Normore and DePriest (2001), who failed to

support congruence and cospeciation in mycobionts and photobionts, suggesting high rates of algal haplotype switching and/or horizontal gene transfer.

Large scale sampling is required to examine geographical patterns in photobiont species and haplotypes (Opanowicz and Grube 2004). Robertson and Piercey-Normore (2007) found that a high level of variation in a small geographic area indicated a lack of sampling to account for all of the genetic variation in the area. One method to determine sufficient sampling size is rarefaction, a type of haplotypic (allelic) species accumulation curve (Werth 2011). The level of sampling is dependent on the spatial scale. Rarefaction showed that sample sizes were sufficient from about 20 individuals for studies within a single local population to 300 – 400 individual samples (or 25 – 30 sampled populations) at the landscape level (Werth 2011). Lindblom (2009) also used rarefaction to determine the level of genetic variation that was missing and found that 23% of intergenic spacer region and 8% of ITS variation was unaccounted for in the sample size collected.

1.2.7 Gene Flow and Dispersal

Gene flow is the dispersal of genetic information between populations, which increases genetic variation within a population by introducing alleles from one population into the other (Templeton 2006). A lack of population structure at a local level may indicate a high level of gene flow (Werth and Sork 2008), since gene flow can facilitate gene transfer between individuals and populations (Yahr et al. 2006), or replace photobionts in the population, changing the dominance of photobionts and their haplotypes. Doering and Piercey-Normore (2009) found that there was low algal variation between and within populations on jack pine (*Pinus banksiana* Lamb.), suggesting that there were high levels of gene flow of *Trebouxia* photobionts within the population. Gene flow may be detected through the analysis of DNA

sequences from sampled locations. Gene flow was found to be occurring in the photobiont of *Cladonia arbuscula* around Payuk Lake but not in the fungal partner (Robertson and Piercey-Normore 2007). In contrast, Fontaine et al. (2013) found that gene flow was low between populations of *De. luridum* found in Canada and Austria because there were few shared haplotypes among the two populations. Mantel's test (isolation by distance; Mantel 1967) is one way to assess gene flow within or among populations since populations closer together should be more similar to each other than populations farther apart, which is true in most cases; however, Werth et al. (2007) found that while isolation by distance in samples of *Lobaria pulmonaria* across a landscape was high, a high level of gene flow was detected within the forest, suggesting that connectivity of the patch and mode of dispersal can also affect gene flow.

The dispersal of genetic variation in lichens occurs either sexually in the form of ascospores in the mycobiont or through asexual means of the lichen thallus, such as conidiospores produced in pycnidia or fragmentation in *Cladonia arbuscula* (Wallr.) Rabenh. (Robertson and Piercey-Normore 2007). For example, both symbionts are codispersed in soredia for *E. mesomorpha*, which was detected due to the high genetic variation found within populations but low variation reported between populations (Piercey-Normore 2006). Due to the physical weight and shape of vegetative propagules, dispersal results in high spatial autocorrelation (Werth et al. 2006b); however, dispersal of *Lobaria pulmonaria* is not restricted due to landscape and distance (Werth et al. 2007). Lichen propagules from *L. pulmonaria* were found to have dispersed great distances into habitats where the lichen was absent, indicating that habitat suitability may be required for colonisation rather than spore dispersal alone (Werth et al. 2006a).

Population structure and gene flow may also be affected by dispersal vectors, such as wind (Tormo et al. 2001) and water currents (Rout and Gaur 1994). In many lichens, propagules, such as soredia, can be dispersed by either wind or water, or from a combination of both (Thomson 1972). In plants, gene flow was found to be bidirectional in the shrub *Myricaria germanica* Desv., indicating that dispersal by water was not as effective as other means of dispersal (Werth and Scheidegger 2014), and could be a combination of many vectors. In other lichens, dispersal is limited based on life history stages. *Lasallia pustulata* (L.) Mérat, a lichen occurring in similar habitats to *De. luridum* since it may grow on rocky outcrops near coasts and flowing streams, as well as boulders in open heathland, employs water dispersal for asexual fragments and wind dispersal for sexual ascospores (Hestmark 1992).

Water dispersal would limit dispersal within the watershed and alter distribution of haplotypes based on water flow direction. For example, Derycke et al. (2006) reported that the numbers of haplotypes of nematodes were fewer upstream compared to downstream, which may increase as a result of the additional tributaries entering the stream system, adding haplotypes to the system in the direction of water flow. The transport of haplotypes may occur in lichens as well. In lichens, fragmentation is probably the most common form of dispersal (Thomson 1972). Water dispersal in the spring runoff carries ice-scoured lichen fragments downstream (Elridge 1996; Thomson 1972); however, the establishment of new thalli requires suitable habitats that may be difficult to obtain due to currents, substrata surface properties, and other environmental characteristics (Armstrong 1981). Some lichens, such as *Cladonia pyxidata* (L.) Hoffm., and *C. pocillum* (Ach.) O.J. Rich., utilise splash cups (Thomson 1972) or water trickles (Bailey 1967) to carry asexual soredia away from the thallus; though compared to dispersal by runoff, splash cups would be a limited but effective means of short-distance dispersal.

Wind dispersal would result in a broader, more scattered dispersal pattern than water dispersal. Wind dispersed lichens would be expected to have smaller propagule sizes to allow for ease in carrying, since smaller propagules would be lighter and therefore have the potential to be carried further (Werth et al. 2014). However, at local scales, size may not be as important as other factors, such as topography, may provide barriers to long distance dispersal (Werth et al. 2014). Contrarily, Muñoz et al. (2004) found that dominant wind direction was more important in long distance dispersal of cryptogamic species in the Southern Hemisphere due to the connectivity of sites experiencing the same wind conditions. Similar wind conditions may contribute to high dispersal rates of lichen fragments over snow in the Arctic, leading to a wide distribution of many lichen species (Thomson 1972). Armstrong (1987) even suggested that wind speed is highly correlated to wind dispersal, but both wind and water can disperse lichen soredia. Regardless, identical haplotypes within a species may indicate a recent dispersal event since many of the genes used to assess genetic variation evolve at fast rates (Moncalvo and Buchanan 2008).

1.2.8 Landscape Genetics and Geographic Information Systems

Visualising, analysing, and understanding the distribution and population genetics of organisms is very complex and dynamic. Landscape genetics, first coined in 2003, is a rapidly evolving field of research that includes spatial analyses, ecology, population genetics, and geography to understand the spatial distribution of genetic variation over a landscape (Storfer et al. 2010). Landscape genetics tries to understand the interaction between the landscape (topography) and microevolutionary processes (i.e. evolutionary processes within species such a gene flow, genetic drift, and selection) (Holderegger and Wagner 2006). Landscape genetics utilises many tools including molecular markers and spatial statistics, such as Mantel's test and

variograms, geographic information systems (GIS) and other programs. The use of specialised spatial statistics quantifies landscape variables and population genetic structure and variation over an area of study (Storfer et al. 2007) and helps to identify barriers to dispersal and gene flow that may not have been identified using more traditional approaches. Several studies have been done on the landscape and regional scales (Fontaine et al. 2013; Slatkin 1993; Fernández-Mendoza et al. 2011), but those at local scales (i.e. within a single lake or forest; Werth 2010) were limited in the types of analyses performed and the interpretations.

Since landscape genetics deals with the spatial distribution of genetic variation over a landscape, parametric statistics cannot be used due to biases in autocorrelation and spatial relatedness. The most common statistics used are those that examine "isolation by distance", where things that are located closer together are more related than those located farther apart (Dale and Fortin 2014). Geographic distance measures, such as the "as the crow flies" (Euclidean), network path distances, and least-cost distances, are commonly used in tests for spatial autocorrelation (Manel and Holderegger 2013; Dale and Fortin 2014). Variogram analyses, which take into account the spatial variance between samples, are also commonly used since they avoid biases due to underestimation of population variance and they estimate spatial genetic variation accounting for isolation-by-distance (Wagner et al. 2005).

Landscape genetics also utilises GIS to model the spatial distribution of genetic variation over a landscape and to predict patterns in dispersal and establishment due to functional connectivity within the landscape (Manel and Holderegger 2013). The use of GIS allows for the overlay of land cover use, topographic features, and other thematic maps with genetic data linked to some sort of spatial context (i.e. GPS coordinates), which can further be used to predict future patterns in distribution (Manel and Holderegger 2013). Hydrological modelling using GIS can be

performed to understand and predict how water moves through a system, which can help elucidate the distribution of aquatic organisms within a landscape. For example, Carey and Woo (1999) modelled snowmelt runoff on two slopes (one north and one south facing) and found that the south slope contributed faster and more runoff than the north slope, which released more soil into the watershed. Modelling runoff can be applied to the study of lichens, since more lichen fragments and potential photobionts can be transported into a water system from various inflow sources. Modelling runoff could have implications in understanding how aquatic and semi-aquatic organisms may be dispersing within the landscape.

1.2.9 Algal Barcoding

Genetic markers are a rapidly evolving tool for studying population genetics (Werth 2010). Depending on the level of variation within the gene, genetic markers can be used to assess interspecific (between species) and intraspecific variation (within a single species to evaluate lineages and strains). In lichenised fungi, commonly used markers include the nuclear ribosomal intergenic spacer region (IGS rDNA), *ef1α* (translation elongation factor 1), *rpb2* (large subunit of RNA polyermase II), *cox1* (cytochrome c oxidase), and the internal transcribed spacer region (ITS rDNA) of the nuclear ribosomal DNA (Pino-Bodas et al. 2013). The IGS had the highest intra- and interspecific variation compared to *rpb2*, with a 100% identification success rate between species, and *ef1α* had the lowest variation and the most failure in identifying species (Pino-Bodas et al. 2013). The *cox1* and ITS showed similar variation and species resolution (Pino-Bodas et al. 2013).

Markers used for algae generally have low variability (Chase et al. 2005), and plant plastid markers are too conserved, making species delimitations within algae very difficult. Interspecific variation is much more easily studied in green algae than intraspecific variation.

Algal DNA barcoding is further challenging by the fact that different markers work best with different groups of algae (Hall et al. 2010), and although the universal plastid amplicon (UPA) is considered to be a universal marker, it has trouble discriminating taxa, and may not be sufficiently variable to use as a reliable marker (Saunders and Kucera 2010). Protist DNA barcoding (for dinoflagellates and related algae) commonly uses markers to assess the large subunit of rDNA (LSU) gene, while the mitochondrial cytochrome oxidase 1 (CO1-5P) is used for brown and red algae, the 3' region of the plastid large subunit of the ribulose-1-5-bisphosphate carboxylase-oxygenase (*rbc*L-3P) for diatoms, and *tufA* (plastid elongation factor Tu gene) for green algae (Saunders and McDevit 2012). Additionally for green algae, the 18S rDNA gene is also used commonly, followed by 28S rDNA, actin protein coding gene, rbcL, and atpB (chloroplast gene markers; Leliaert et al. 2012). Filamentous lichen photobionts, such as *Trentepohlia,* are studied using the small subunit of the ribosomal DNA and rbcL genes to distinguish between species (Nyati et al. 2007). Single celled green algal photobionts are studied utilising a wide variety of genetic markers.

The nuclear genomes contains many different genes with a balance between conserved regions and highly variable regions that can be used to discriminate between species. The *tufA* gene can be used to discriminate among species and genera, but the lack of introns provides low variability for intraspecific discrimination (intraspecific divergence of 0.52%; Saunders and Kucera 2010). The actin protein coding gene is also commonly used to distinguish between species due to two isoforms which were thought to result from gene duplications (Kroken and Taylor 2000).

The nuclear ribosomal DNA gene regions also offer the ability to discriminate among species. The ITS regions of the ribosomal rDNA can be used to discriminate taxa to the species

level due to varying sizes of the ITS regions, and they have been used to distinguish species of *Prototheca* Krüger (achlorophyllous algae) and lichen photobionts (Hirose et al. 2013), such as those in the Trebouxiophyceae (Cordeiro et al. 2005) and those that associate with the fungal Physciaceae (Helms et al. 2001). The ITS is good universal marker for plants and animals because it is flanked by conserved regions (LSU, SSU and 5.8S rDNA) to make universal primers, but also high success rate in distinguishing taxa to the generic, and many to the species level (Yao et al. 2010). The large and small subunits (LSU (26S rDNA) and SSU (18S rDNA), respectively) are part of the ribosomal DNA gene complex, which consists of both highly conserved and highly divergent regions (Sonnenberg et al. 2007). The 26S rDNA region can be used to distinguish between phyla (del Campo et al. 2010). The divergent domains D2/D3 of the nuclear ribosomal LSU are variable at the species level, though it has large regions of highly conserved sequences (Saunders and Kucera 2010). There is also variation in the number and pattern of introns in the SSU rDNA (Piercey-Normore 2004), making it a good marker for assessing interspecific variation. Indeed, the 18S rDNA has been used to assess the phylogeny of *Planophila* Gerneck (Chlorophyta), which was not monophyletic (Friedl and O'Kelly 2002), and to identify environmental DNA of algae (Theroux et al. 2010). Sherwood et al. (2000) found that sequence divergences in the Prasiolales (algae related to *Diploshaera*) for *rbc*L and 18S rDNA were 0 – 6.1% and 0.4 – 3.8% respectively. The *rbc*L sequences were 1078 bp long, with 490 bp of invariant sites, 486 phylogenetically informative sites, and 102 autapomorphies. In comparison, the 18S rDNA sequences were 1433 bp long, with 872bp invariant sites, 357 informative sites, and 204 autapomorphies, but was weaker than *rbc*L (Sherwood et al. 2000).

Chloroplast genomes are useful in phylogenetic reconstructions because of their condensed gene content compared to nuclear genomes (Leliaert et al. 2012). Chloroplast genes,

contained within 3 – 275 chloroplast DNAs per plastid (Zoschke et al. 2007), are usually also single copy, not multi-copy within the genome as they are in some of the nuclear DNA genes such as rDNA. Chase et al. (2005) found that the *rbc*L marker was very successful in phylogenetic studies between species, but not lineage reconstructions due to its slow evolutionary rate and unambiguous sequence alignments (Nozaki et al. 1995), making it good for generic or higher levels of phylogeny. Kulichová et al. (2014) found 29 operational taxonomic units (OTUs; based on sequence similarity) from 122 colonies of single celled green algae, which showed similar levels of variation as the 18S rDNA gene.

The *rbcL* gene is good for determining variation within genera (Nelsen et al. 2011; Saunders and Kucera 2010), but is best at detecting variation at the species level (Saunders and Kucera 2010). Hodkinson et al. (2014) used the *rbc*L gene to identify the photobionts of *Sulzbacheromyces* Hodkinson & Lücking and *Lepidostroma* Mägd. & S. Winkl. lichenised fungi. These photobionts were found to be closely related to lichenised *Diplosphaera* (Hodkinson et al. 2014). The *rbc*L marker is commonly used in lichenised photobionts because it has high success in sequencing and PCR (> 80%; Saunders and Kucera 2010). The *rbc*L region has been found to contain group 1 introns (Hanyuda et al. 2000), which could help to discriminate against haplotypes in the same species, although variation may be lower than other genetic markers (Wongsawad and Peerapornpisal 2014) since it has very small intraspecific divergence (0.41% – 6.1%; Saunders and Kucera 2010 and Sherwood et al. 2000, respectfully). The chloroplast large-subunit rDNA (LSU rDNA) has a diversity of group 1 introns which, when present, can also be used to differentiate between species of lichen photobionts (del Campo et al. 2010).

Mitochondrial genomes can also be used, but they have a much slower rate of evolution (and therefore variability) in plants compared to animals (Robba et al. 2006). One mitochondrial

gene that is used to study algae is the cox1 (mitochondrial cytochrome c oxidase). This gene is often used to discriminate between red algae species since it has 0 – 4 bp of intraspecific variation and 28 – 148 bp of interspecific variation based on 539 bp long gene (Robba et al. 2006). However, the presence of group I and sometimes group II introns makes it hard to amplify and sequence so it is not often used (Saunders and Kucera 2010).

The discrimination among lineages and strains within an algal species is much more difficult than interspecific variations. The markers must be conserved enough to discern differences between species, but variable enough to identify the subtle differences among strains. Many intraspecific markers including inter-simple sequence repeats (ISSR), randomly amplified polymorphic DNA (RAPD), restriction fragment length polymorphisms (RFLPS), and amplified fragment length polymorphisms (currently used in plants and animals) are inexpensive ways to screen multiple loci (Werth 2010) and detect variation within a species. Some markers, such as simple sequence repeats (SSRs; a type of microsatellite), can be designed specific to the lichen symbionts (Werth 2010) and are highly polymorphic, but may not be applicable to all species. RAPDs and SSRs are used to differentiate between populations and species (Murtagh et al.1999; Honegger et al. 2004), but are usually applied to axenic cultures of mycobionts rather than photobionts. RAPD fingerprinting can be used to assess subspecific diversity (Nyati et al. 2013).

Microsatellite markers (inter-simple sequence repeat (ISSR)) are highly reproducible, highly specific, and can identify more complex patterns than RAPDs. They are designed to anneal to microsatellite sequences, and as a result use longer primers for more stability (16 – 20 bp). Microsatellites consist of repetitive sequences and they can vary at their respective loci (Oppermann et al. 1997). Polymorphisms within larger repeat regions are called variable number of tandem repeats (VNTR; Nakamura et al. 1987). Due to multiple banding patterns, they are

also good for assessing intraspecific variation (Wongsawad and Peerapornpisal 2014; Dal Grande et al. 2014adal). Mini- and microsatellites, tRNA fingerprinting, and RAPDs are most common in fungal studies (Nyati et al. 2013). They provide a rapid method for assessing genetic diversity within a population or species, although they are not necessarily associated with a specific gene (Oppermann et al. 1997). One type of microsatellite that is used to DNA fingerprint cyanobacteria and cyanobionts is the highly iterated palindrome (HIP1; Bittencourt-Oliveira et al. 2007). The HIP1 is an octameric palindrome sequence abundant in coding regions and only found in cyanobacteria (Robinson et al. 1995). It is often used to characterise cyanobacteria that are associated with angiosperms (Rasmussen and Svenning 1998).

Some genes can be used to assess inter- and intraspecific variation of species. The ITS rDNA and actin protein coding genes are two such genes commonly used in photobiont phylogenies. The ITS rDNA regions separate the rDNA subunit regions (Coleman and Mai 1997). The 5.8S rDNA gene is highly conserved and is approximately 158 bp long and is shared among most taxa (Coleman and Mai 1997). On either side of the 5.8S rDNA region, are two ITS regions: ITS1 is on the 5’ end of the 5.8S rDNA region and ITS2 is on the 3’ end. The ITS1 and ITS2 regions are based on ring structure rather than a hairpin which is normally used (Coleman et al. 1998; Mai and Coleman 1997); however, they contain four hairpin structures around an open ring, with conserved areas that are specific subsequences believed to be involved enzymatic interactions during RNA processing (Beiggi and Piercey-Normore 2007). The ITS secondary structure contains four helices, with helix I being the most divergent (Skaloud and Peksa 2010). In fungi, ITS2 is considered more conserved than ITS1 based on secondary structures (Coleman 2003; Mai and Coleman 1997; Beiggi and Piercey-Normore 2007), though there are variations due to hairpin structure at the distal end of the ITS2. In the ITS2 region, nucleotide changes

occur most frequently in helix IV, followed by helix I (Coleman 2003). Helix III is the most conserved (5' end), and helix II has a pyrimidine-pyrimidine bulge and is also conserved (Coleman 2003). Generally, ITS2 is longer than ITS1 (>200 bp compared to <200 bp) with ~43 – 63% GC content (Beiggi and Piercey-Normore 2007). Many studies use the differences between ITS1 and ITS2 to differentiate between algal photobionts in lichens. Werth (2012) found that *Ramalina menziesii* was associating with multiple species of *Trebouxia* during its juvenile stages, and also found that haplotypes of the same alga were shared among fungal mycobionts (8 haplotypes) using the ITS rDNA gene. Beck et al. (1998) also found multiple strains within species of *Trebouxia* using ITS rDNA.

The ITS rDNA gene region is considered to be highly variable because the spacer regions are removed, before maturation of the ribosome (Coleman 2015). Although the variability within the ITS rDNA region is considered to be high and it can help discriminate both between and within species, actin markers showed phylogenies that were better resolved with stronger support for clades than the ITS rDNA gene region in lichen symbionts (Skaloud and Peksa 2010). On the other hand, group I introns are common in the 18S rDNA regions and may range from short 200 – 500 bp regions to several thousand bp regions. When these are functional, they can self-splice and some may be found throughout the genome (Friedl et al. 2000), and when present they may be useful to distinguish among species. There has been some evidence to suggest they can be transferred from the free-living alga to the lichen photobiont or vice-versa via horizontal gene transfer. Horizontal gene transfer (lateral gene transfer) of group I introns is common in green algae and helps to rapidly spread evolutionary innovations across lineages (Leliaert et al. 2012).

The actin protein coding gene functions to produce actin, a cytoskeletal protein that has many cellular functions (Wu et al. 2009 and references therein). It is a single copy gene in

unicellular organisms (Bhattacharya and Ehlting 1995), but a multi-copy gene family in plants (Wu et al. 2009). There are two types of actin in lichen photobionts (type I (α-actin*)* and type II (β-actin)) and both of these actin proteins coding genes are more variable than the ITS rDNA, with 37 phylogenetically informative sites. Type II is believed to be a pseudogene, caused by a duplication event during the evolution of Trebouxiophyceae, and is highly variable due to abundant synonymous DNA substitutions. The gene region is ~ 682 bp long with 279 variable sites (41%) and 188 (27.6%) informative sites, with 95% of the variation in the introns (Nelsen and Gargas 2006). There is also an intron located at nucleotide 738 (Kroken and Taylor 2000). They also contain splicosomal introns in codon 123 (glutamine) and some green algal species have some introns with microsatellite repeats (CA repeat; Wu et al. 2009). Some actin genes diverged faster than others, indicating divergent evolution or expression of different alleles of actin (Wu et al. 2009), and are believed to have approximately six times more variation than the ITS rDNA (Nelsen and Gargas 2006). Actin type I introns are often used to distinguish cryptic species and are commonly used in population genetics studies (Nelsen and Gargas 2006). The versatility of the actin and ITS rDNA genes in assessing intraspecific variation make these genes ideal candidates for investigating population structure in *Diplosphaera chodatii* within a single lake.

CHAPTER 2 : MATERIALS AND METHODS

2.1 Overview

The methods are described for isolation and culture of lichen algae (photobionts) from the thallus and free-living algae around the thallus on the rock surface as well as the DNA isolation, PCR, and sequencing of the algal genes. The photobiont was examined for genetic variation and spatial distribution by collecting the lichen thallus from rock around the margin of Payuk Lake and using algal-specific primers to amplify and sequence two genes. The pattern of haplotype variation in these genes was compared with bedrock topology of the lake to estimate the hydrological movement and potential photobiont dispersal and gene flow by testing four hypotheses. The possibility for free-living algae to contribute to the lichen photobiont population was examined by sampling the free-living algal diversity present on the rock adjacent to the thallus. Representatives of the algae from the thallus and from the free-living samples were cultured and examined microscopically for identification to genus, though only the lichenised alga was sequenced.

2.2 Field Collections

The Mistik Creek chain of lakes (Figure 2.1) is located approximately 32 km southeast of Flin Flon, Manitoba, Canada. On September 10-14th, 2014 and June 25-30th, 2015, the collection of 102 lichen thallus (and therefore photobiont) samples was made in 34 collection sites from Payuk Lake, Manitoba (Figure 2.2), with three replicates collected within three meters of each other in each site. These numbers resulted in a photobiont sample size high enough to compare the genetic diversity in a local population study (Werth 2011). Thallus collections were made in the inflow of Payuk Lake at Mistik Creek (18 samples; Figure 2.3A), the inflow of Payuk Lake at Twin Creek (6 samples; Figure 2.3B), Payuk Lake (72 samples; Figure 2.3C), the

outflow of Payuk Lake into Mistik Creek (6 samples; Figure 2.3D), and three additional samples were collected for reference from the Whiteshell Provincial Park in July 2015 (Permit number PP-PHQ-15-015). The 34 collection sites were recorded using a Garmin GPS map 76C x GPS unit (datum NAD83, UTM zone 14N) and were at least 25 m apart. They were selected based on accessibility and the presence of *Dermatocarpon luridum* thalli along the lake margin. Environmental parameters (Appendix A) for each collection site included the slope (degrees) and rock aspect (North, South, East, West), which were measured using a Suunto MC-2 Global Compass (Suunto, Vantaa, Finland). Additionally, the general rock type (granite, rhyolite, basalt) and surrounding vegetation were recorded. A photograph of each *D. luridum* thallus was taken and the height above the water was recorded using a metric ruler. Portions of each *D. luridum* thallus were moistened with lake water to scrape the thallus from the rock with a knife without breaking it into many pieces and placed into separate ziplock bags. Lichen samples were cleaned of debris and 1 cm thallus portions (approximately <20 mg dry weight) were placed in 1.5 mL Eppendorf tubes and stored at -20°C for use in molecular analyses, while the rest of the thallus was transferred to paper envelopes to be deposited as vouchers in the cryptogamic division of the University of Manitoba Herbarium (WIN). Since algal turnover within an established lichen thallus is thought to be very low due to the slow growth in lichens (Ahmadjian 1993), temporal variation between the fall (2014) and spring (2015) collections is expected to be negligible.

Free-living algae surrounding each lichen thallus were collected at each collection site to examine algal diversity and compare with the lichen photobiont. Prior to scraping off the lichen thallus, algae were collected by brushing the surrounding rock with a new toothbrush and rinsing the brush in a 20 mL sterile plastic vial containing MilliQ sterile water between brushings. The samples were then stored at -20 °C for further microscopic examination and culturing.

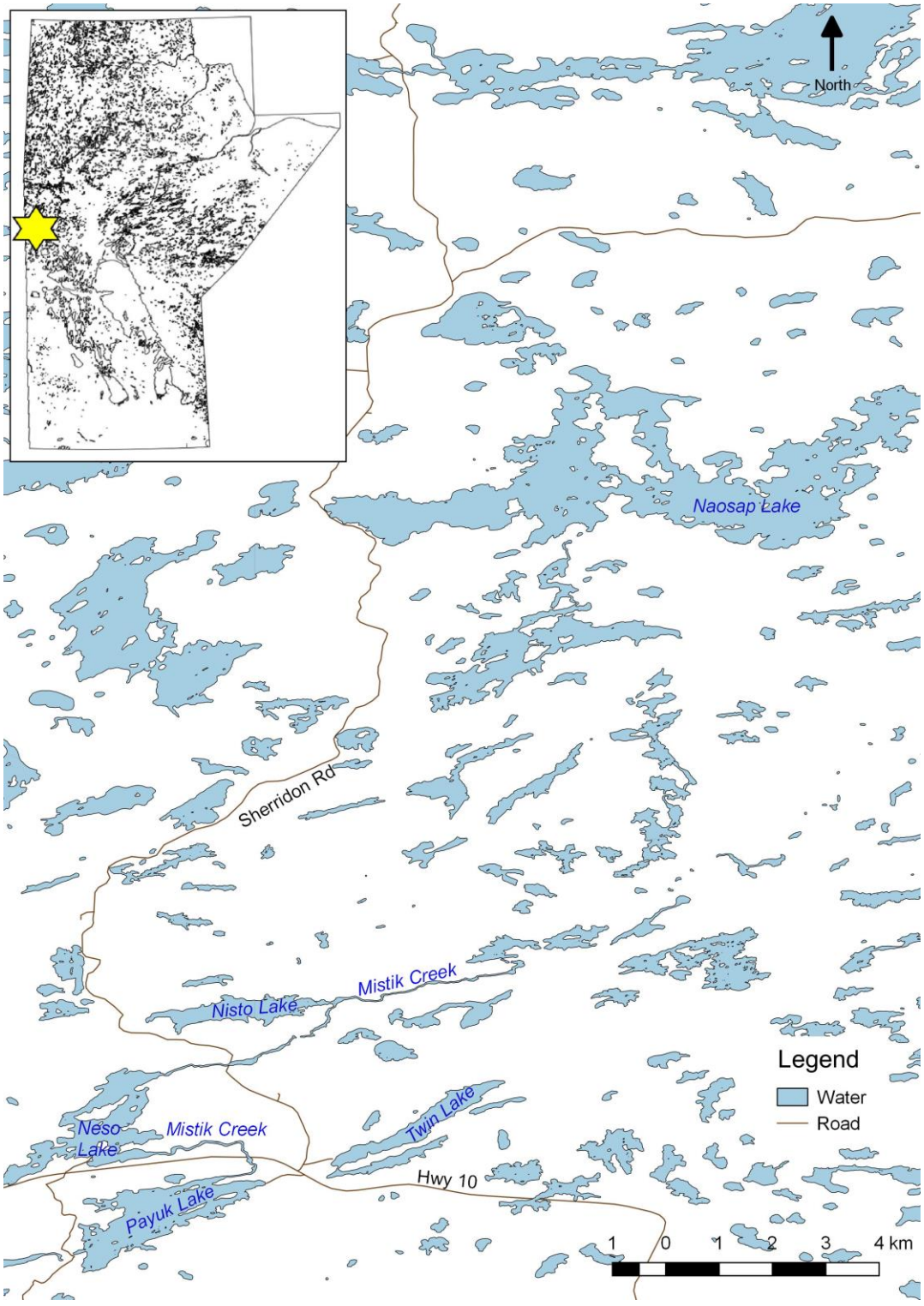

Figure 2.1. Map of the Mistik Creek chain of lakes located approximately 32 km from Flin Flon, Manitoba, Canada. Map was produced using Quantum GIS v. 2.18 Las Palmas (Quantum GIS Development Team 2017), with base maps downloaded from CanVec (GeoGratis, Natural Resources Canada).

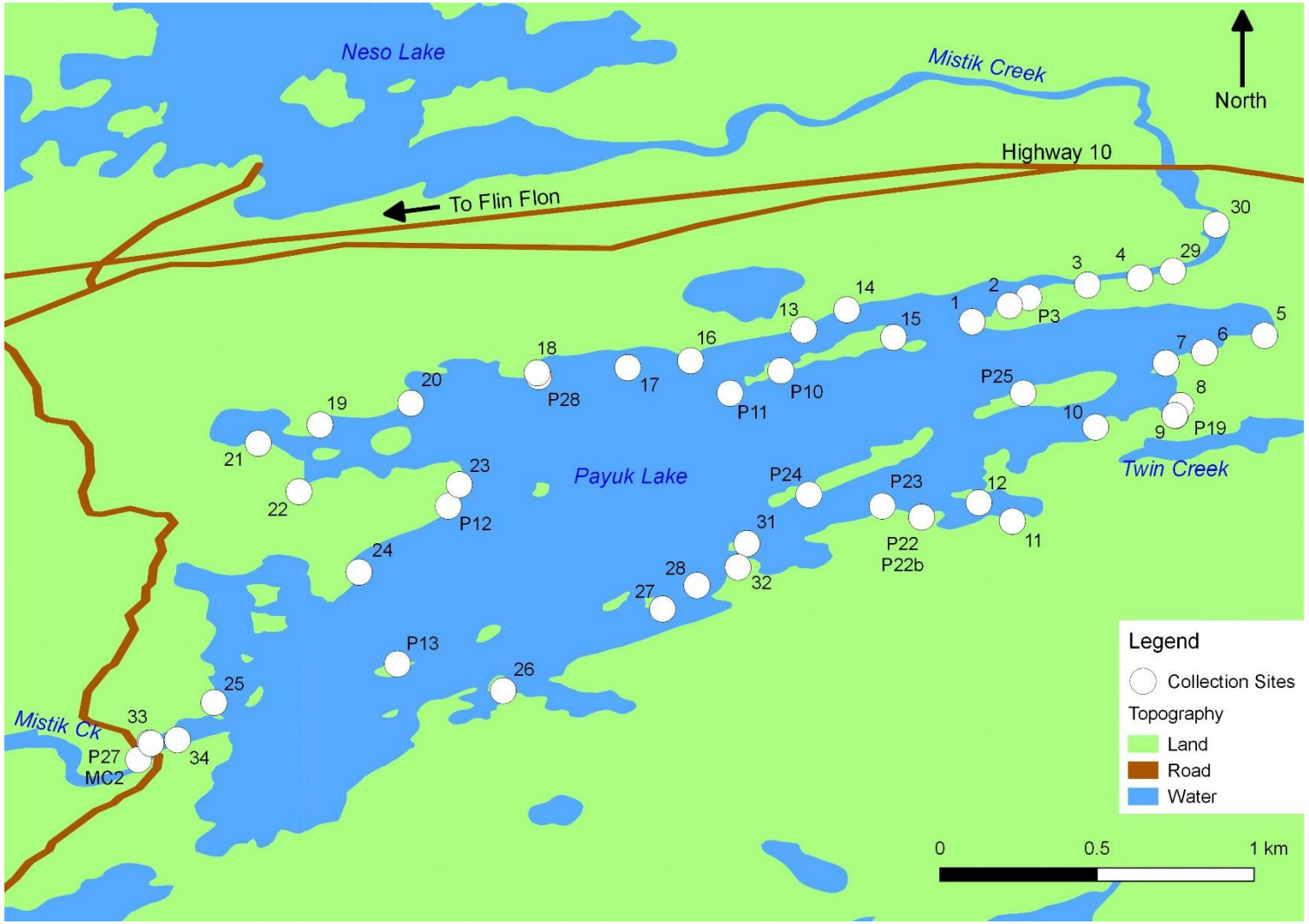

Figure 2.2. Collection sites of *Dermatocarpon luridum* thalli from Payuk Lake, Manitoba. Numbers without letters represent samples collected in this study. Numbers with letters represent samples collected in Fontaine et al. (2013) where P is Payuk, MC is Mistik Creek. Each number in this study represents collections in triplicate (see Table 2.2). Map was produced using Quantum GIS v. 2.18 Las Palmas (Quantum GIS Development Team 2017), with base maps downloaded from CanVec (GeoGratis, Natural Resources Canada).

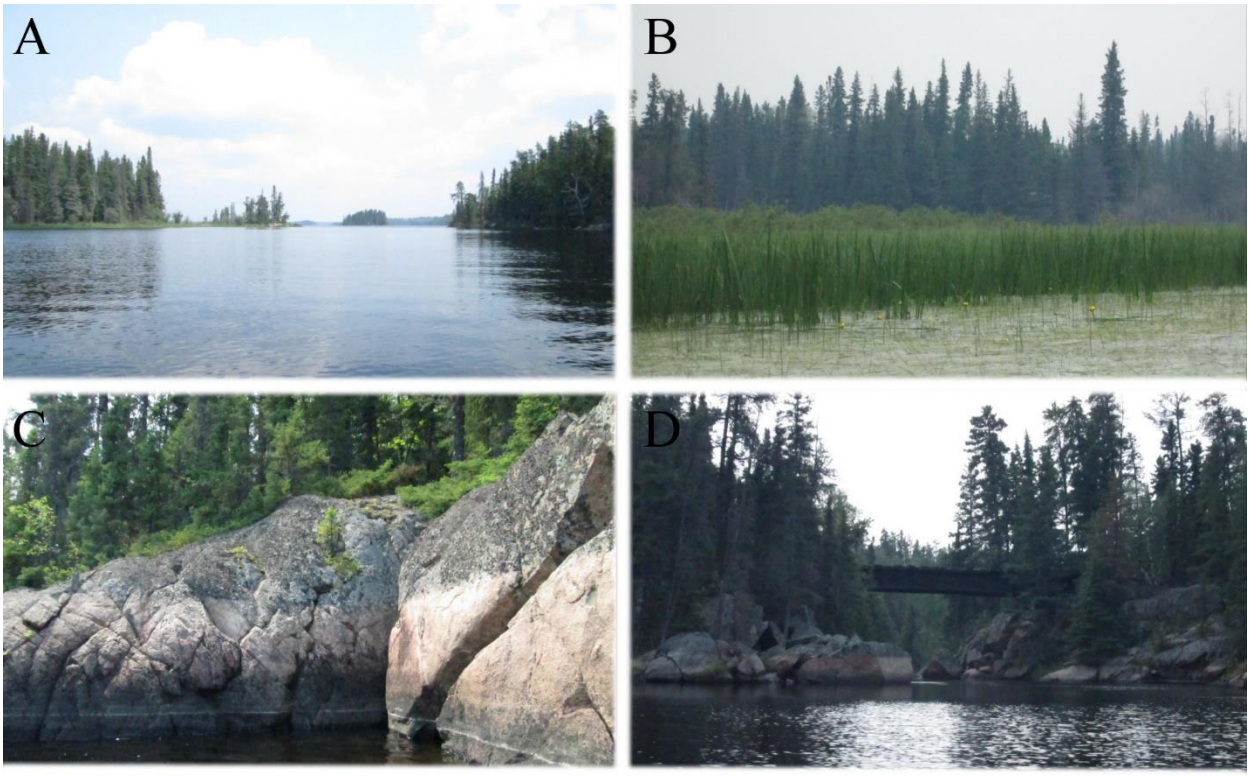

Figure 2.3. Photos of collection sites around Payuk Lake, showing A: Mistik Creek inflow; B: Twin Creek inflow; C: Middle region with high rock faces; D. Mistik Creek outflow.

2.3 Algal Culturing

Six thallus samples were randomly chosen for the verification of photobiont identity using a random number table with numbers between 1 and 102. Ten mg of crushed lichen tissue (see section 2.4) was placed into a clean 1.5 mL Eppendorf tube. The photobiont was isolated from the rest of the lichen thallus using the Percoll method (Gasulla et al. 2010), with modifications. Briefly, the powder was resuspended in 200 µL sterile isotonic buffer (0.3M sorbitol in 50 mM HEPES, pH 7.5), which was then loaded onto 1.5 mL of 80% Percoll in isotonic buffer in a 10 mL centrifuge tube and spun in a Sorvall Legend X1R centrifuge (Thermo Fisher Scientific, Waltham, MA, USA) at 5000 rpm for 20 min. A total of 400 µL of the green layer (just below the surface of the supernatant) was pipetted into a new 10 mL centrifuge tube and diluted two-fold in sterile distilled water. The samples were then centrifuged at 2000 rpm for 10 mins. The supernatant was discarded and the pellet was resuspended in 2 mL of sterile distilled water and 1 drop of Tween 20. The samples were subjected to sonification using a Fisher Vortex Genie 2 (Thermo Fisher Scientific, Waltham, MA, USA) five times. Each sonification round consisted of 1 min steady sonification at 40 KHz, followed by centrifugation at 5000 rpm for 5 mins. Finally, the samples were resuspended in 1 mL of sterile distilled water in a 1.5 mL Eppendorf tube. Isolation of free-living algae followed the same protocol, though culturing differed from that of the photobiont.

The photobiont samples were then streaked onto slants containing standard BBM media (Bischoff and Bold 1963; Appendix B) on 2% agar. The cultures were placed in a 20 °C incubator and left to grow for one month. The cultures were then subcultured by transferring a portion of the single green algal mass from the slants into autoclaved flasks containing liquid BBM media using a flame-sterilised metal rod and incubated at 20 °C.

The free-living algal samples were directly inoculated into flasks containing liquid BBM media and incubated at 20 °C under 24 hour light conditions. The algal cultures were examined after 10 months using a Zeiss AxioImager.Z1 Microscope (Carl Zeiss Microscopy, LLC, Thornwood, NY, USA) under bright field (BF) and differential interference contrast (DIC). Photographs of each algal specimen were taken with a Zeiss AxioCam 105 Colour Camera (Carl Zeiss Microscopy, LLC, Thornwood, NY, USA). Algal specimens were identified to genus using Wehr and Sheath (2003).

2.4 DNA extraction, PCR, and sequencing

The thallus samples of *D. luridum* that were placed in the 1.5 mL Eppendorf tubes (approximately < 20 mg dry weight) were crushed to a powder in liquid nitrogen. DNA extraction of the lichen thallus using 10 mg of crushed tissue was performed using DNeasy Plant Mini Kit (Qiagen Inc, Toronto, Ontario), following the manufacturer's protocol. Polymerase chain reaction (PCR) was performed to amplify two algal loci. The algal internal transcribed spacer ribosomal DNA (ITS rDNA) region, already sequenced for *Diplosphaera chodatii* in a different study, followed the procedure by Fontaine et al. (2012). The algal-specific forward primer was STICHO-ITS-F-5' (Table 2.1; Fontaine et al. 2012), and the universal reverse primer was ITS4-3' (Table 2.1; White et al. 1990). Additional algal specific primers located in the 5.8 ribosomal region were designed in this study to troubleshoot difficult sequences (Figure 2.4), using the *Diplosphaera chodatii* specific forward primer Dch-5.8S-F (Table 2.1) and the reverse primer Dch-5.8-R (Table 2.1), along with another *Diplosphaera chodatii* specific ITS reverse primer Dch-ITS-R (Table 2.1). The gene region was amplified in 20 µL (for checking amplification success) and 50 µL (for sequencing preparation) reactions using 1X PCR Buffer (200 mM Tris-HCl, pH 8.4, 500 mM KCl, 2 mM $MgCl_2$; GeneDireX, FroggaBio, Toronto,

Ontario, Canada), 2 Units *Taq* DNA Polymerase (GeneDireX, FroggaBio, Toronto, Ontario, Canada), 200 µM of each dNTP (GeneDireX, FroggaBio, Toronto, Ontario, Canada), 0.5 µM of each of the forward and reverse primers, and 5-25 ng of DNA template. The PCR was performed on a Biometra T-Gradient thermal cycler (Montreal Biotech Inc, Dorval, Quebec, Canada) using an initial 3 mins at 94 °C, followed by 30 cycles of denaturation at 94°C for 1 min, annealing at 58.5 °C for 30 secs, and elongation at 72 °C for 45 secs, and ending with a hold at 6 °C.

The algal β-actin type 1 gene (*Actin*) was used because of its ability to vary within a species due to different intron lengths (Kroken and Taylor 2000; Piercey-Normore 2006; Nelsen and Gargas 2006). Furthermore, it had already been sequenced (Fontaine et al. 2012) in the same algal species, though the intron located at nucleotide site 738 (Kroken and Taylor 2000) was not sequenced, providing an opportunity for adding previous data to this study to address questions on temporal changes in population structure. The forward and reverse primers were Dch-βactin-F and Dch-βactin-R (Table 2.1) respectively, both of which were newly designed in this study using *D. chodatii* β-actin sequences from GenBank (Figure 2.4). The gene region was amplified in 20µL and 50µL reactions using 1X PCR Buffer (200 mM Tris-HCl, pH 8.4, 500 mM KCl, 2 mM $MgCl_2$; GeneDireX, FroggaBio, Toronto, Ontario, Canada), 2.5 Units *Taq* DNA Polymerase (GeneDireX, FroggaBio, Toronto, Ontario, Canada), 200 µM of each dNTP (GeneDireX, FroggaBio, Toronto, Ontario, Canada), 0.5 µM of each of the forward and reverse primers, and 5-25 ng of DNA template. The PCR was performed on a Biometra T-Gradient thermal cycler (Montreal Biotech Inc, Dorval, Quebec, Canada) using an initial 3 mins at 94 °C, followed by a touchdown sequence of 2 cycles of denaturation at 94°C for 1 min, annealing at 54 °C for 30 secs, and elongation at 72 °C for 30 secs; 2 cycles of denaturation at 94°C for 1 min, annealing at 53 °C for 30 secs, and elongation at 72 °C for 30 secs; then 26 cycles of denaturation at 94°C for

1 min, annealing at 52 °C for 30 secs, and elongation at 72 °C for 30 secs; and ending with a hold at 6 °C.

The PCR product was prepared for DNA sequencing by precipitation using ethanol and cleaned by excising the DNA bands from gel electrophoresis on a 1% agarose gel in 1X Tris-borate (TBE) buffer, followed by centrifugation in spin columns using the Wizard SV-Gel and PCR Clean-up kit (Promega, Madison, Wisconsin, USA) following manufacturer's directions. Resuspension of the cleaned PCR product was performed in 32 μL of autoclaved sterile distilled water instead of 50 μL as recommended by the manufacturer. DNA sequencing was performed initially using a cycle-sequence reaction in Big Dye v.3.1 (Applied Biosystems, Foster City, CA) and cleaned using ethylenediaminetetraacetic acid (EDTA), following the manufacturer's instructions. The product was resuspended in Hi-Di formamide (Applied Biosystems, Foster City, CA) and sequenced using a 3130 Genetic Analyzer (Applied Biosystems, Foster City, CA). The sequences were manually cleaned in ChromasPro v2 (Technelysium Pty Ltd, South Brisbane, Australia) and aligned in MEGA 6 (Tamura et al. 2013). The sequences were then submitted to GenBank, adding an additional 80 ITS rDNA and 52 β-actin sequences of *Diplosphaera chodatii* to their database (Table 2.2). Twenty-four previously published sequences from collections in the summer of 2010 (Fontaine et al. 2013) were obtained from GenBank, along with one sample from the University of Texas and one sample of *Trebouxia jamesii*, to be used as baseline data for the study and in phylogenetic analyses and aligned with the study sequences (Table 2.3).

Table 2.1. Internal transcribed spacer (ITS) region of rDNA and β-actin primers used for polymerase chain reaction (PCR) and DNA sequencing.

Primer Name	Sequence	Gene	Use	Source
STICHO-ITS-F-5'	5'-GGATCATTGAATCTATCAACAAC-3'	ITS rDNA	PCR and Sequencing	Fontaine et al. (2012)
Dch-ITS-R	5'-TGGTGGCCGAGCGGACGATT-3'	ITS rDNA	PCR and Sequencing	This study
ITS4-3'	5'-TCCTCCGCTTATTGATATGC-3'	ITS rDNA	PCR and Sequencing	White et al. (1990)
Dch-5.8S-F-5'	5'-CGGATATCTTGGCTCCCGCAT-3'	5.8S Ribosomal region in ITS	Sequencing	This study
Dch-5.8S-R-3'	5'-ACCGAAGTCTCGAGCGCAATA-3'	5.8S Ribosomal region in ITS	Sequencing	This study
Dch-βactin-F	5'-CAACACAGCGAGTGCCCTAT-3'	β-actin protein	PCR and Sequencing	This study
Dch-βactin-R	5'-TGTACCGCACCTGTAAGCGC-3'	β-actin protein	PCR and Sequencing	This study

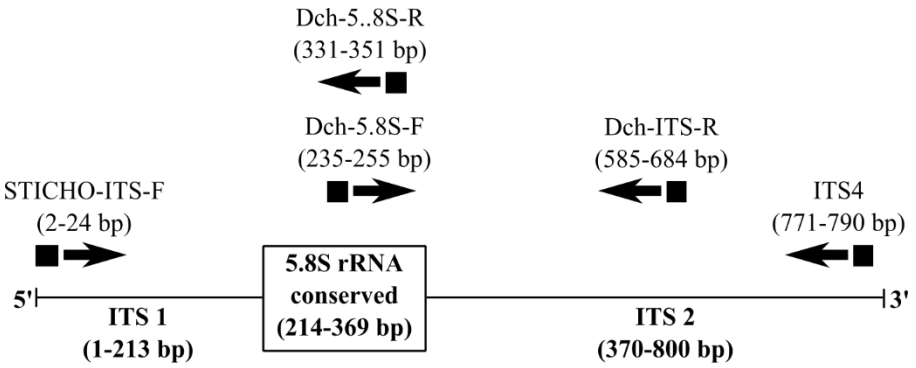

ITS rDNA Gene Region

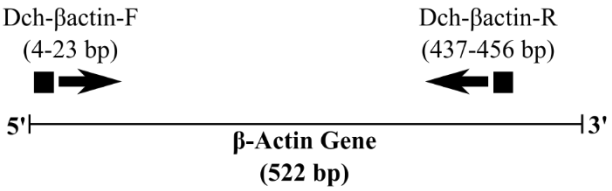

β-Actin Gene Region

Figure 2.4. Primer map showing the relative binding locations and direction of amplification of internal transcribed spacer (ITS) region of the rDNA gene and β-actin protein gene primers.

Table 2.2. Collection sites, photobiont samples, and sequence accession numbers used in this study. Collection sites 1-34 and from Whiteshell Provincial Park (WS) were sampled in triplicate from this study. Collection sites with a letter before the number were taken from Fontaine et al. (2013). Photobiont samples D (*Dermatocarpon luridum* from Payuk Lake) and WS (*De. luridum* from Whiteshell) were collected and sequenced in this study, photobiont samples with P (from Payuk Lake) and MC (Mistik Creek) were collected from Fontaine et al. (2013). Latitude and longitude are included. GenBank Accession Numbers are indicated and a dash refers to samples that were not sequenced. Collection site numbers correspond with those in Figure 2.2.

	Latitude	Longitude		GenBank Accession Number	
Collection Site	(Decimal degrees)	(Decimal degrees)	Sample	ITS	Actin
Whiteshell	49.8095	-95.2384	WS1	MF124964	-
Whiteshell	49.8095	-95.2384	WS2	-	MF124892
Whiteshell	49.8095	-95.2384	WS3	-	-
1	54.6502	-101.5122	D1	MF124939	MF124907
1	54.6502	-101.5122	D2	MF124949	
1	54.6502	-101.5122	D3	MF124954	-
2	54.6510	-101.5104	D4	-	MF124896
2	54.6510	-101.5104	D5	MF124961	-
2	54.6510	-101.5104	D6	-	-
3	54.6520	-101.5065	D7	MF124962	-
3	54.6520	-101.5065	D8	-	-
3	54.6520	-101.5065	D9	MF124963	-
4	54.6524	-101.5040	D10	MF124940	-
4	54.6524	-101.5040	D11	MF124941	MF124893
4	54.6524	-101.5040	D12	MF124942	-
5	54.6495	-101.4978	D13	MF124943	-
5	54.6495	-101.4978	D14	MF124944	MF124906
5	54.6495	-101.4978	D15	-	-
6	54.6487	-101.5008	D16	MF124945	MF124912
6	54.6487	-101.5008	D16b	MF124946	-
6	54.6487	-101.5008	D17	MF124947	-
6	54.6487	-101.5008	D18	MF124972	MF124905
7	54.6482	-101.5027	D19	MF124948	MF124910
7	54.6482	-101.5027	D20	-	MF124909
7	54.6482	-101.5027	D21	MF124950	-
8	54.6461	-101.5020	D22	-	MF124908
8	54.6461	-101.5020	D23	MF124951	-
8	54.6461	-101.5020	D24	MF124952	-
9	54.6456	-101.5022	D25	MF124953	MF124894
9	54.6456	-101.5022	D26	-	-
9	54.6456	-101.5022	D27	MF125004	-

Table 2.2. continued.

Collection Site	Latitude (Decimal degrees)	Longitude (Decimal degrees)	Sample	GenBank Accession Number ITS	Actin
10	54.6450	-101.5061	D28	-	MF124937
10	54.6450	-101.5061	D29	-	-
10	54.6450	-101.5061	D30	-	-
11	54.6404	-101.5103	D31	MF124999	MF124903
11	54.6404	-101.5103	D32	-	-
11	54.6404	-101.5103	D33	MF124998	MF124895
12	54.6413	-101.5119	D34	MF124955	-
12	54.6413	-101.5119	D35	MF124956	-
12	54.6413	-101.5119	D36	MF124957	MF124897
13	54.6498	-101.5205	D37	MF124967	-
13	54.6498	-101.5205	D38	MF124966	-
13	54.6498	-101.5205	D39	MF125003	MF124911
14	54.6508	-101.5184	D40	MF124958	-
14	54.6508	-101.5184	D41	MF124959	MF124933
14	54.6508	-101.5184	D42	MF124960	MF124931
15	54.6494	-101.5161	D43	MF124970	-
15	54.6494	-101.5161	D44	MF124969	-
15	54.6494	-101.5161	D45	-	-
16	54.6483	-101.5261	D46	MF124974	-
16	54.6483	-101.5261	D47	-	-
16	54.6483	-101.5261	D48	-	-
17	54.6479	-101.5292	D49	-	MF124914
17	54.6479	-101.5292	D50	MF124976	MF124913
17	54.6479	-101.5292	D51	-	-
18	54.6477	-101.5337	D52	MF124975	-
18	54.6477	-101.5337	D53	MF124968	MF124899
18	54.6477	-101.5337	D54	MF124977	-
19	54.6451	-101.5444	D55	MF124979	MF124898
19	54.6451	-101.5444	D56	MF124978	MF124916
19	54.6451	-101.5444	D57	MF124981	MF124919
20	54.6462	-101.5399	D58	MF124980	MF124915
20	54.6462	-101.5399	D59	-	-
20	54.6462	-101.5399	D60	MF124982	-
21	54.6442	-101.5474	D61	-	MF124900
21	54.6442	-101.5474	D62	-	-
21	54.6442	-101.5474	D63	-	MF124918

Table 2.2. continued.

Collection Site	Latitude (Decimal degrees)	Longitude (Decimal degrees)	Sample	GenBank Accession Number ITS	Actin
22	54.6418	-101.5454	D64	MF1249783	-
22	54.6418	-101.5454	D65	-	MF124917
22	54.6418	-101.5454	D66	-	-
23	54.6422	-101.5375	D67	-	MF124924
23	54.6422	-101.5375	D68	-	-
23	54.6422	-101.5375	D69	-	MF124901
24	54.6379	-101.5425	D70	-	-
24	54.6379	-101.5425	D71	MF124984	MF124922
24	54.6379	-101.5425	D72	-	MF124921
25	54.6314	-101.5496	D73	MF124985	MF124920
25	54.6314	-101.5496	D74	-	-
25	54.6314	-101.5496	D75	MF124965	MF124923
26	54.6320	-101.5354	D76	MF124987	MF124935
26	54.6320	-101.5354	D77	MF124986	-
26	54.6320	-101.5354	D78	-	-
27	54.6360	-101.5275	D79	-	-
27	54.6360	-101.5275	D80	-	-
27	54.6360	-101.5275	D81	MF124989	-
28	54.6372	-101.5258	D82	MF124988	MF124926
28	54.6372	-101.5258	D83	-	MF124925
28	54.6372	-101.5258	D84	-	-
29	54.6527	-101.5023	D85	MF124994	-
29	54.6527	-101.5023	D86	-	-
29	54.6527	-101.5023	D87	MF124993	MF124936
30	54.6550	-101.5002	D88	MF124992	MF124927
30	54.6550	-101.5002	D89	MF124991	-
30	54.6550	-101.5002	D90	MF124990	-
31	54.6393	-101.5233	D91	MF125001	MF124938
31	54.6393	-101.5233	D92	MF125000	MF124934
31	54.6393	-101.5233	D93	-	MF124932
32	54.6381	-101.5238	D94	-	-
32	54.6381	-101.5238	D95	MF124973	-
32	54.6381	-101.5238	D96	MF125002	MF124904
33	54.6294	-101.5527	D97	MF124971	MF124930
33	54.6294	-101.5527	D98	MF124997	MF124929
33	54.6294	-101.5527	D99	-	MF124928

Table 2.2. continued.

Collection Site	Latitude (Decimal degrees)	Longitude (Decimal degrees)	Sample	GenBank Accession Number	
				ITS	Actin
34	54.6296	-101.5514	D100	-	MF124902
34	54.6296	-101.5514	D101	MF124996	-
34	54.6296	-101.5514	D102	MF124995	-
P3	54.6514	-101.5094	P3	KF317571.1	KF317550.1
P10	54.6478	-101.5217	P10	KF317572.1	KF317551.1
P11	54.6467	-101.5242	P11	KF317573.1	-
P12	54.6411	-101.5381	P12	KF317574.1	-
P13	54.6333	-101.5406	P13	KF317575.1	-
P19	54.6456	-101.5022	P19	JX645008.1	KF317552.1
P22	54.6406	-101.5147	P22	KF317576.1	-
P22b	54.6406	-101.5147	P22b	JX645017.1	-
P23	54.6411	-101.5167	P23	JX645018.1	KF317553.1
P24	54.6417	-101.5203	P24	KF317577.1	-
P25	54.6467	-101.5097	P25	KF317578.1	-
P27	54.6294	-101.5528	P27	KF317579.1	-
P28	54.6475	-101.5336	P28	JX645015.1	KF317554.1
MC2	54.6286	-101.5533	MC2	KF317580.1	-

Table 2.3. Additional sequences collected from Naosap Lake (Na), Nisto Lake (Ni) and Neso Lake (Ne) further upstream from Payuk Lake (from Fontaine et al. 2013; Figure 2.1) and their accession numbers that were used in phylogenetic analyses. AV037 was a *Trebouxia jamesii* sequence used as an outgroup. UTEX_1177 was a known sample of *Diplosphaera chodatii* from the University of Texas.

	GenBank Accession Number	
Sample	ITS	Actin
AV037	KT819982.1	-
UTEX_1177	HQ129931	-
Na1	KF317592.1	KF317563.1
Na3	KF317593.1	-
Na7	KF317594.1	-
Na11	KF317595.1	-
Na15	-	KF317564.1
Na16	KF317596.1	-
Na20	KF317597.1	-
Na22	-	KF317565.1
Ne1	KF317581.1	-
Ne3	KF317582.1	-
Ne4	KF317583.1	KF317555.1
Ne6	KF317584.1	KF317556.1
Ne10	KF317585.1	-
Ne14	-	KF317557.1
Ne18	-	KF317558.1
Ne23	KF317586.1	KF317559.1
Ne29	-	KF317560.1
Ni1	KF317587.1	-
Ni7	KF317588.1	-
Ni10	-	KF317561.1
Ni15	-	KF317562.1
Ni21	KF317589.1	-
Ni23	KF317590.1	-
Ni30	KF317591.1	-

2.5 GIS Analyses

To obtain the spatial distances between all of the samples, geographic information systems (GIS) were used (Appendix C). Baseline GIS data of Payuk Lake were downloaded from the publically available datasets offered through CanVec (GeoGratis, Natural Resources Canada; https://www.nrcan.gc.ca/earth-sciences/geography/topographic-information/free-data-geogratis/11042, accessed April 2015). A digital elevation model (DEM) of Payuk Lake and surrounding areas was provided by Garry Lux from the Manitoba Government in Flin Flon, Manitoba. All of the data were defined to be in the NAD83 UTM 14N projection.

The most basic measurement of spatial distance is that of "as-the-crow-flies", or the Euclidean straight line distance between samples. To create a distance matrix to be used in Mantel's test for spatial autocorrelation, the sample locations were imported into QGIS 2.18.2 Las Palmas (QGIS Core Development Team 2017) as a .csv file and converted to a point feature. The Euclidean distance between each of the samples relative to all of the other samples was calculated using the "distance matrix" tool within the "analysis" toolset of vector analysis, using a linear matrix. The results were exported as an Excel table showing all of the pairwise Euclidean distances between each of the samples.

A second method to measure the distances between two sample sites is along the shoreline, which takes into account the curvature of the bays within the lake (as in the perimeter of the lake). To obtain a distance matrix outlining the shoreline distances between all of the samples for use in Mantel's test (see *Data Analysis*), the lake feature was converted from a polygon to a polyline feature. The locations of the samples were snapped to the shoreline polyline feature. Shortest path analysis was performed using the "v.net.allpairs" command within the QGIS GRASS 7 algorithms in the toolbox to obtain all of the shortest pairwise distances

between all samples following the shoreline. The results were exported as an Excel table showing all of the pairwise shoreline distances between each of the samples.

Since water moves through the lake as runoff and through main streams, a hydrological model showing the net flow accumulation of water through the lake was generated. Since water flows along the path of least resistance (i.e. downhill or through a watershed), the distance between all of the samples along this flow accumulation "network" can then be determined for use in Mantel's test. The following procedures were performed using the "Hydrology" toolset within the "Spatial Analyst" toolbox in ArcGIS 10.2 (ESRI 2013). Using the DEM of Payuk Lake, a flow direction layer of water through the lake was created using the "Flow Direction" tool. Sinks (where water accumulates due to no net flow in any direction) were identified using the "sinks" tool within and removed using the "fill" tool. The flow direction was recalculated once the sinks were removed. Next, a flow accumulation network was created using the "flow accumulation" tool. As water moves within a system, net accumulation of water occurs in the direction of flow within the system. Downstream has a higher net accumulation than upstream due to runoff and stream flow. To create the stream network used in the calculation of distance in the network, flow accumulation was converted to a stream order raster using the "stream order" tool and transformed into a feature class using the "stream to feature" tool. Values of flow accumulation were than extracted from the accumulation raster and added to the stream order feature using the "stream link" tool. The flow lengths (of the network) upstream and downstream were calculated using the "flow length" tool, with the upstream and downstream parameter selected respectively. Raster values (indicating the lengths) were extracted using the "extract values to points" tool within the "Extraction" toolset and exported into Excel. Using the baseline data of Payuk Lake, Mistik and Twin creeks polylines were merged together into a single

polyline using the Editor tool extension and added to the flow accumulation polyline feature. The sample locations were then snapped to the closest spot along the new stream polyline using the "snap" tool within the "editing tools" toolset. The raster values of the flow accumulation underneath the samples along the network were extracted (the higher the number, the farther downstream the sample was located) using the tool "extract values by points" within the "extraction" toolset. Next, the net flow accumulation polyline feature was imported into QGIS 2.18.2, where the Euclidean distance of the samples along the net flow accumulation network was calculated using the "distance matrix" tool within the "analysis" toolset of vector analysis, using a linear matrix. Lastly, a path distance (equivalent to shoreline distance) was calculated between all of the samples along the flow accumulation network using the same steps to obtain the shoreline distance. The pairwise distances matrices were then exported into Excel for use in Mantel's test.

Mantel's test determines if there is isolation by distance between locations in a geographic area. The farther apart the locations, the less likely they will be similar to each other. Similarly, this test can be applied to test for similarity between samples collected since closely related samples would occur closer together. Since a watershed behaves differently than static geographic locations, four pairwise measures of distance were defined and calculated between the collected samples: the Euclidean distances within Payuk Lake; the distance along the shoreline of the lake to account for topography; Euclidean distances along a net flow accumulation network; and a path distance along a net flow accumulation network (taking into account water flow direction).

2.6 Data Analysis

To ensure pairwise comparison of base pairs for haplotype analyses with all samples (those sequenced in this study and acquired through GenBank), the sequences were trimmed to be all the same length. A combined concatenated ITS/β-actin alignment was also created using the trimmed sequences from both to determine if unresolved nodes in the single-gene phylogenies could be resolved (Gontcharov et al. 2004).

To determine the relationship of the 102 *Diplosphaera chodatii* samples with each other, along with previous known samples collected from Payuk Lake, maximum likelihood (ML) trees of the ITS rDNA, β-actin, and combined ITS rDNA/ β-actin alignments were produced in MEGA 6 (Tamura et al. 2013), using all sites with a Kimura 2-parameter model and 1000 bootstrap permutations. Maximum likelihood was used instead of neighbour-joining due to its higher robustness in dealing with variance caused by small or varying sample sizes (Will 2012). Due to the lack of resolution in the ITS rDNA tree, the ITS rDNA alignment was split into the ITS1 region with partial 5.8S ribosomal DNA gene (1-315bp) and the ITS2 region with partial 5.8S ribosomal DNA gene (316-607bp). Also, due to lack of resolution, the combined ITS rDNA /β-actin alignment will not be used in subsequent analyses. Pairwise genetic distances for use in Mantel's test were computed for each of the ITS1, ITS2, and β-actin in MEGA 6 using the Kimura 2-parameter model, 1000 bootstrap permutations, complete deletion of missing base pairs, and using transversions and transitions. The trees were visualised in FigTree v1.4.3 (Rambout 2016).

The ITS1, ITS2, and β-actin sequence alignments were exported as a phylip file and were assessed in TCS 1.21 (Clement et al. 2000), using the 5^{th} state criterion and 95% probability of parsimony (Fontaine et al. 2013), for the number of haplotypes present and haplotype networks

(to assess the relatedness of each sequence with all others). Each single change (base pair change, insertion, or deletion) from the first assessed sequence was considered to be a new haplotype and so on.

Intensive sampling is required to determine if there are spatial patterns in the distribution of photobionts and their haplotypes (Opanowicz and Grube 2004), as well as determine whether all of the genetic variation was accounted for (Werth 2011). Rarefaction analyses were performed in R using the "rarefy" function from the "vegan" package on the ITS1, ITS2, and β-actin genes to determine if all of the genetic variation was sampled within Payuk Lake (Werth 2011). The haplotype network of each of the ITS1, ITS2, and β-actin genes were then mapped in QGIS to assess the distribution of genetic variation around Payuk Lake.

To determine if there is population structure and gene flow of lichenised *D chodatii* within Payuk Lake, Analysis of Molecular Variance (AMOVA) was used (Excoffier et al. 1992). However, in order to determine population structure, populations must be defined. Populations within Payuk Lake were defined based on ecological and geological hypotheses according to direction of water movement within the lake (Figure 2.5). The first hypothesis (Inflow-Outflow-Bay; Figure 2.5A) subdivides the lake according to an inflow region, and outflow region, and an isolated bay region. Samples collected within those regions are classified as a single population. The second hypothesis (Bay Topography; Figure 2.5 B) subdivides the lake based on topographical features, with Mistik Creek and Twin Creek as two separate inflow regions, a middle "mixing" region, an isolated bay, and the Mistik Creek outflow. The third hypothesis (Hydrology; Figure 2.5C) subdivides the lake based on the flow of water (which may affect dispersal if *D. chodatii* is dispersed by water), with two inflow regions (Mistik and Twin Creeks), and middle "mixing" region, and the Mistik Creek outflow. The last hypothesis (Wind;

Figure 2.5D), adds an element of predominant wind patterns across the surface of the lake. There are two inflow regions (Mistik and Twin Creek), a wind region that may push surface water against the direction of flow within the middle of the lake (and disperse *D chodatii* if it is wind dispersed), and the Mistik Creek outflow region. GenAlEx v6.501 (Peakall and Smouse 2012; Peakall and Smouse 2006) was used to perform AMOVA, using 999 permutations, and to obtain a PhiPT fixation index (analogous to F_{st} fixation index) to assess gene flow. Since only one lake was being assessed, the number of populations was determined by how Payuk Lake was subdivided (Figure 2.5), and the number of regions was set to one. Mantel's test was also performed to assess gene flow by means of isolation by distance (Mantel 1967) using the genetic distance and geographical distance matrices obtained earlier. Mantel's test was performed in R using the "mantel" function from the "ecodist" package, and 999 Monte Carlo permutations.

Lastly, to determine which definition of "population" for *De. luridum* (and therefore *Di. chodatii*) around Payuk Lake best explained the genetic variation and gene flow within the lake, model selection using a modified Akaike's Information Criterion (AIC; Akaike 1974) was performed using the sum of squares within populations (output from AMOVA) rather than the error sum of squares from a typical analysis of variance. The corrected AIC (AIC_c) was used to assess the best definition since the sample size divided by the number of "model" parameters (number of subdivisions within the lake) was less than 40. Levels of significance for all statistical tests were assessed at $\alpha<0.05$.

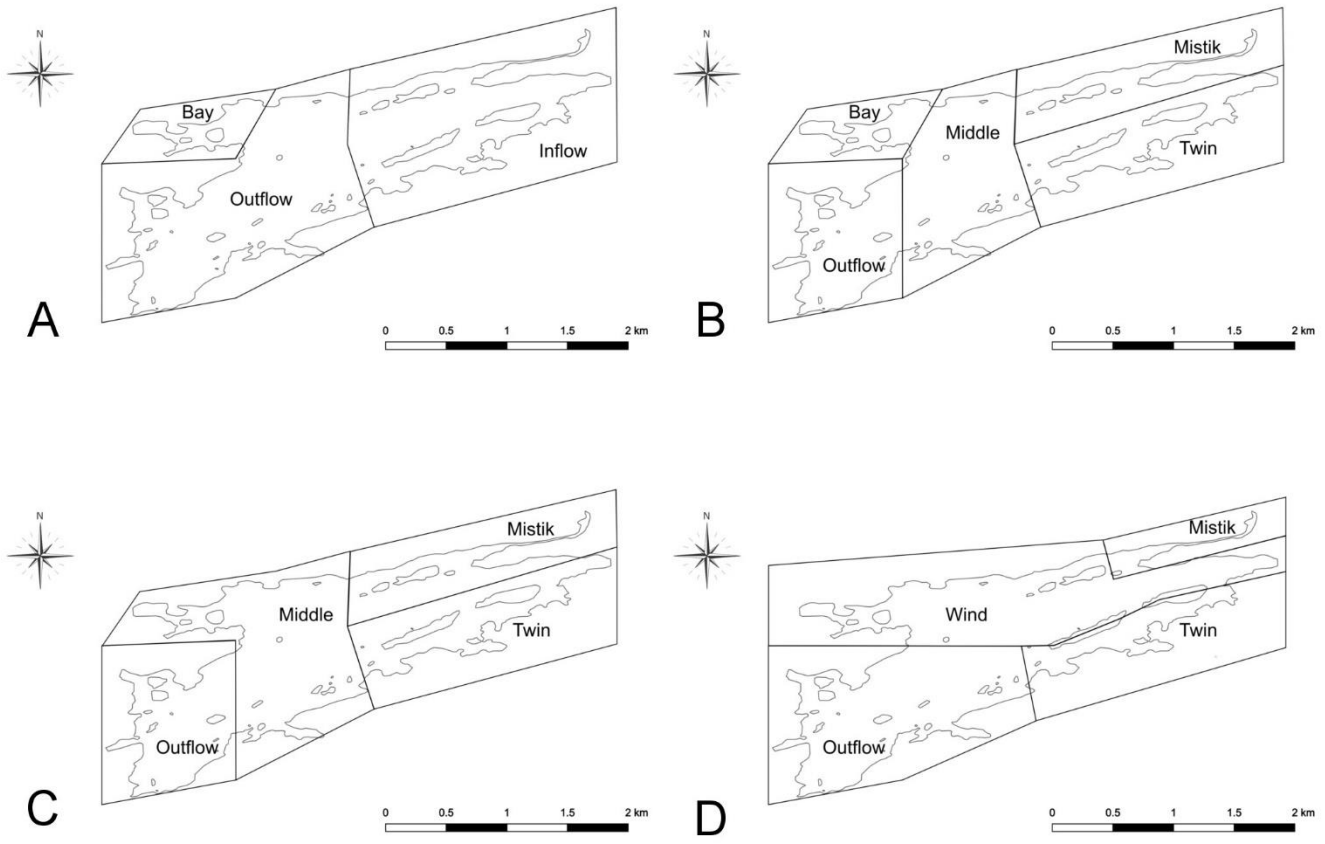

Figure 2.5. Map of Payuk Lake divided into geographic sections to show the definitions of populations for four ecologically meaningful hypotheses used in analyses of population structure and gene flow. A: Inflow-outflow-bay; B: Bay topography; C: Hydrology; D: Wind.

CHAPTER 3 : RESULTS

3.1 Photobiont ITS rDNA Phylogeny

The ITS rDNA phylogeny represents 79 *Diplosphaera chodatii* sequences from thallus samples collected from Payuk Lake, plus an additional sample collected from Whiteshell Provincial Park, and 19 NCBI GenBank Accessions for a total sample size of 99 analysed sequences. The ITS rDNA sequences were 680-805 bp long; trimmed, the final alignment of all the sequences was 607 bp. Overall, the maximum likelihood (ML) tree showed low resolution (bootstrap values < 50% are not shown) among the samples (Figure 3.1), with a transition/transversion (Ts/Tv) ratio of 0.7173, a shared branch lengths (sbl) of 0.72047016, and a log likelihood value of -3433.71. While there was little resolution within the tree, samples collected from Payuk Lake grouped together with *D. chodatii* samples collected farther upstream from other lakes in the watershed (Ne, Ni, Na samples), as well as with a known *D. chodatii* sample (UTEX_1177_HQ129931, University of Texas) obtained from GenBank, which matched the study samples (100% coverage, an E-value of 0.0, and identity of 97%). Furthermore, the Whiteshell sample (WS1) clustered with samples collected from Payuk Lake and others farther upstream, indicating similar ITS rDNA genotypes across vast geographic distances.

The lack of distinct clades within the ITS rDNA maximum likelihood tree may be due to noise in the phylogenetic signal for ITS rDNA, incongruence between the ITS1 and ITS2 regions, or the presence of highly variable indels within the ITS2 region of the ITS rDNA gene (Figure 3.2). Within this region, there are two indel regions. The first occurs at nucleotide positions 399-403 (5bp long) and the second at nucleotide positions 446-456 (11bp long). Within these two indels, at least five variations of base pairs were present in the first indel (none, TGTGT, ACCGGA, GTTGGA, and lacking base pairs except having extra G's at the end) and at

least four were present in the second indel (TACC-----GGCA, --AT-------, ACAT-------, TGTCTCACCGGGA), resulting in tens of combinations of genetic variants and therefore few distinct groups. Evolutionary divergence has been shown to occur in other organisms for the ITS1 and ITS2 (Torres et al.1990), though the ITS1 and ITS2 does exhibit coevolution within taxa (Hausner and Wang 2005). As a result, further analyses were undertaken using the ITS1 and ITS2 regions, each analysed separately, of the ITS rDNA gene. The ITS1 alignment was 315 bp long and the ITS2 alignment was 292 bp long.

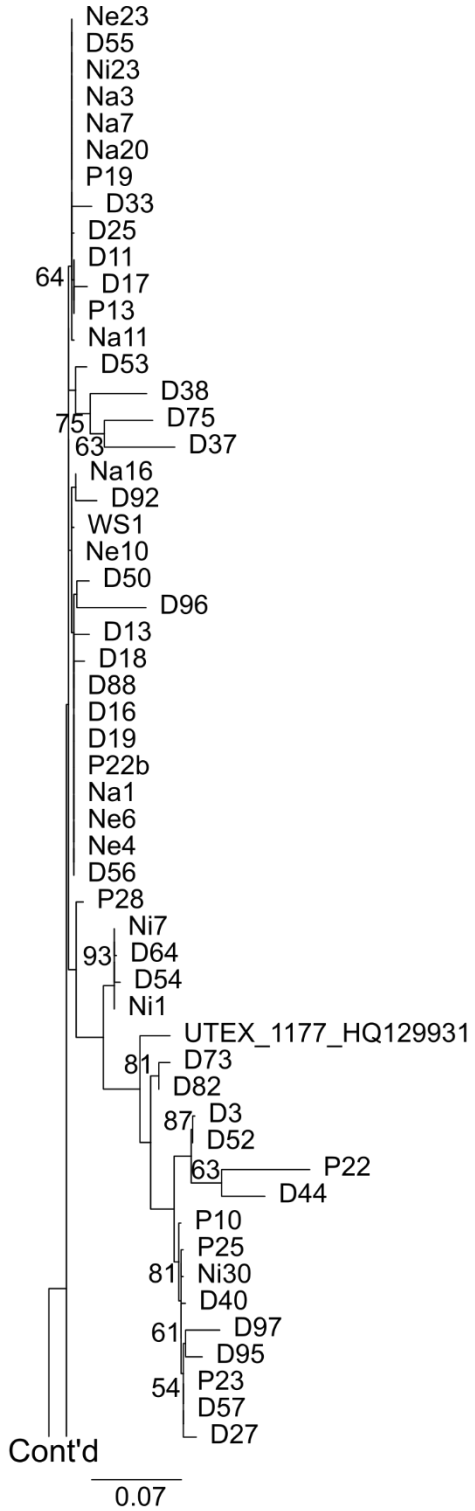
Ne23
D55
Ni23
Na3
Na7
Na20
P19
D33
D25
D11
64
D17
P13
Na11
D53
D38
75
D75
63
D37
Na16
D92
WS1
Ne10
D50
D96
D13
D18
D88
D16
D19
P22b
Na1
Ne6
Ne4
D56
P28
Ni7
93
D64
D54
Ni1
UTEX_1177_HQ129931
81
D73
D82
87
D3
D52
63
P22
D44
P10
P25
81
Ni30
D40
61
D97
D95
54
P23
D57
D27
Cont'd
0.07

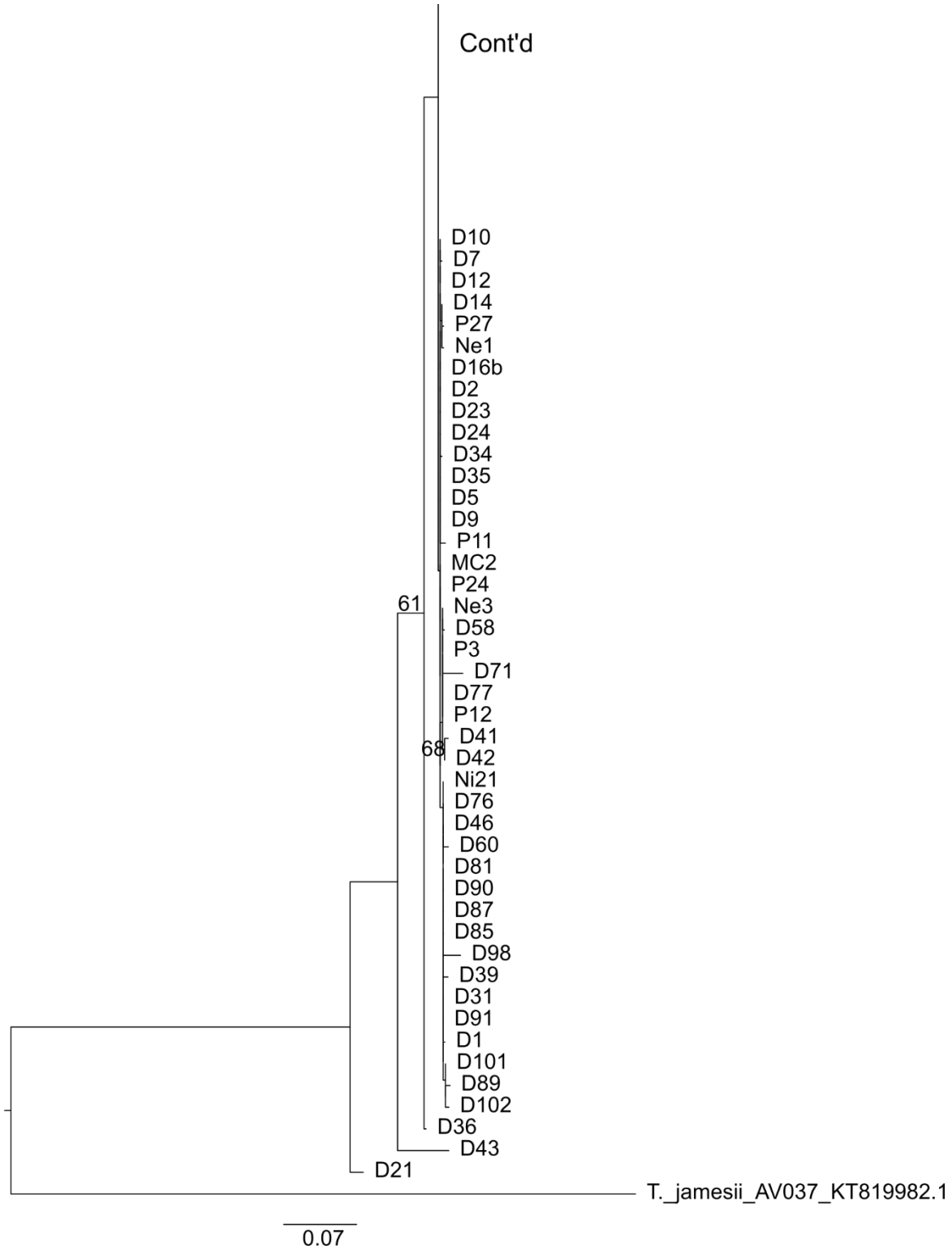

Figure 3.1. Maximum likelihood tree of the full internal transcribed spacer (ITS) region of the rDNA gene within lichenised *Diplosphaera chodatii*. Bootstrap values above 50% are included in the tree. *Trebouxia jamesii* is the assigned outgroup. Letters in the sample names refer to the locations in which they were collected (Table 2.2 and 2.3).

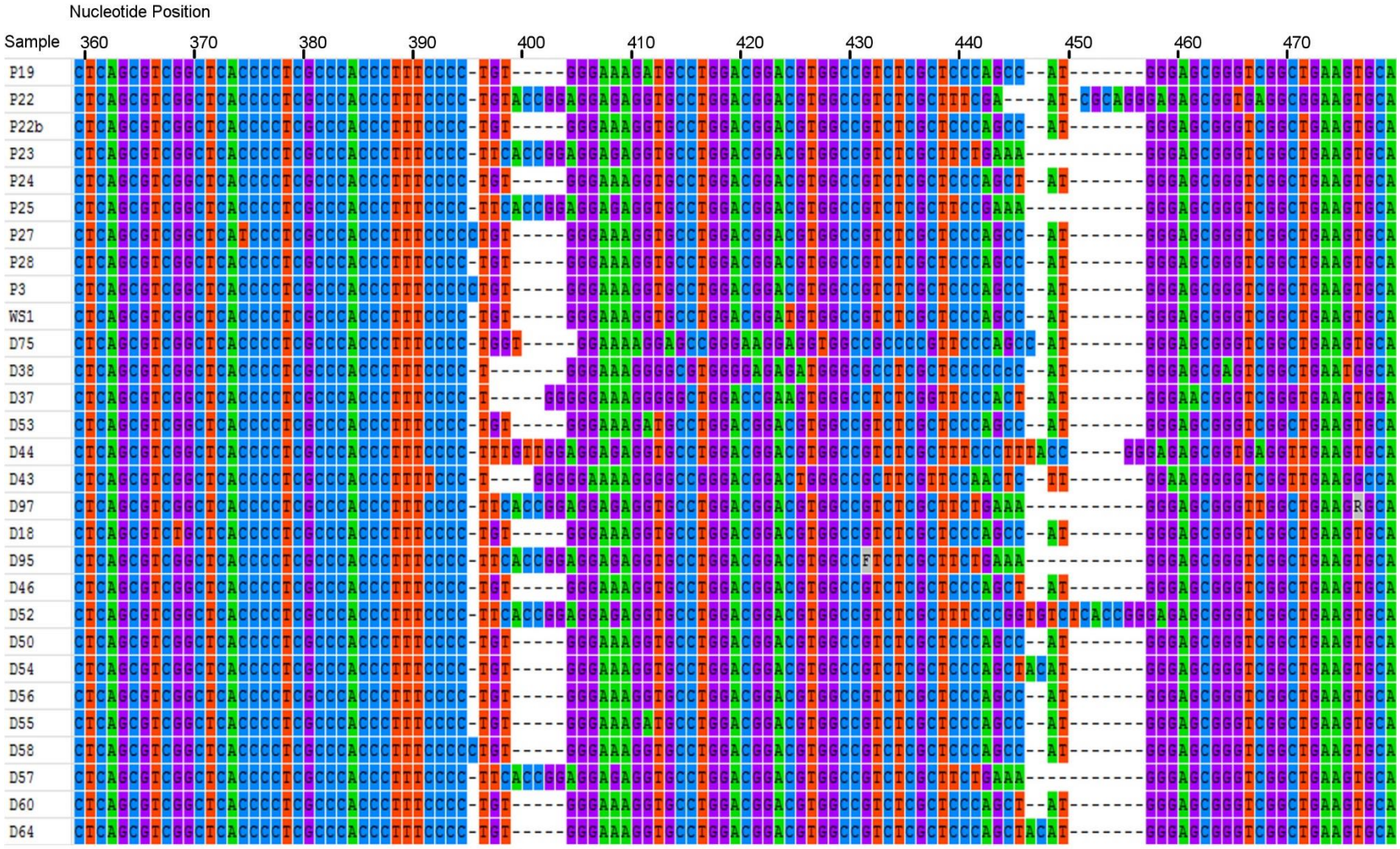

Figure 3.2. Sequence alignment of the internal transcribed spacer region (ITS2) of the rDNA gene within lichenised *Diplosphaera chodatii* showing two indel regions, one on the left (399-403bp) and the other on the right (446-456bp). Samples are indicated to the left and sequence position is indicated at the top of the alignment. See Table 2.2 for sample information.

The ITS1 phylogeny showed more resolution than the full ITS rDNA phylogeny with four main clades (Clades A, B, C, and D; Figure 3.3), and with a Ts/Tv ratio of 0.6647, a sbl value of 0.27028389, and a log likelihood value of -977.59. The clades do not correspond with the geographic locations of the samples within the lake. For example, samples collected from the inflow sources of Payuk Lake (D1-4, D29, D30, and P3; Figure 2.2; Table 2.2) grouped with samples collected in other areas within the lake within clade B. As with the full ITS rDNA phylogeny, the Whiteshell sample also fell in the main clade (Clade B). Samples P22b, D18, and D50 fell outside the main clade due to 5-6 single base pair changes randomly throughout the sequences. Sample D96 was assigned as an internal outgroup due to multiple single base pair changes randomly throughout the sequences. Samples that had most dominant haplotypes (haplotypes 2 and 3; Figure 3.3) resolved broadly into Clade B. Within Clade B, Clade C contained samples (D13, D16, D19, D56, and D88) that contained a single haplotype (haplotype 3), with two unique haplotypes. Clade D showed good bootstrap support and fell within haplotype network N1-A and contained samples with an abundant (but not dominant) haplotype (haplotype 11), with one sample containing a unique haplotype in haplotype network N4.

The ITS2 phylogeny showed two clades (A and B), and several samples outside of the clades (Figure 3.4), with a Ts/Tv ratio of 0.6707, a sbl value of 1.2677250, and a log likelihood value of -2036.98. Again, the Whiteshell sample falls within the main clade with samples collected from Payuk Lake. There is low resolution within clade A (most bootstrap values are less than 50%) but 5 samples (D21, D43, D38, D37, D75) have long branches indicating many nucleotide changes due to the presence of 4 bp in indel 1 and nothing in indel 2, with additional single base pair changes randomly throughout the sequences. These samples were, for the most part, located on the northern shore of Payuk Lake. The samples that have 74% bootstrap support

(D95 and D97) were found on the southern shore, close to the outflow. Haplotypes from the *Di. chodatii* samples did fall into broad clades (Figure 3.4). Clade A contained samples of the most dominant haplotypes 2 and 29, while Clade B consisted of unique haplotypes. Furthermore, samples from Clade A were also found within the haplotype network N1 (Figure 3.4). Haplotype networks N2, N3, and N4 were not resolved within the ML phylogeny. Within Clade A, two subgroups contained only a single haplotype (haplotype 3 with 63% bootstrap support and haplotype 32 with 62% bootstrap support).

Within the ITS1 and ITS2 phylogenies, samples D73 and D82 always occurred together, with strong bootstrap support (> 80%). These samples are found on the southern shore of Payuk Lake, towards the outflow region.

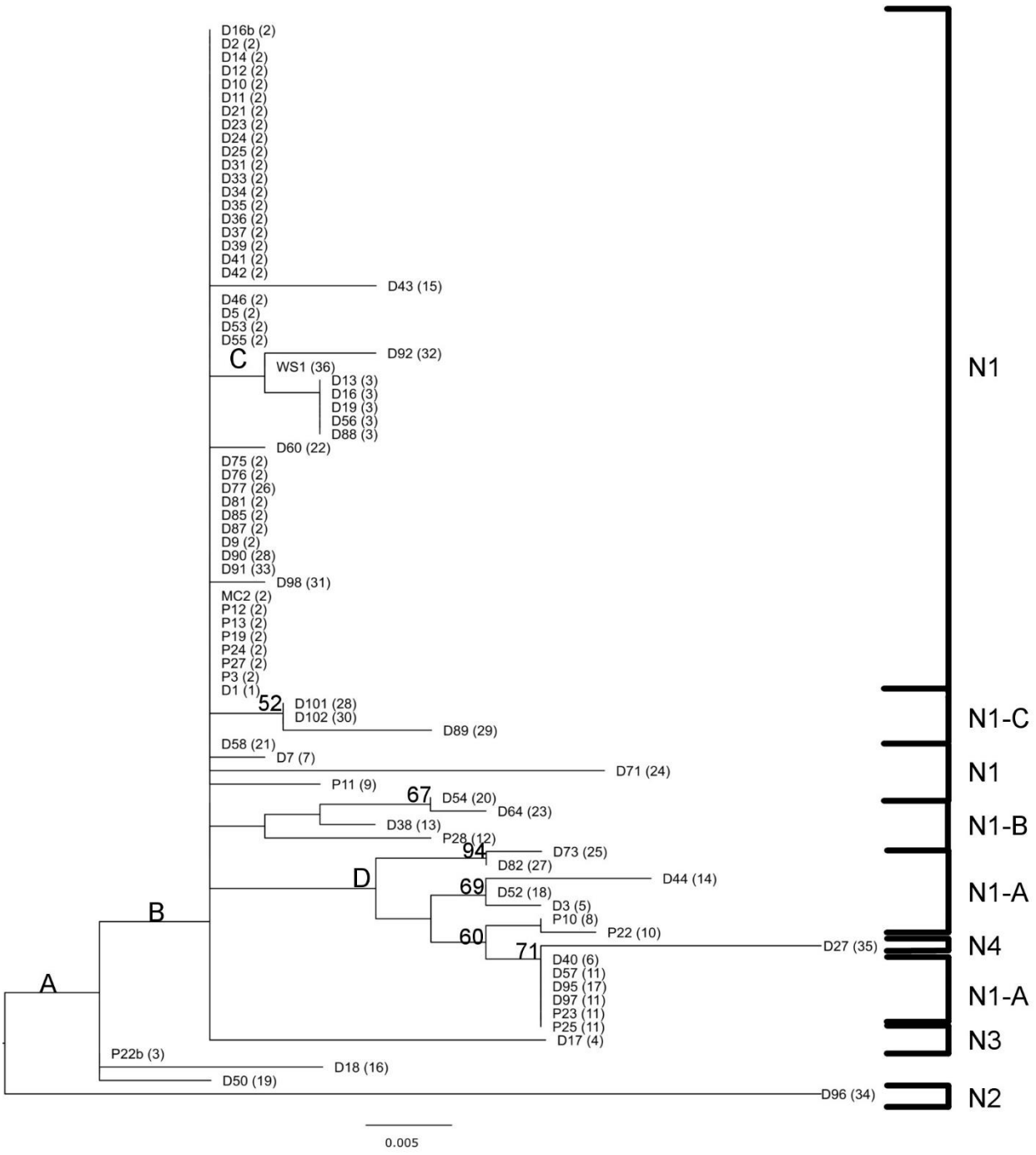

Figure 3.3. Maximum likelihood tree of the internal transcribed spacer (ITS1) region of the rDNA gene within lichenised *Diplosphaera chodatii*. Letters A-D represent clades. Bootstrap values above 50% are included. Letters before the sample numbers represent collection locations (Table 2.2) and numbers in brackets following the sample name are the haplotypes (from this study only). Bolded brackets on the right indicate clusters of haplotype networks (N#; Figure 3.8).

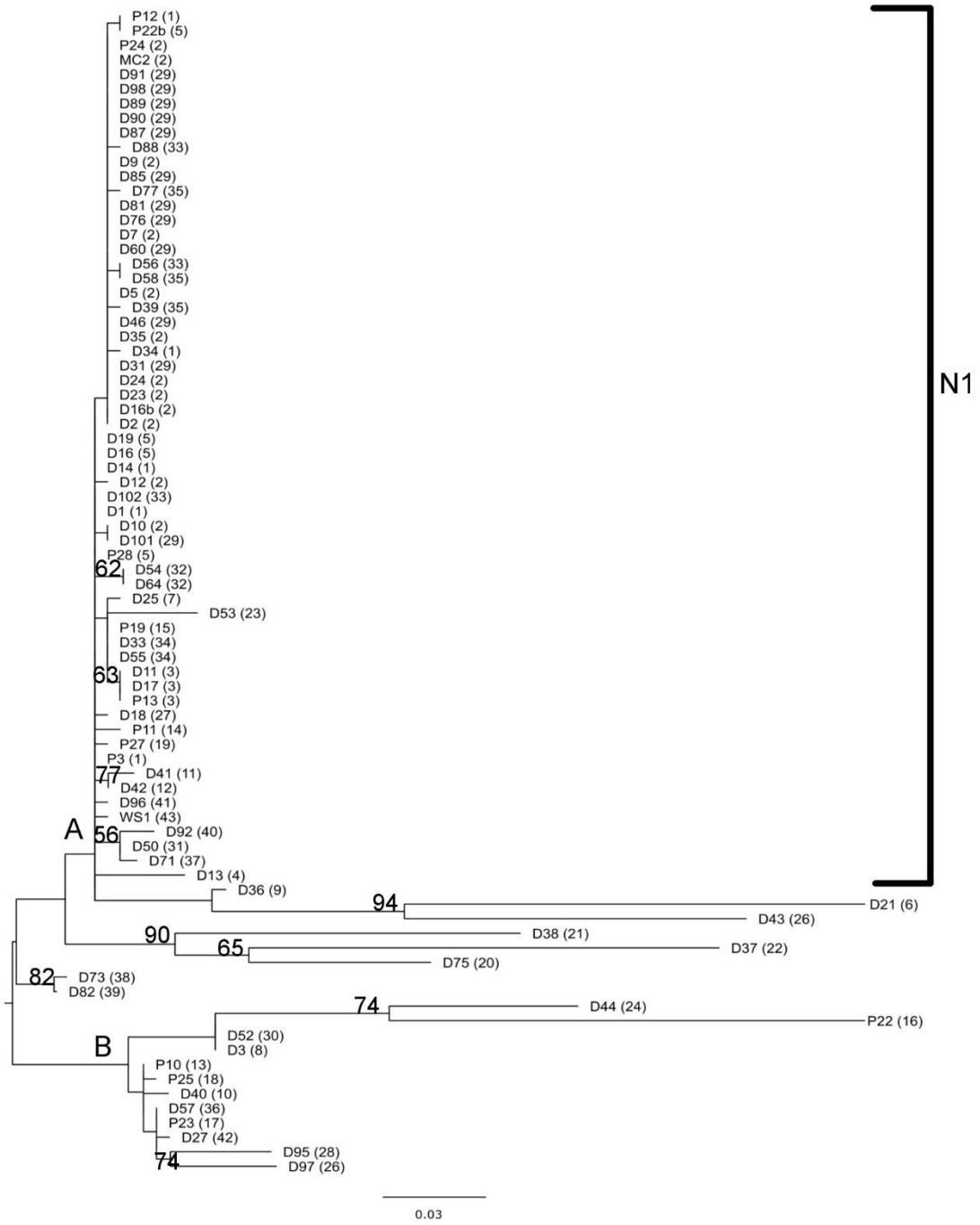

Figure 3.4. Maximum likelihood tree of the internal transcribed spacer (ITS2) region of the rDNA gene within lichenised *Diplosphaera chodatii*. Letters A and B represent clades. Bootstrap values above 50% are included. Letters before the sample numbers represent collection locations (Table 2.2) and numbers in brackets following the sample name are the haplotypes (from this study only). The bolded bracket on the right indicates the cluster in the haplotype network (N#; Figure 3.9).

3.2 Photobiont β-actin Phylogeny

The β-actin phylogeny represents 51 *Diplosphaera chodatii* sequences from samples collected from Payuk Lake, plus an additional sample collected from Whiteshell Provincial Park, and 11 NCBI GenBank Accessions for a total of 63 analysed sequences. The β-actin sequences were 461-470 bp long; trimmed, the final alignment of all the sequences was 401 bp. The β-actin phylogeny showed three main clades (Clades A, B, C; Figure 3.5), and had a Ts/Tv ratio of 1.2004, a sbl value of 0.13256, and a log likelihood value of -908.52. Clade A includes all samples except the outgroup (D87). Clade B includes all the samples except D16, D18, D49, D57, D96, and D87. Both clades A and B have low bootstrap support. Clade C exhibited strong bootstrap support (84%). Payuk Lake samples were in the same clades as samples collected from lakes further upstream (FontaineNe, FontaineNi, FontaineNa; Figure 2.1), and the Whiteshell sample (WS2) fell within clade C with other Payuk Lake samples. Samples with the dominant haplotypes fell within Clades B and C. The most common haplotypes 1 and 12 fell within Clade B, and showed some intermixing between the samples that had those haplotypes. These samples also fell within the dominant haplotype network N1. Clade C represented samples consisting of the common (but not dominant) haplotypes 5 and 6, and also separated out into its own haplotype network (N2; Figure 3.5), with good bootstrap support. The basal portion of Clade B contained samples that contained unique haplotypes. Haplotype 11 clustered in Clade A. The separation of Clade C may be due to the presence of a single indel region with the β-actin alignment (Figure 3.6). The indel was situated at sites 129-134 and exhibited two variations: either ----G- or ATTTGA. Within Clade B, samples D39, D91, and D93 had long branches, which may be due to the presence of ten or more ambiguous nucleotides at the ends of the sequences relative to the rest of the alignment.

3.3 Combined ITS/β-actin Phylogeny

The combined ITS/β-actin represents 36 *Diplosphaera chodatii* sequences from samples collected from Payuk Lake only (Figure 3.7). The 36 samples represent samples for which both β-actin and ITS rDNA sequences were available. The final sequence alignment was 1008 bp long. The maximum likelihood tree, based on the Kimura 2 parameter model, showed three main clades, with a Ts/Tv ratio of 0.7907, a sbl value of 0.19456, and a log likelihood value of -2667.88. Clades A, B, and C have low bootstrap support but clade D has strong bootstrap support. Clade A (bootstrap is 54%) includes most of the samples. Clade B (bootstrap is 54%) includes sample D75, along with the samples found in Clade D (bootstrap is 94%; D73, D82, P10, D57, P23, and D97). Clade C (bootstrap is 50%), contains samples found in all areas of the lake except the outflow. Clade D on the tree is a result of the effect of the ITS portion of the combined sequence because topology follows similarly to ITS1 (Figure 3.3), with moderate bootstrap support > 89%. The other clade is a result of both the ITS and β-actin portions of the combined sequence. The branch lengths are long in all of the clades, possibly due to the presence of the indels in ITS2 rDNA region, as well as the β-actin portion. No parts of the maximum likelihood tree match or are similar to the topology of the ITS2 tree alone (Figure 3.4).

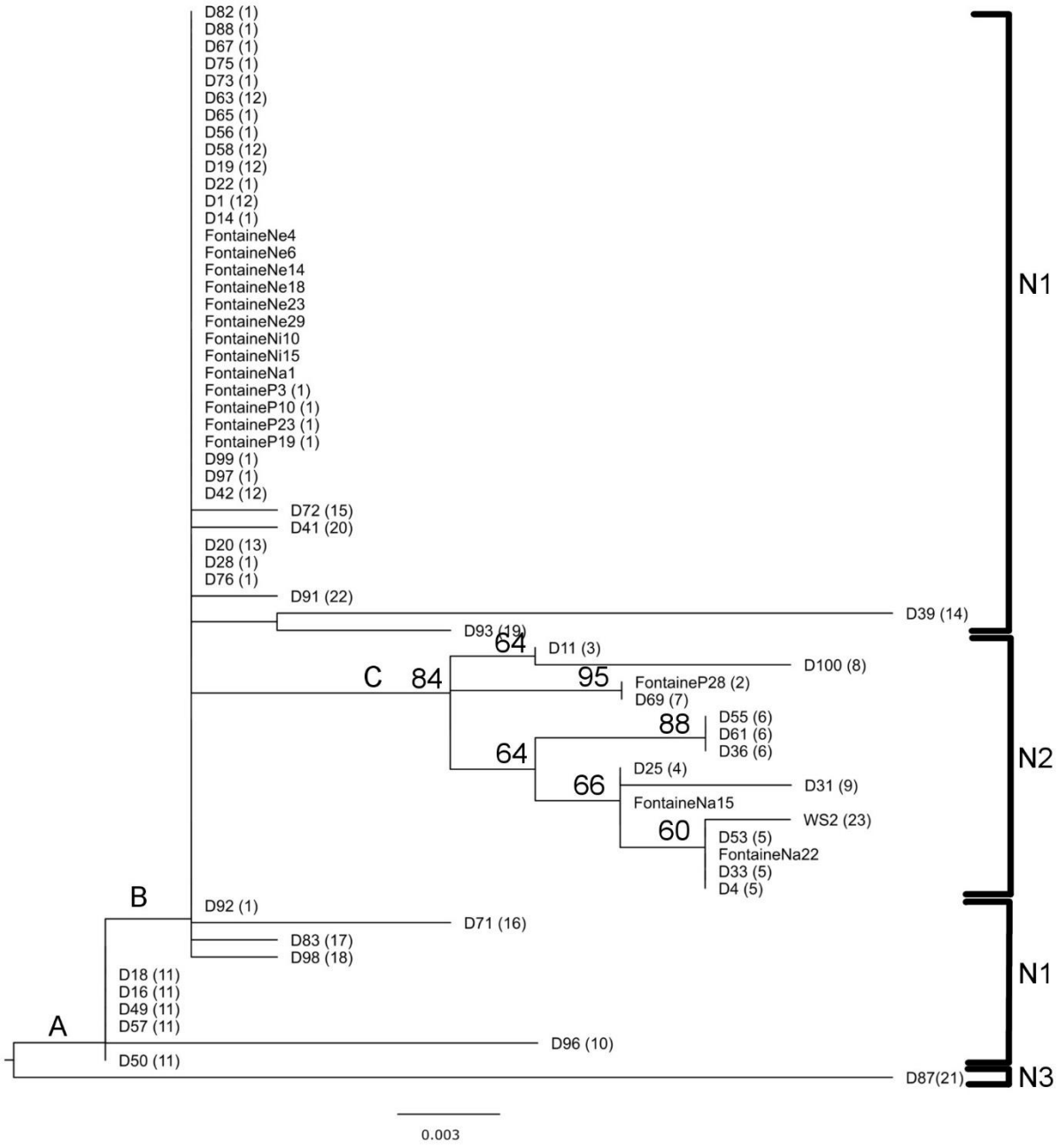

Figure 3.5. Maximum likelihood tree of the β-actin protein gene within lichenised *Diplosphaera chodatii*. Letters A-C represent clades. Bootstrap values above 50% are included. Letters before the sample numbers represent collection locations (Table 2.2 and Table 2.3), and numbers in brackets following the sample name are the haplotypes (from this study only). Bolded brackets to the right indicate clusters of haplotype networks (N#; Figure 3.10).

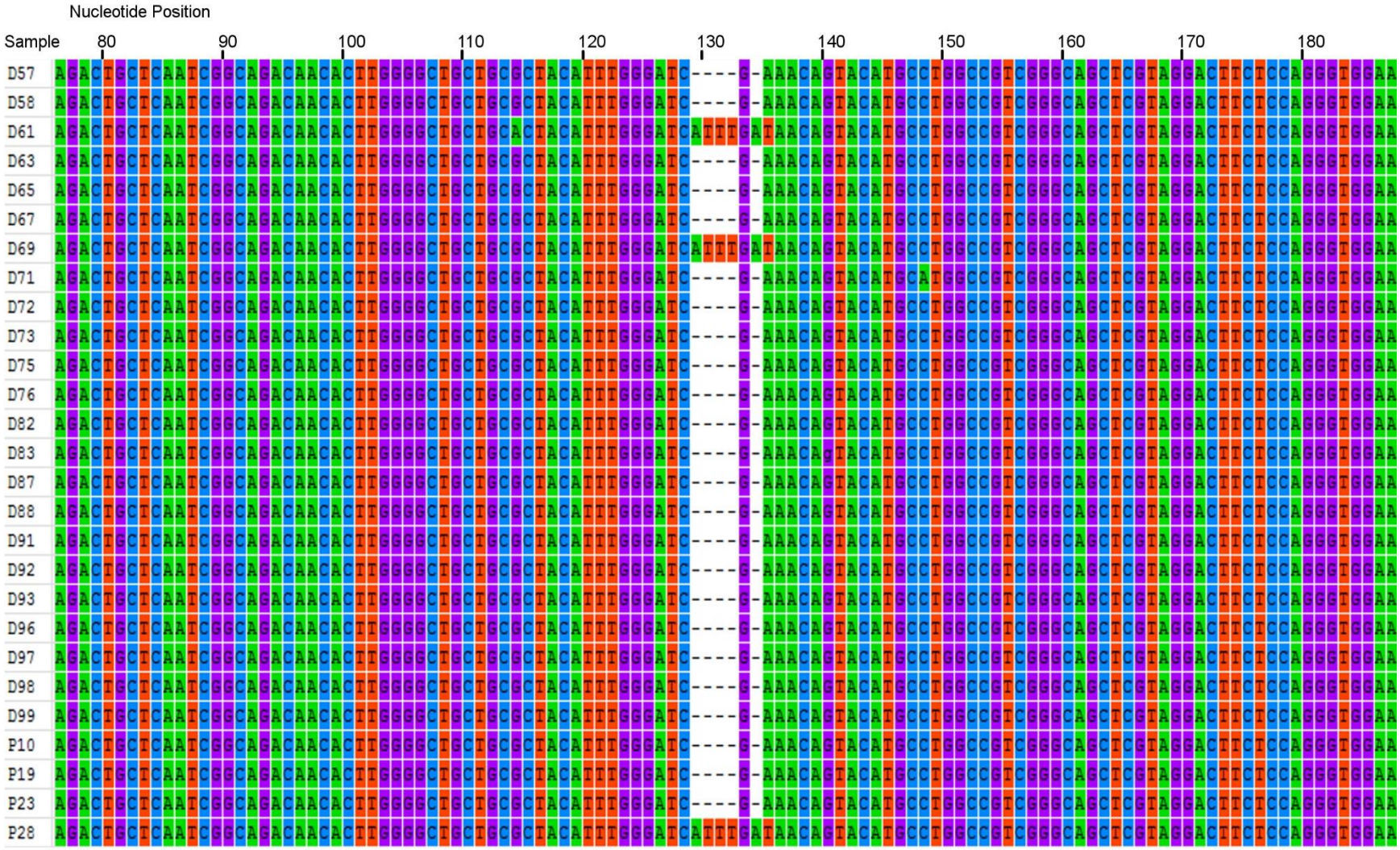

Figure 3.6. Sequence alignment of the β-actin protein gene within lichenised *Diplosphaera chodatii* showing one indel region (129-134bp). Samples are indicated to the left and sequence position is indicated at the top of the alignment. See Table 2.2 for sample information.

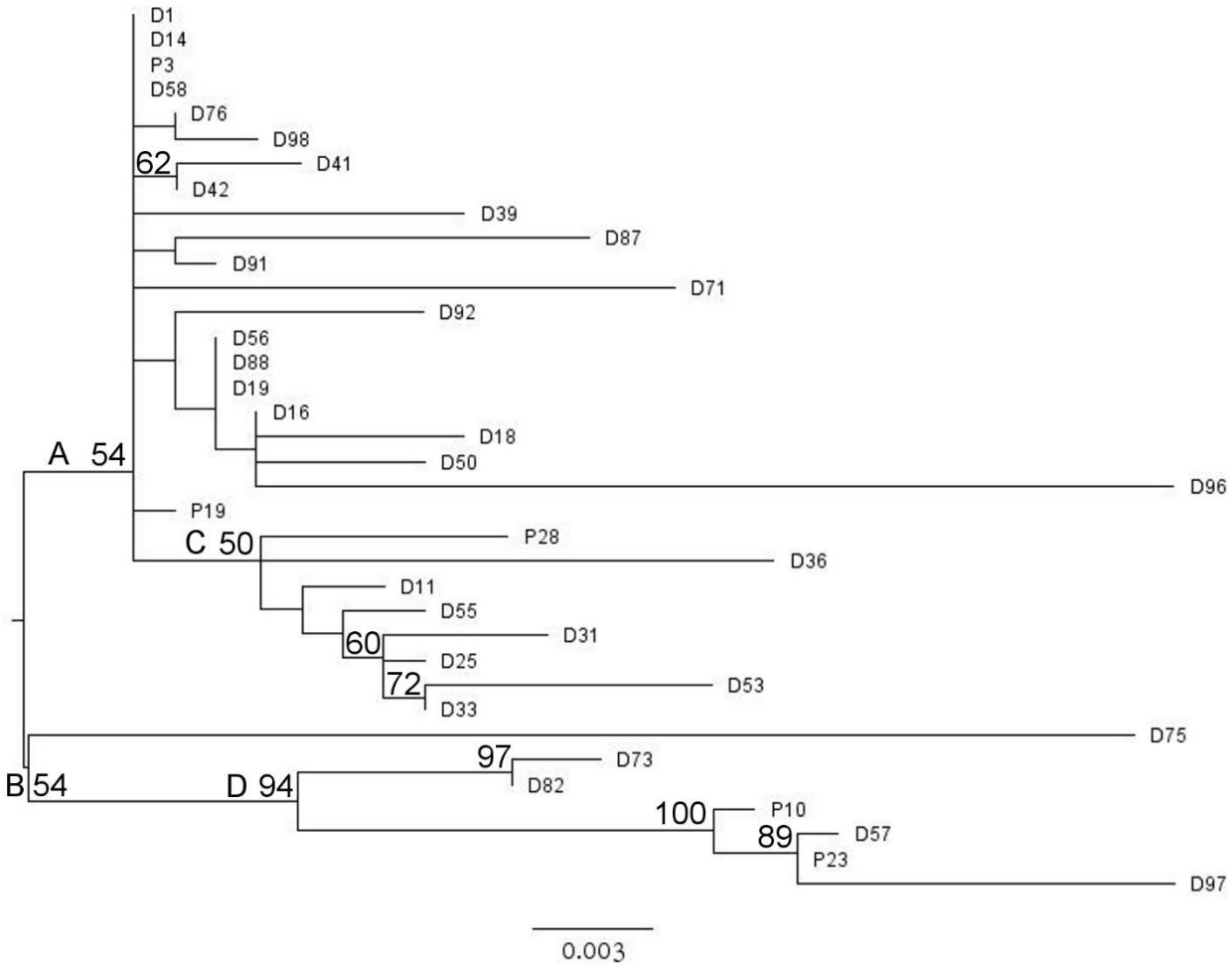

Figure 3.7. Maximum likelihood tree of the combined full internal transcribed spacer region of rDNA and β-actin genes within lichenised *Diplosphaera chodatii*. Letters A-D represent clades. Bootstrap values above 50% are included. Only the samples with two genes sequenced are included in the phylogeny. The letters before the sample numbers represent collection locations (Table 2.2).

3.4 Haplotype Networks

The ITS1 region of the ITS rDNA gene within *Diplosphaera chodatii* contained 36 haplotypes within 80 samples examined (35 haplotypes when excluding the Whiteshell sample, WS1). There were four haplotype networks produced (N1, N2, N3, and N4) based on the total number of base pair changes from the dominant haplotypes computed from TCS (Figure 3.8). Haplotype network 1 (N1) contained the most haplotypes (haplotypes=72), and can be subdivided into three subnetworks within the main network, based on isolated branches that are not connected with other samples within the main network (N1). Subnetwork N1-A contained 13 samples and occurred separately from the other samples in N1. Subnetwork N1-B was defined based on the topology within the maximum likelihood tree (Figure 3.3) and contained four samples, but hey are still connected to samples within N1 and therefore not completely separate. There were also four samples within subnetwork N1-C, and these matched the topology of the maximum likelihood tree. Haplotype networks N2, N3, and N4 are considered "unique" networks since they contained only a single haplotype from a single sample. The sample in N2 contained extra G base pair substitutions in nucleotide positions 17-44 of the alignment compared to the other samples, N3 contained more T and C substitutions (where Cs switched with Ts and vice-versa) in nucleotide positions 158-184, and the sample in N4 contained extra C substitutions at nucleotide positions 70-98 throughout the sequence alignments. Subnetwork N1-A is different from the rest of N1 due to the presence of Cs instead of Ts at nucleotide positions 87, 133, and 155, T instead of C at nucleotide positions 84, A instead of G at nucleotide position 94, and an additional G at nucleotide position 98 in the sequence alignment.

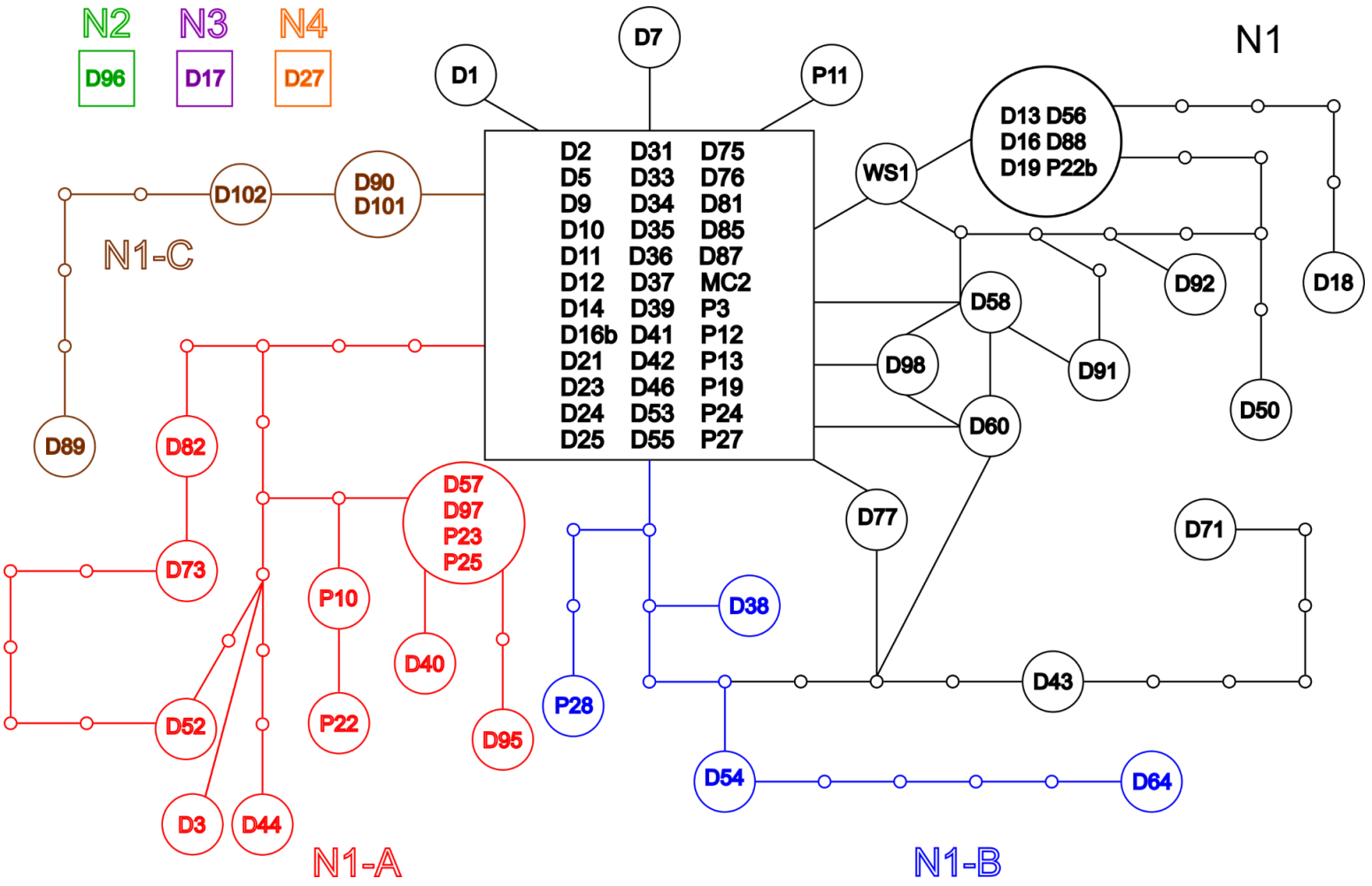

Figure 3.8. Haplotype networks of the internal transcribed spacer 1 region (ITS1) of the rDNA gene within lichenised *Diplosphaera chodatii* collected from Payuk Lake, Manitoba (D, P, and MC samples), and one sample from Whiteshell Provincial Park (WS). Squares represent the first and dominant haplotype designated to a network, circles with samples represent related haplotypes (size is proportional to the number of samples that have the haplotype), and small hollow circles represent single base pair changes from the dominant haplotype. The colors represent networks and subnetworks (see text for explanation).

The ITS2 region of the rDNA gene within *Diplosphaera chodatii* contained 43 haplotypes within 80 sequences examined (42 haplotypes when excluding the Whiteshell sample, WS1). There were 15 haplotype networks defined (Figure 3.9). Haplotype network 1 (N1) contained the largest number of related haplotypes (59 sequences). Haplotype networks N2 (6 sequences), N3 (2 sequences), and N4 (2 sequences) were differentiated based on variations of base pairs within the indel regions of ITS2, with 95% level of parsimony (Figure 3.2). Haplotype network 2 (N2) contained the sequence TTCACCGGA in indel 1 and GAAA------ in indel 2. Haplotype network 3 (N3) contained the same sequence TTCACCGGA in indel 1, but was different in indel 2 (CCCGGTGTCTCACCGGA). Haplotype network 4 (N4) contained two completely different variations in the indels, with TTTTGTGC in indel 1 and –AA------- in indel 2. The other 11 haplotype networks were considered "unique" since they contained only a single haplotype from a single sample collected from the lake.

The β-actin gene within *D. chodatii* contained 23 haplotypes from 52 sequences examined (22 haplotypes excluding the Whiteshell samples, WS2). There were three haplotype networks defined (Figure 3.10). The first network N1 contained 38 sequences (13 haplotypes), the second network N2 contained 13 sequences (9 haplotypes), and the last network N3 was unique and contained a single haplotype from a single specimen. The difference between haplotype N1 and N2 was based on the indel region (Figure 3.6). N1 contained missing base pairs within the indel region (----G-A) while N2 contained the sequence ATTTGAT within the indel region. N3 was separate due to the presence of ambiguities in the first 12 base pairs of the sample sequence. The Whiteshell sample fell within haplotype N2.

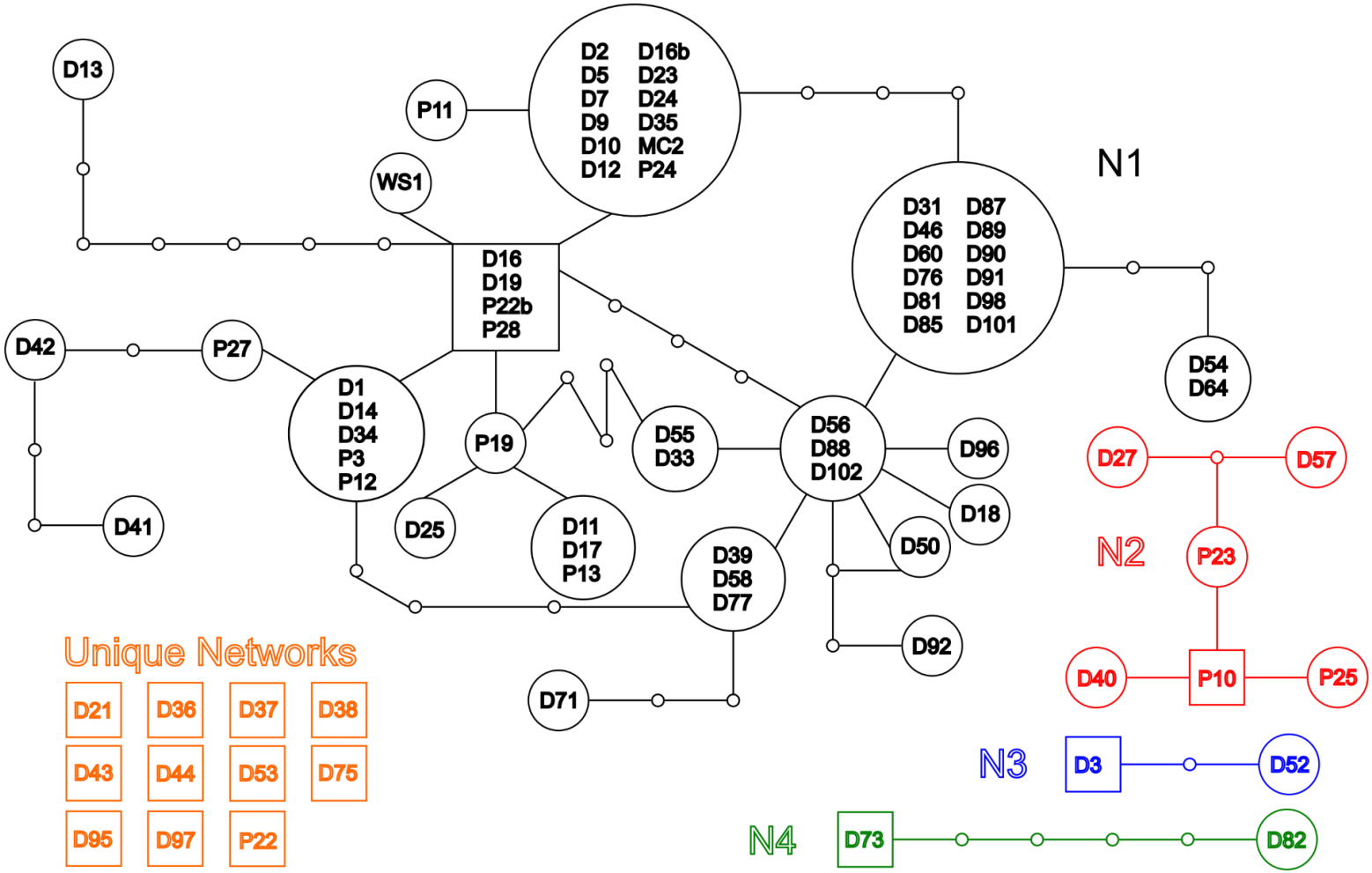

Figure 3.9. Haplotype networks of the internal transcribed spacer 2 region (ITS2) of the rDNA gene within lichenised *Diplosphaera chodatii* collected from Payuk Lake, Manitoba (D, P, and MC samples), and one sample from Whiteshell Provincial Park (WS). Squares represent the first and dominant haplotype designated to a network, circles with samples represent related haplotypes (size is proportional to the number of samples that have the haplotype), and small hollow circles represent single base pair changes from the dominant haplotype. The colors represent networks and subnetworks (see text for explanation).

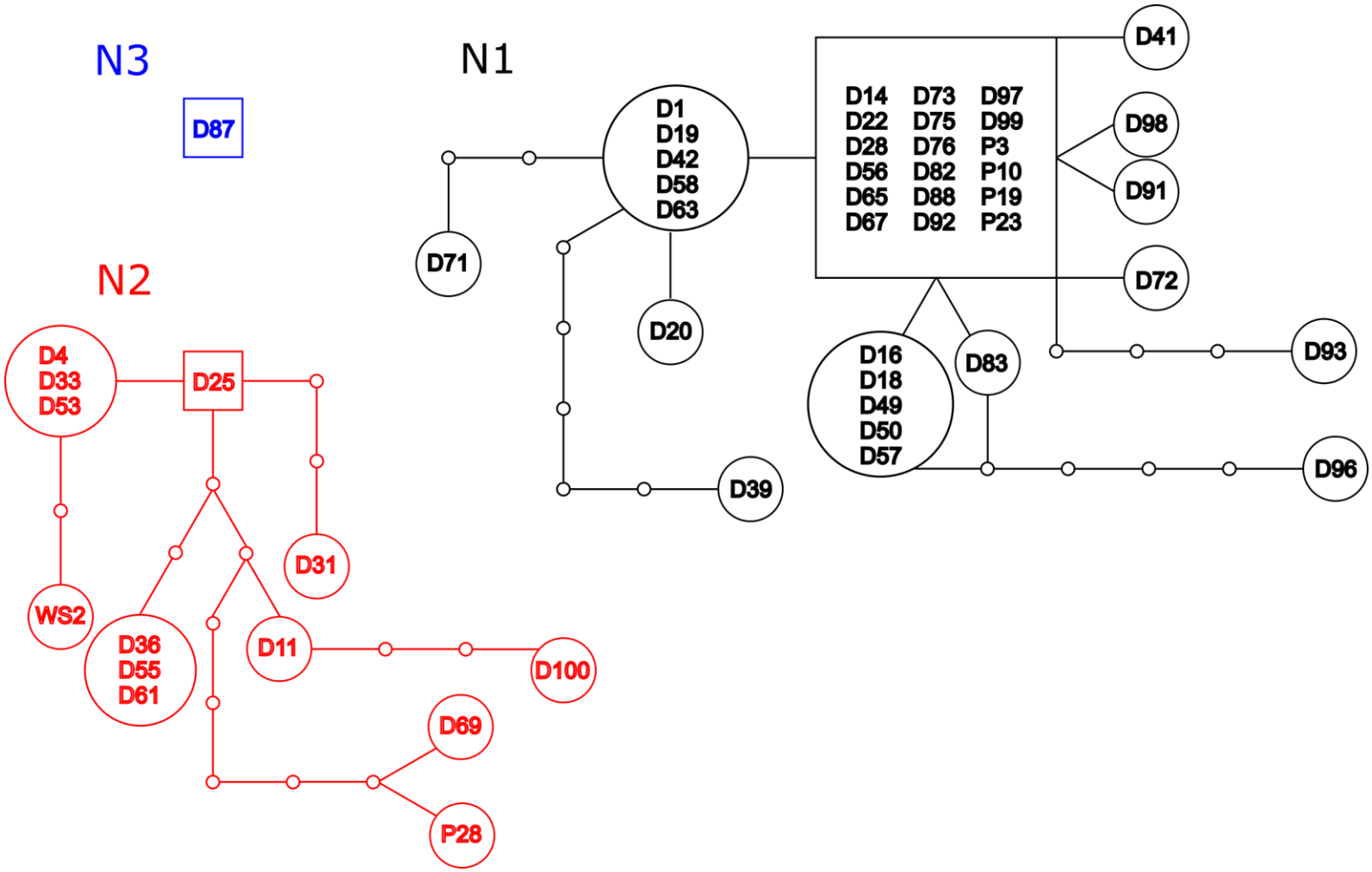

Figure 3.10. Haplotype networks of the β-actin gene within lichenised *Diplosphaera chodatii* collected from Payuk Lake, Manitoba (D and P samples), and one sample from Whiteshell Provincial Park (WS). Squares represent the first and dominant haplotype designated to a network, circles with samples represent related haplotypes (size is proportional to the number of samples that have the haplotype), and small hollow circles represent single base pair changes from the dominant haplotype. The colors represent networks and subnetworks (see text for explanation).

3.5 Haplotype Distribution

There were many haplotypes found within each of the ITS1, ITS2, and β-actin genes despite a large sampling size. For ITS1 and ITS2 (Figure 3.11 and Figure 3.12, respectively), a new haplotype was found in approximately every two specimens sequenced. For the β-actin gene, a new haplotype was found every two to three specimens sampled (Figure 3.13).

Patterns of genetic variation corresponded with geographic patterns around the lake. In the ITS1 rDNA, the three unique haplotype networks were found on the Twin Creek (southeast) side of the lake (Figure 3.14). Furthermore, the most dominant haplotype network (N1) was found throughout the lake, in both the inflows (Mistik Creek and Twin Creek), in the middle of the lake, and in the outflow. However, even within N1, patterns were seen in the distribution of subnetworks (Figure 3.14). Subnetwork N1-A did not occur in the outflow of the lake and was isolated on islands and secluded points around the lake. Subnetwork N1-B only occurred on the Mistik Creek (northern) side of the lake and in the isolated bay on the northwest side of the lake. Subnetwork N1-C occurred in both the Mistik Creek inflow, as well as the outflow, but not throughout the lake (Figure 3.14).

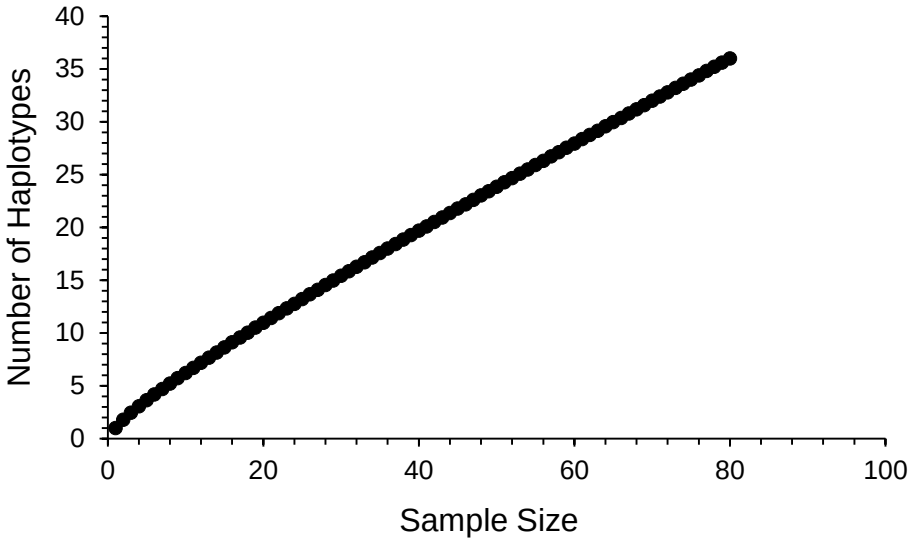

Figure 3.11. Rarefaction curve of the internal transcribed spacer region 1 (ITS1) of the rDNA gene of lichenised *Diplosphaera chodatii* collected from Payuk Lake, Manitoba.

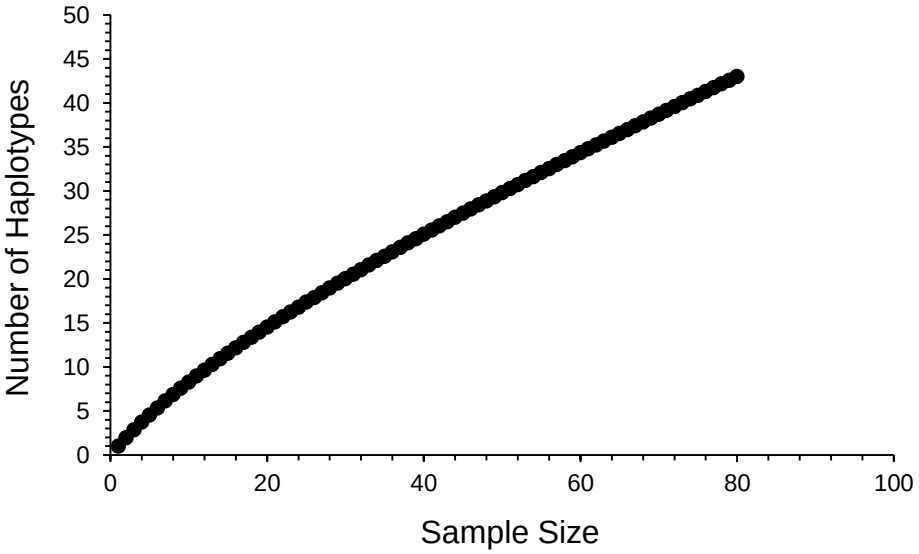

Figure 3.12. Rarefaction curve of the internal transcribed spacer region 2 (ITS2) of the rDNA gene of lichenised *Diplosphaera chodatii* collected from Payuk Lake, Manitoba.

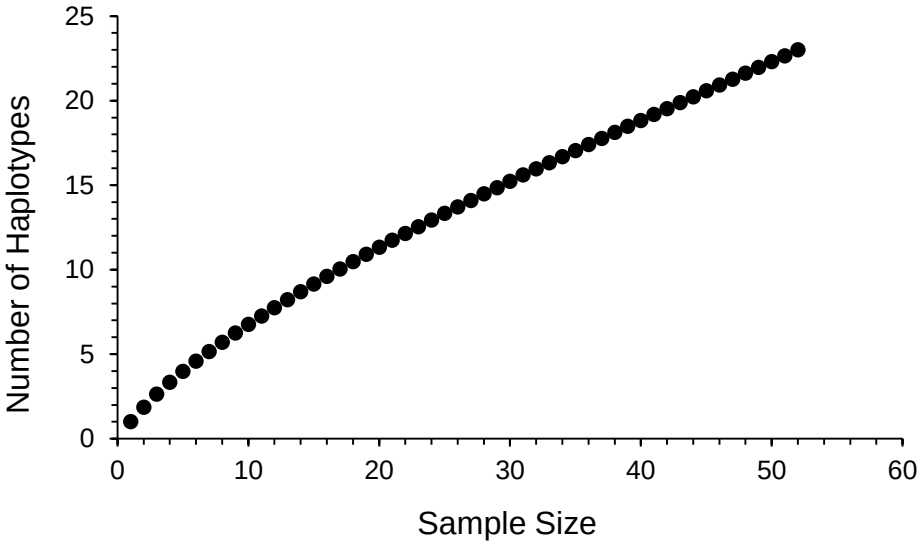

Figure 3.13. Rarefaction curve of the β-actin protein gene of lichenised *Diplosphaera chodatii* collected from Payuk Lake, Manitoba.

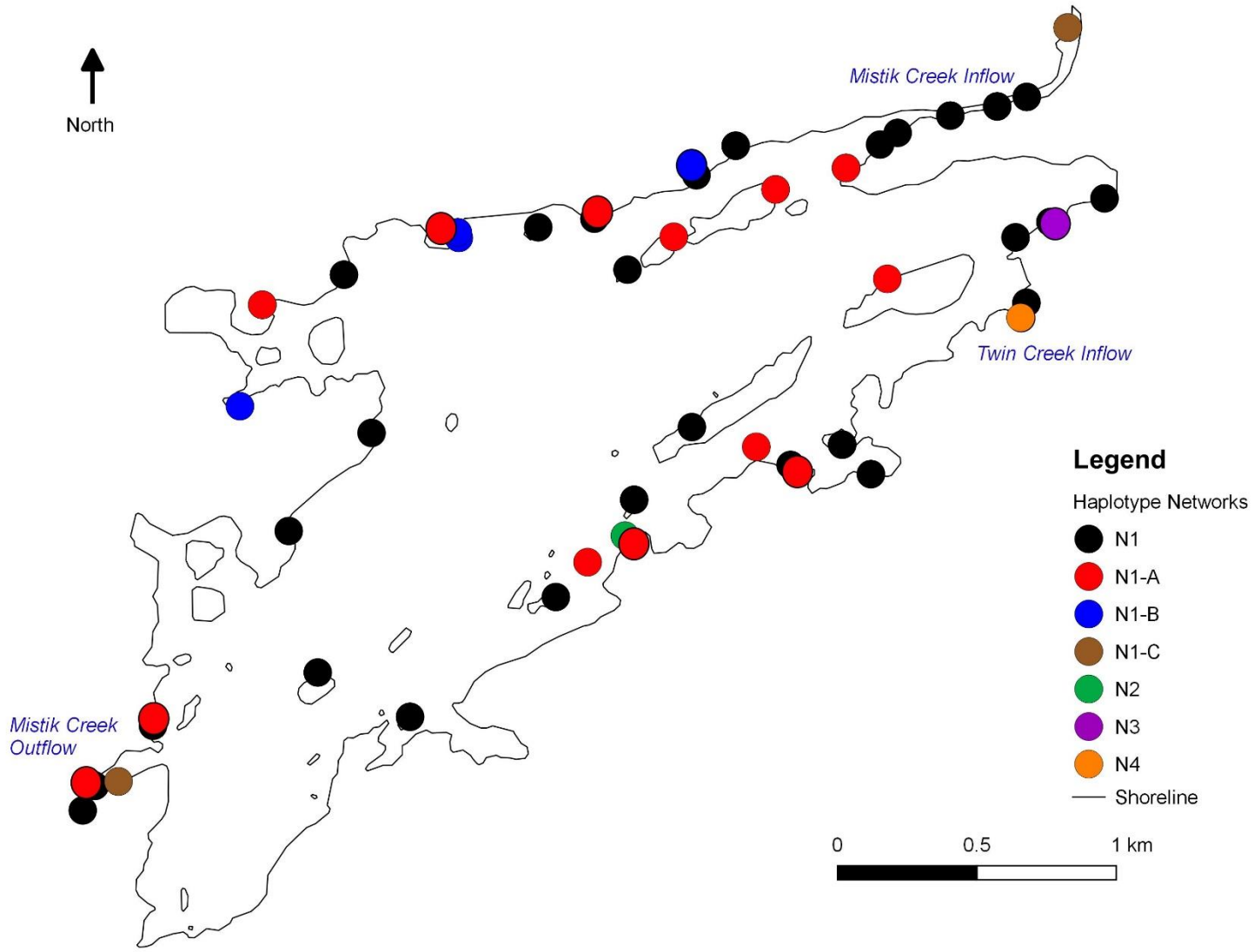

Figure 3.14. Distribution of haplotype subnetworks of the internal transcribed spacer region 1 (ITS1) of lichenised *Diplosphaera chodatii* in Payuk Lake, Manitoba. The colors represent haplotype networks and correspond with those in Fig 3.8.

The ITS2 also had interesting distribution patterns around Payuk Lake. The dominant haplotype network (N1) was found throughout the lake, as well as in both inflows and the outflow (Figure 3.15). Haplotype network 2 (N2) was only within the middle of the lake, on the Twin Creek side and in the Mistik Creek inflow (but not in the creek itself), and not in the outflow. Haplotype network 3 (N3) only occurred on the Mistik Creek (northern) side of the lake and was not present in the outflow. Haplotype network 4 (N4) was found on the Twin Creek (southern) side of the lake and the outflow, but not on the northern shore (Figure 3.15). Unique haplotypes were found throughout the lake. Four unique networks were found in Mistik Creek, four were found within Twin Creek, one was found in the middle region of the lake, and two were found in the outflow.

For the β-actin gene, the two dominant haplotype networks (N1 and N2) were found throughout the lake (Figure 3.16). Both networks were present in Mistik Creek, Twin Creek, the middle regions of the lake including the isolated bay in the northwest side of the lake, as well as in the outflow. The unique haplotype network N3 was found only in the Mistik Creek inflow, more specifically on a rock within the creek itself.

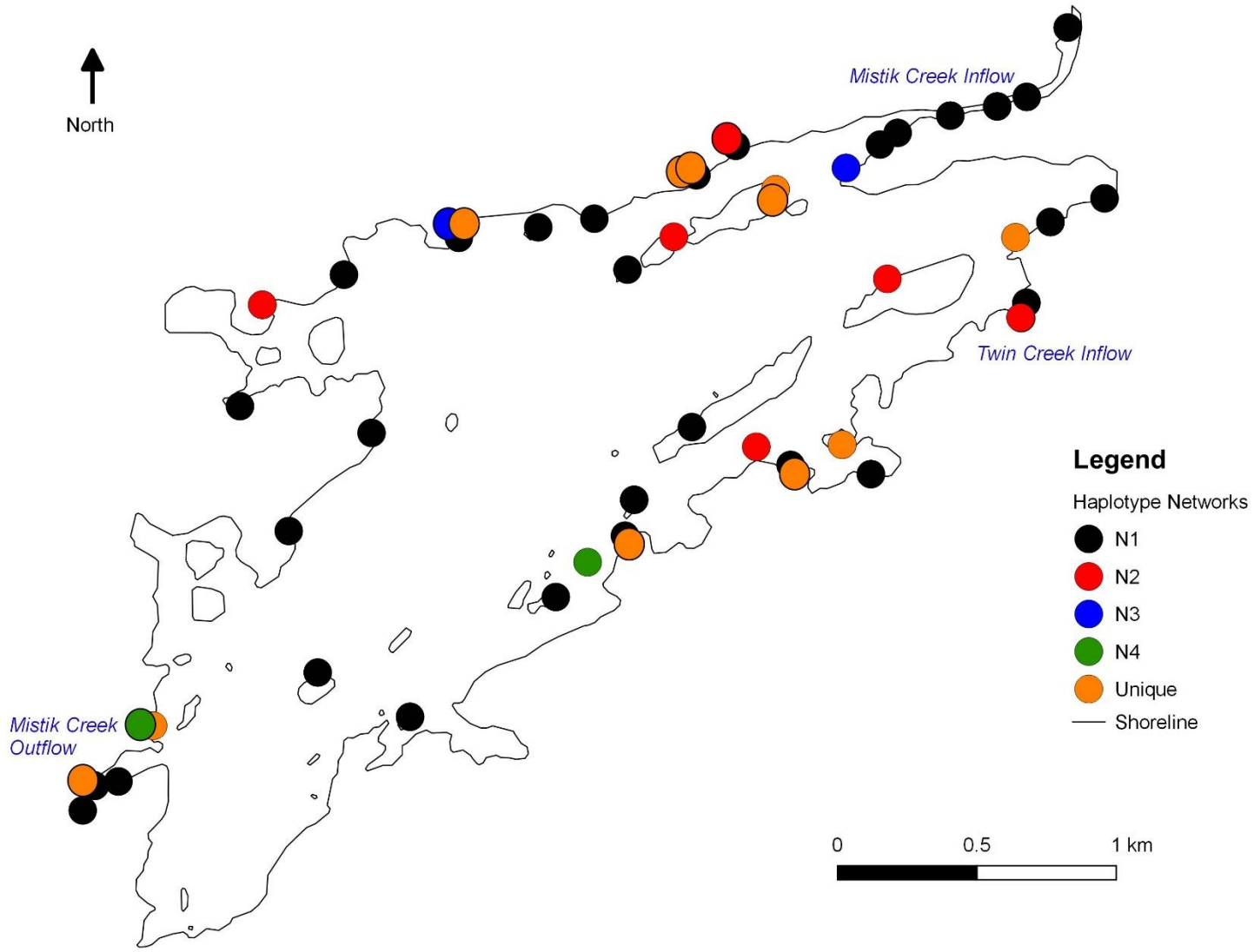

Figure 3.15. Distribution of haplotype networks of the internal transcribed spacer region 2 (ITS2) of lichenised *Diplosphaera chodatii* in Payuk Lake, Manitoba. The colors represent haplotype networks and correspond with those in Fig 3.9.

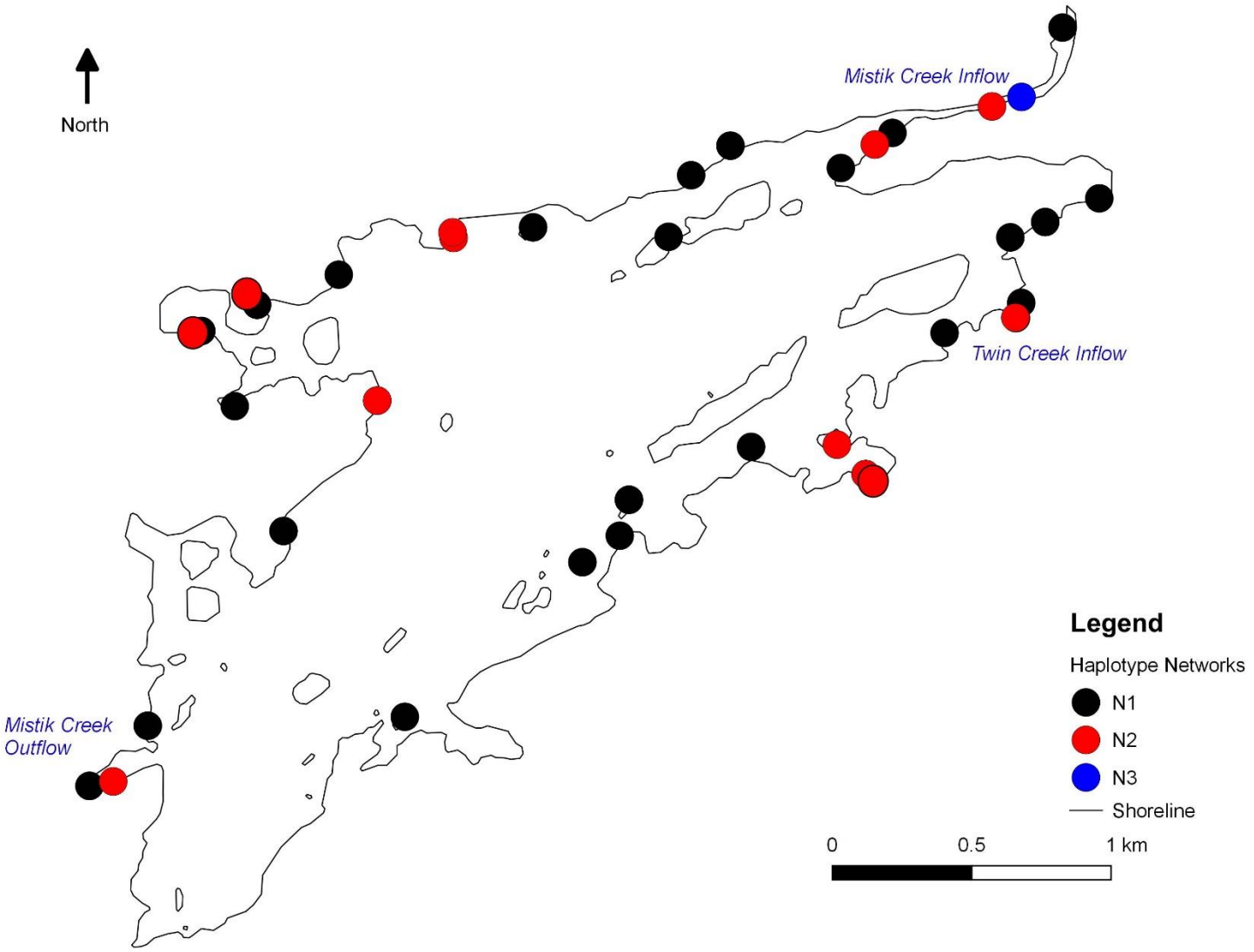

Figure 3.16. Distribution of haplotype networks of the β-actin protein gene of lichenised *Diplosphaera chodatii* in Payuk Lake, Manitoba. The colors represent haplotype networks and correspond with those in Fig 3.10.

3.6 Hydrology and Gene Flow

The hydrological net flow accumulation model revealed the patterns of movement of water through Payuk Lake (Figure 3.17). Supporting personal observation, Payuk Lake has two major inflow sources: Mistik Creek on the northeast side of the lake, and Twin Creek on the southeast side of the lake. Water moves through the lake in the northeast to southwest direction, to the Mistik Creek outflow at the southwest bay. The southernmost bay has some boggy seepage, but that is offset by the accumulation of run-off entering the lake from surrounding cliffs. Additional water enters the lake as runoff from steep cliffs in the isolated bay on the northwest shore, and multiple points of entry from steep cliffs on the southern shore.

Mantel's test for spatial relatedness indicated that there was no isolation-by-distance occurring among *Diplosphaera chodatii* samples found within Payuk Lake based on the ITS1, ITS2, and β-actin genes (Table 3.1), regardless of the geographic distance measure defined (p value > 0.05 in all cases). This large scale test indicated that gene flow is occurring in Payuk Lake, but it cannot detect smaller scale variations within the lake. Analysis of Molecular Variance also indicated high gene flow within Payuk Lake for the ITS1, ITS2, and β-actin genes for most landscape hypotheses (p-value > 0.05), but there was one landscape hypothesis for each gene that showed significant population structure (small scale variation; Table 3.2). For both the ITS1 and ITS2 genes, the "Wind" landscape hypothesis showed significant variation within populations (PhiPT=0.031, p=0.039 and PhiPT=0.016, p=0.053 respectively).

The ITS1 gene showed significant differences between the Outflow population and Mistik Creek (p=0.018), Twin Creek (p=0.011), and Wind populations (p=0.025) (Table 3.3). Haplotype 2 was the most common, occurring in 45.6% (36/79) of the samples, and was present evenly throughout the four populations (Wind, Outflow, Twin Creek, and Mistik Creek) (Table

3.4). Haplotypes 2, 3, 11, and 28 had more than one occurrence while the rest of the haplotypes only occurred in a single sample from a single population (Table 3.4). The Wind population had the highest number of haplotypes compared to the other populations within the Wind landscape hypothesis, with a total of 18/35 haplotypes present, and Mistik Creek had the lowest, with seven haplotypes present (Table 3.4). Between the Outflow population and the rest of them, there were two shared haplotypes, with 15 of 18 haplotypes unique to Wind, six of nine haplotypes unique to Twin Creek, and four of seven haplotypes unique to Mistik Creek compared with the Outflow (Table 3.4).

In ITS2 alone, there were significant differences between the Mistik Creek population and the Wind (p-value=0.024) and Outflow populations (p=0.005) (Table 3.5). Haplotypes 2 and 29 were the most dominant, with 12/79 occurrences each (Table 3.6). Nine haplotypes (haplotypes 1, 2, 3, 5, 29, 32, 33, 34, and 35) occurred more than once, while the rest only had a single occurrence from a single population (Table 3.6). The Wind population had the highest number of haplotypes compared to the other populations within the Wind landscape hypothesis, with a total of 26/42 haplotypes present, and the Mistik Creek population had the lowest, with six haplotypes present (Table 3.6). Between Wind and Mistik Creek populations, five haplotypes were shared, while Wind had 17 unique haplotypes and Mistik Creek only had one (Table 3.6). Mistik Creek and the Outflow populations contained five shared haplotypes, with one and six unique haplotypes, respectively (Table 3.6).

For the β-actin gene, the "Hydrology" landscape hypothesis showed significant variation within populations (PhiPT=0.069, p=0.02; Table 3.2). There were significant differences between the Middle population and Twin Creek population (p=0.027), and the Outflow population and Mistik Creek and Middle populations ((p=0.014 and 0.001, respectively; Table

3.7). Haplotype 1 was the most dominant, with 18/51 occurrences each (Table 3.8). Five haplotypes (haplotypes 1, 5, 6, 11, and 12) occurred more than once, while the rest only had a single occurrence from a single population (Table 3.8). The Twin Creek population had the highest number of haplotypes compared to the other populations within the Hydrology landscape hypothesis, with a total of 11/22 haplotypes present, and the Outflow population had the lowest, with five haplotypes present (Table 3.8). There was one shared haplotype between Mistik Creek and Outflow, one shared haplotype between Middle and Outflow, and five shared haplotypes between Twin Creek and Middle populations (Table 3.8).

Akaike's Information Criterion supported the results of the AMOVA (Table 3.9). The best landscape hypotheses for the ITS1 and ITS2 genes were "Wind" (ΔAIC_c= 0.00 for both), followed by the "In-Out-Bay" hypothesis (ΔAIC_c=0.49 and 0.32, respectively; Table 3.9). The best landscape hypotheses for the β-actin gene were "Hydrology" (ΔAIC_c=0.00), followed by "In-Out-Bay" (ΔAIC_c=0.51; Table 3.9).

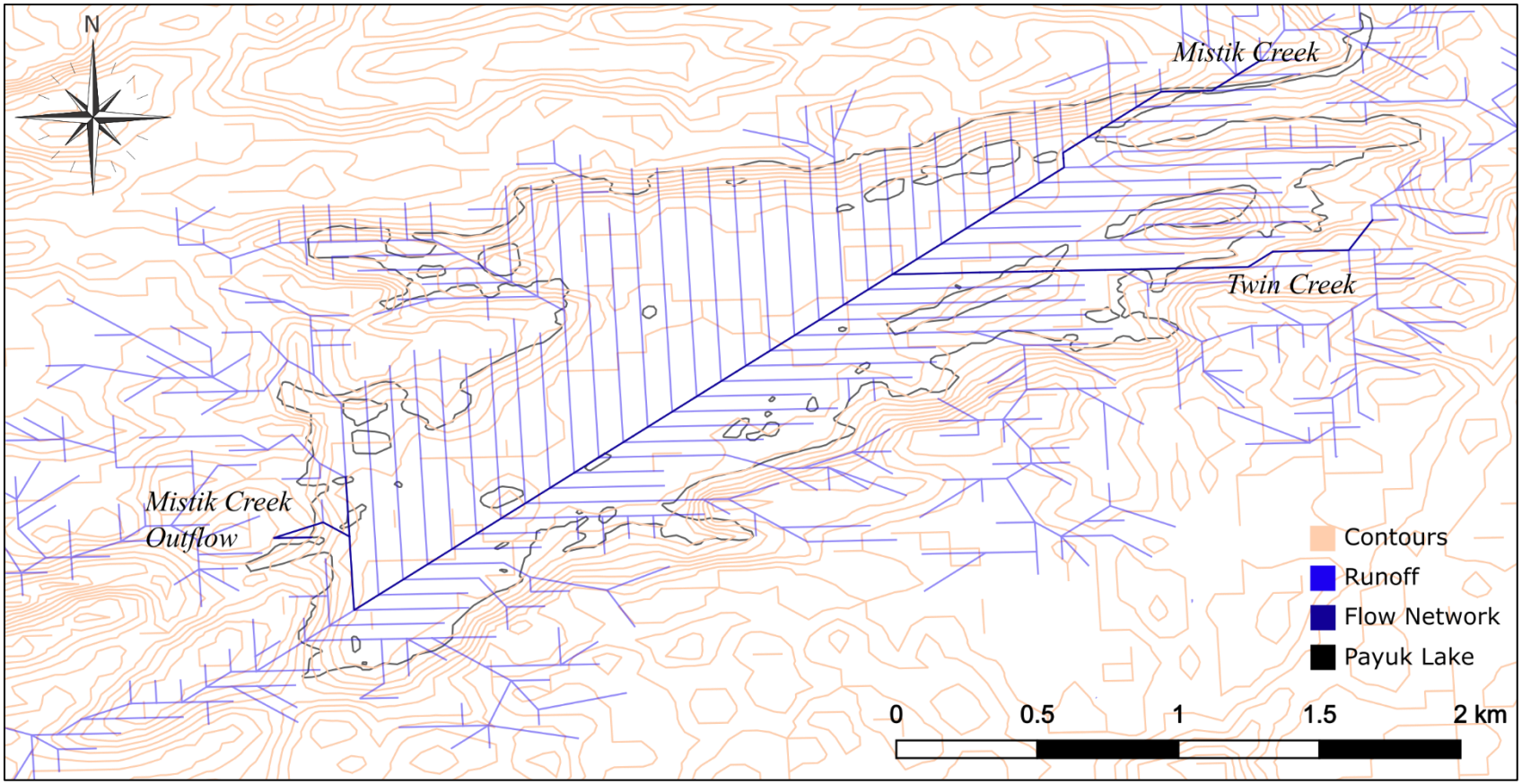

Figure 3.17. Hydrological net flow accumulation network map of Payuk Lake, Manitoba.

Table 3.1. Summary of Mantel tests for isolation by distance using four distance measures for the internal transcribed spacer region (ITS1 and ITS2) rDNA and β-actin (Actin) genes of *Diplosphaera chodatii*.

Gene	Distance Measure	Mantel Stat	P-value
Actin	Euclidean	-0.073	0.886
	Shoreline	0.019	0.271
	Network Euclidean	-0.103	0.941
	Network Path	-0.115	0.923
ITS1	Euclidean	-0.066	0.861
	Shoreline	0.080	0.102
	Network Euclidean	-0.070	0.865
	Network Path	-0.090	0.908
ITS2	Euclidean	-0.090	0.941
	Shoreline	-0.003	0.481
	Network Euclidean	-0.086	0.894
	Network Path	-0.061	0.773

Table 3.2. Summary of Analysis of Molecular Variance (AMOVA) of four different landscape hypotheses for each of the β-actin (Actin) protein gene and internal transcribed spacer regions (ITS1 and ITS2) of the rDNA gene in lichenised *Diplosphaera chodatii* from Payuk Lake, Manitoba. DF= degrees of freedom; MS= mean square error. Significant values are bolded.

Gene	Population Classification	AMOVA Analysis	DF	MS	Estimated Variation	% Total Molecular Variation	PhiPT	P-Value
Actin	Hydrology	Among Pop.	3	0.783	0.030	7%		
		Within Pop.	47	0.407	0.407	93%	0.069	**0.02**
	Wind	Among Pop.	3	0.425	0.000	0%		
		Within Pop.	47	0.430	0.430	100%	-0.001	0.45
	In-Out-Bay	Among Pop.	2	0.619	0.013	3%		
		Within Pop.	48	0.422	0.422	97%	0.030	0.16
	Bay Topography	Among Pop.	4	0.415	0.000	0%		
		Within Pop.	46	0.431	0.431	100%	-0.004	0.47
ITS1	Hydrology	Among Pop.	3	0.513	0.007	2%		
		Within Pop.	75	0.389	0.389	98%	0.016	0.18
	Wind	Among Pop.	3	0.620	0.012	3%		
		Within Pop.	75	0.385	0.385	97%	0.031	**0.04**
	In-Out-Bay	Among Pop.	2	0.426	0.002	0%		
		Within Pop.	76	0.393	0.393	100%	0.004	0.36
	Bay Topography	Among Pop.	4	0.350	0.000	0%		
		Within Pop.	74	0.397	0.397	100%	-0.008	0.53
ITS2	Hydrology	Among Pop.	3	0.418	0.000	0%		
		Within Pop.	75	0.476	0.476	100%	-0.007	0.64
	Wind	Among Pop.	3	0.614	0.008	2%		
		Within Pop.	75	0.469	0.469	98%	0.016	**0.05**
	In-Out-Bay	Among Pop.	2	0.348	0.000	0%		
		Within Pop.	76	0.478	0.478	100%	-0.014	0.74
	Bay Topography	Among Pop.	4	0.436	0.000	0%		
		Within Pop.	74	0.476	0.476	100%	-0.006	0.58

Table 3.3. Pairwise PhiPT values (lower diagonal) and p-values (upper diagonal) from Analysis of Molecular Variance of the internal transcribed spacer region (ITS1) rDNA of lichenised *Diplosphaera chodatii* collected from Payuk Lake, Manitoba, using the Wind landscape hypothesis. Significant values are bolded.

	Population			
Population	Mistik	Twin	Wind	Outflow
Mistik	-	0.353	0.419	**0.018**
Twin	0.000	-	0.325	**0.011**
Wind	0.000	0.000	-	**0.025**
Outflow	0.105	0.085	0.062	-

Table 3.4. Frequency and number of haplotypes for the internal transcribed spacer region (ITS1) rDNA of lichenised *Diplosphaera chodatii* collected from Payuk Lake, Manitoba, using the Wind landscape hypothesis. Total count is the number of occurrences of each haplotype.

	Population				
Haplotype	Wind	Mistik Creek	Twin Creek	Outflow	**Total Count**
1	0	1	0	0	**1**
2	10	9	10	7	**36**
3	4	1	1	0	**6**
4	1	0	0	0	**1**
5	0	1	0	0	**1**
6	1	0	0	0	**1**
7	0	1	0	0	**1**
8	1	0	0	0	**1**
9	1	0	0	0	**1**
10	0	0	1	0	**1**
11	2	0	1	1	**4**
12	1	0	0	0	**1**
13	1	0	0	0	**1**
14	1	0	0	0	**1**
15	1	0	0	0	**1**
16	1	0	0	0	**1**
17	0	0	1	0	**1**
18	1	0	0	0	**1**
19	1	0	0	0	**1**
20	1	0	0	0	**1**
21	1	0	0	0	**1**
22	1	0	0	0	**1**
23	1	0	0	0	**1**
24	0	0	0	1	**1**
25	0	0	0	1	**1**
26	0	0	0	1	**1**
27	0	0	0	1	**1**
28	0	1	0	1	**2**
29	0	1	0	0	**1**
30	0	0	0	1	**1**
31	0	0	0	1	**1**
32	0	0	1	0	**1**
33	0	0	1	0	**1**
34	0	0	1	0	**1**
35	0	0	1	0	**1**
No. of Haplotyes	**18**	**7**	**9**	**9**	

Table 3.5. Pairwise PhiPT values (lower diagonal) and p-values (upper diagonal) from Analysis of Molecular Variance of the internal transcribed spacer region (ITS2) rDNA of lichenised *Diplosphaera chodatii* collected from Payuk Lake, Manitoba, using the Wind landscape hypothesis. Significant values are bolded.

	Population			
Population	Mistik	Twin	Wind	Outflow
Mistik	-	0.368	**0.024**	**0.005**
Twin	0.000	-	0.393	0.202
Wind	0.039	0.000	-	0.459
Outflow	0.089	0.013	0.000	-

Table 3.6. Frequency and number of haplotypes for the internal transcribed spacer region (ITS2) rDNA of lichenised *Diplosphaera chodatii* collected from Payuk Lake, Manitoba, using the Wind landscape hypothesis. Total count is the number of occurrences of each haplotype.

	Population				
Haplotype	Wind	Mistik Creek	Twin Creek	Outflow	**Total Count**
1	1	2	1	1	**5**
2	1	6	4	1	**12**
3	1	1	0	1	**3**
4	1	0	0	0	**1**
5	3	0	1	0	**4**
6	1	0	0	0	**1**
7	0	0	1	0	**1**
8	0	1	0	0	**1**
9	0	0	1	0	**1**
10	1	0	0	0	**1**
11	1	0	0	0	**1**
12	1	0	0	0	**1**
13	1	0	0	0	**1**
14	1	0	0	0	**1**
15	0	0	1	0	**1**
16	0	0	1	0	**1**
17	0	0	1	0	**1**
18	1	0	0	0	**1**
19	0	0	0	1	**1**
20	0	0	0	1	**1**
21	1	0	0	0	**1**
22	1	0	0	0	**1**
23	1	0	0	0	**1**
24	1	0	0	0	**1**
25	1	0	0	0	**1**
26	0	0	0	1	**1**
27	1	0	0	0	**1**
28	0	0	1	0	**1**
29	2	4	2	4	**12**
30	1	0	0	0	**1**
31	1	0	0	0	**1**
32	2	0	0	0	**2**
33	1	1	0	1	**3**
34	1	0	1	0	**2**
35	2	0	0	1	**3**
36	1	0	0	0	**1**
37	0	0	0	1	**1**
38	0	0	0	1	**1**
39	0	0	0	1	**1**
40	0	0	1	0	**1**
41	0	0	1	0	**1**
42	0	0	1	0	**1**
No. of Haplotypes	**26**	**6**	**14**	**12**	

Table 3.7. Pairwise PhiPT values (lower diagonal) and p-values (upper diagonal) from Analysis of Molecular Variance of β-actin protein gene of lichenised *Diplosphaera chodatii* collected from Payuk Lake, Manitoba, using the Hydrology landscape hypothesis. Significant values are bolded.

	Population			
Population	Mistik	Twin	Middle	Outflow
Mistik	-	0.087	0.381	**0.014**
Twin	0.057	-	**0.027**	0.414
Middle	0.000	0.079	-	**0.001**
Outflow	0.144	0.002	0.184	-

Table 3.8. Frequency and number of haplotypes for the β-actin protein gene of lichenised *Diplosphaera chodatii* collected from Payuk Lake, Manitoba, using the Hydrology landscape hypothesis. Total count is the number of occurrences of each haplotype.

	Population				
Haplotype	Middle	Mistik Creek	Twin Creek	Outflow	**Total Count**
1	5	3	6	4	**18**
2	1	0	0	0	**1**
3	0	1	0	0	**1**
4	0	0	1	0	**1**
5	1	1	1	0	**3**
6	2	0	1	0	**3**
7	1	0	0	0	**1**
8	0	0	0	1	**1**
9	0	0	1	0	**1**
10	0	0	1	0	**1**
11	3	0	2	0	**5**
12	2	2	1	0	**5**
13	0	0	1	0	**1**
14	0	1	0	0	**1**
15	0	0	0	1	**1**
16	0	0	0	1	**1**
17	1	0	0	0	**1**
18	0	0	0	1	**1**
19	0	0	1	0	**1**
20	0	1	0	0	**1**
21	0	1	0	0	**1**
22	0	0	1	0	**1**
No. of Haplotypes	**8**	**7**	**11**	**5**	

Table 3.9. Summary of Akaike's Information Criterion (AIC) for landscape hypotheses within Payuk Lake, Manitoba, for the β-actin protein (Actin) gene and internal transcribed spacer region (ITS1 and ITS2) of the rDNA gene within lichenised *Diplosphaera chodatii*. K=number of parameters; n=sample size; AIC_c=corrected AIC value; ΔAIC_c=difference in the corrected AIC value when compared to the minimum AIC value. Significant results are bolded.

Gene	Landscape Hypothesis	Parameters	K	n	AICc	ΔAICc
Actin	In-Out-Bay	inflow+outflow+mistik bay	3	51	-40.59	0.51
	Hydrology	**mistik+twin+middle+outflow**	**4**	**51**	**-41.11**	**0.00**
	Wind	mistik+twin+wind+outflow	4	51	-38.33	2.78
	Bay Topography	mistik+twin+middle+bay+outflow	5	51	-36.84	4.26
ITS1	In-Out-Bay	inflow+outflow+mistik bay	3	79	-70.45	0.49
	Hydrology	mistik+twin+middle+outflow	4	79	-70.07	0.87
	Wind	**mistik+twin+wind+outflow**	**4**	**79**	**-70.94**	**0.00**
	Bay Topography	mistik+twin+middle+bay+outflow	5	79	-67.40	3.54
ITS2	In-Out-Bay	inflow+outflow+mistik bay	3	79	-55.13	0.32
	Hydrology	mistik+twin+middle+outflow	4	79	-54.13	1.32
	Wind	**mistik+twin+wind+outflow**	**4**	**79**	**-55.45**	**0.00**
	Bay Topography	mistik+twin+middle+bay+outflow	5	79	-52.95	2.50

3.7 Algal Morphological Diversity

Eight taxa of algae were identified in this study (Table 3.10). The first taxon was that of the photobiont, *Diplosphaera chodatii*. This species was characterised by its unicellular, ellipsoidal to spherical shape, ranging in size from 3 – 5 μm × 4 – 8 μm, and containing parietal chloroplasts (Figure 3.18; Table 3.10). Four other green algae were identified, and were all unicellular and spherical, either occurring singly or in a mucilaginous colony, ranging in size from 3 μm – 16.8 μm in diameter, and containing central or evenly interspersed chloroplasts (Figure 3.18; Table 3.10). There were two unidentified unicellular and spherical Chlorophyte green algae (Figure 3.18; Table 3.10), ranging from 4 μm × 4.4 μm to 5.4 μm × 5.5 μm in diameter. One of the unknown Chlorophytes had granular bodies present. Lastly, there was one unidentified cyanobacterium present (Figure 3.18; Table 3.10), with spherical cells arranged in a single trichome and heterocysts spaced throughout.

Cultures that originated from thallus material had the lowest diversity of algal taxa (Table 3.11). Two cultures (D71 and D81) contained axenic samples of the study species, *Diplosphaera chodatii,* while the rest of the cultures isolated from thalli had other algae growing in the media. The environmental cultures (from rock scrapings, noted as E12, E33, and E40) had the highest diversity of algal taxa present (Table 3.11). Sample E12 had six of the eight identified taxa, including *Diplosphaera chodatii* in free-living form. The presence of free-living *Diplosphaera chodatii* in the environmental sample was also supported by PCR (Figure 3.19) where *Diplospharea* specific primers produced a single band at 750 bp in the same position as the ITS band produced in the lichenised *Diplosphaera* sample.

Table 3.10. Characteristics of cultured algae isolated from the lichen thallus of *Dermatocarpon luridum* collected from Payuk Lake, Manitoba.

Algal ID	Phylum	Colony	Shape	Size	Chloroplast Location	Mucilage	Other Characteristics
Diplosphaera chodatii	Chlorophyta	Unicellular	Ellipsoidal to spherical	3-5µm × 4-8µm	Parietal	No	
Diplosphaera -like	Chlorophyta	Unicellular	Ellipsoidal	3µm × 5µm	Parietal	No	
Trebouxia -like	Chlorophyta	Unicellular	Spherical	8.7µm × 9.1µm (single cell), 16.8µm × 16.8µm (with spores)	Central	Yes	Spores inside (4.9µm × 5.2µm)
Coccomyxa -like	Chlorophyta	Multiple unicells in mucilage	Spherical	3.5µm × 3.9µm (cell), 7.1µm × 7.7µm (with mucilage)	Central	Yes	
Chlorella -like	Chlorophyta	Unicellular	Spherical	11.2µm × 12.1µm	Evenly interspersed	No	Large central vacuole
Unknown Chlorophyte 1	Chlorophyta	Unicellular	Spherical	5.4µm × 5.5µm	Central	No	Granular bodies present
Unknown Chlorophyte 2	Chlorophyta	Unicellular	Spherical	4.0µm × 4.4µm	Evenly interspersed	No	
Unknown Cyanobacterium	Cyanophyta	Filamentous, single trichomes	Spherical	< 3µm	N/A	Yes	Heterocysts present

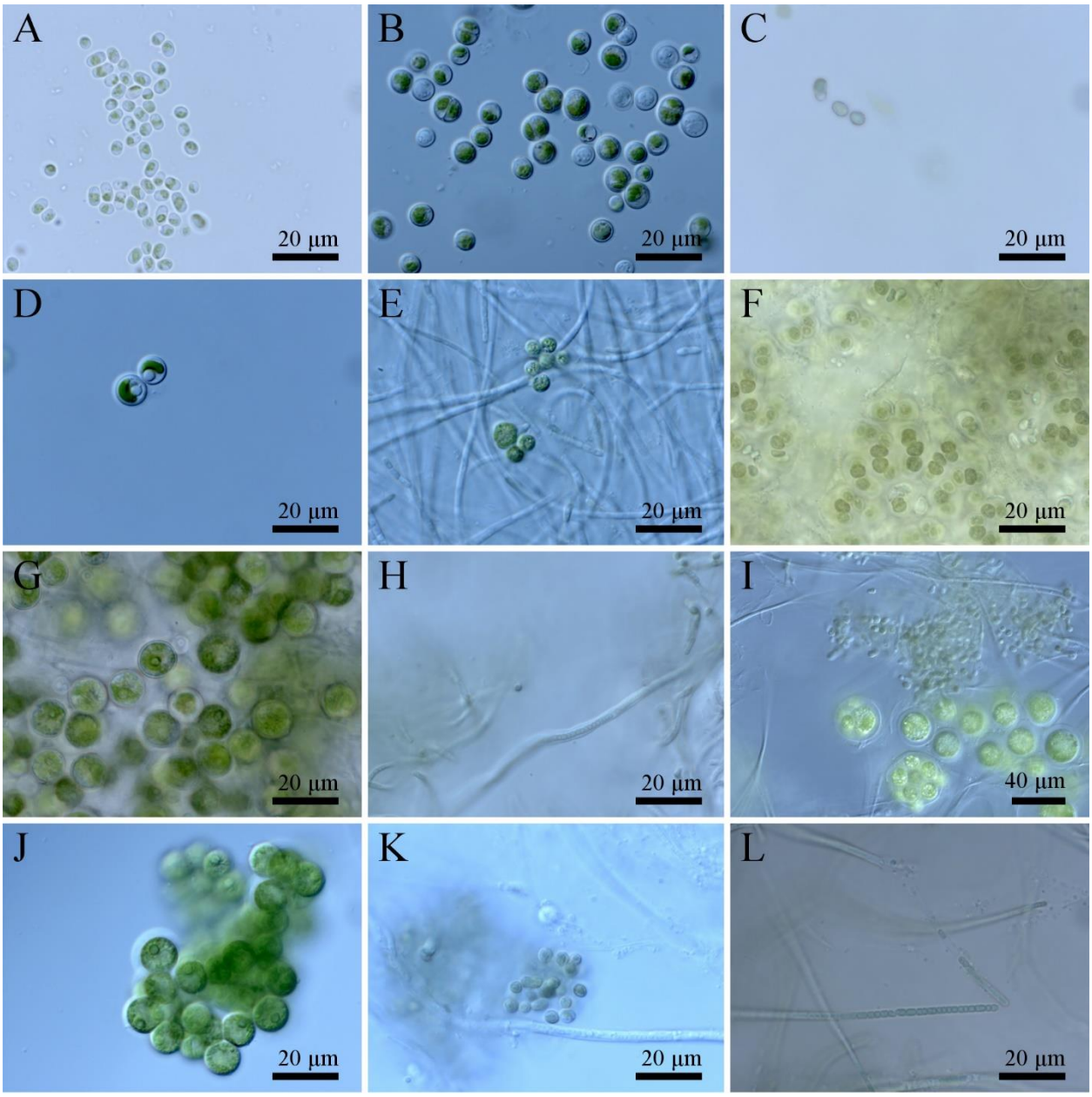

Figure 3.18. Bright field (BF) and differential interference contrast (DIC) of isolated lichenised and associated algae from *Dermatocarpon luridum* from Payuk Lake, MB. A-C: Isolated *Diplosphaera chodatii*; A: axenic known culture (100x BF); B: lichenised (100x DIC); C: *Di. chodatii*-like alga from rock scrapings surrounding *De. luridum* (100x, BF). D-H: Isolated algae associated with *De. luridum* thallus; D: *Di. chodatii*-like alga (100x DIC); E: unknown Chlorophyte 1 (100x DIC); F: *Coccomyxa*-like green alga (100x BF); G: *Chlorella*-like green alga (100x BF); H: unknown cyanobacterium, lacking chloroplasts (100x BF). I-L: Isolated from rock scrapings surrounding *De. luridum*; I: *Trebouxia*-like green alga (40x DIC); J: *Chlorella*-like green alga (100x DIC); K: unknown Chlorophyte 2 (100x DIC); L: unknown cyanobacterium (100x BF). Photo credits: Kyle Fontaine.

Table 3.11. The presence (x) and absence (-) of cultured algae associated with 12 thalli of *Dermatocarpon luridum* and three rock scrapings from Payuk Lake, Manitoba. Samples with D (*Dermatocarpon* thallus) indicate a lichenised culture and E (Environmental sample) indicate cultures from rock scrapings surrounding thalli of *Dermatocarpon luridum*.

		Algal ID							
Culture Type	Sample	*Diplosphaera chodatii*	*Diplosphaera*-like	*Trebouxia*-like	*Coccomyxa*-like	*Chlorella*-like	Unknown Chlorophyte 1	Unknown Chlorophyte 2	Unknown Cyanobacterium
Slant	D51	-	x	-	-	x	-	-	x
	D52	-	-	-	-	-	-	-	-
	D71	x	-	-	-	-	-	-	-
	D73	-	-	-	-	-	-	-	x
	D81	x	-	-	-	-	-	-	-
Subcultured Liquid	D51	-	-	-	-	-	-	-	-
	D52	-	-	-	-	x	x	-	-
	D71	x	-	-	-	-	-	-	-
	D73	-	-	-	-	-	-	-	-
	D81	-	-	x	-	-	x	-	-
Liquid	D87	-	-	-	x	-	-	-	-
	D89	-	-	-	-	-	x	-	-
	E12	-	x	x	x	x	-	x	x
	E33	-	-	-	-	x	x	-	x
	E40	-	-	-	-	-	-	x	x

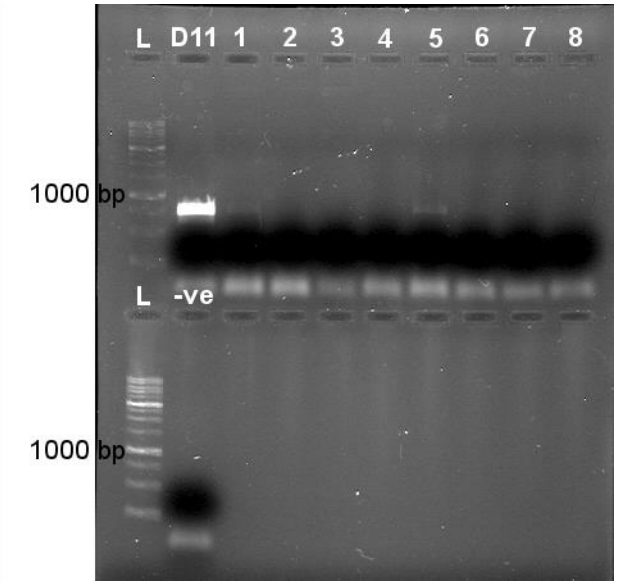

Figure 3.19. Gel image of a 1% agarose gel showing the amplified product of the internal transcribed spacer region (ITS) of a lichenised (D11) and environmental sample of *Diplosphaera chodatii* collected from Payuk Lake, Manitoba. L: 1kb DNA ladder; -ve is the negative control. Lanes 1-4 are a dilution series (1:10, 1:100, 1:1000, and 1:10000 respectively) of environmental sample E24. Lanes 5-8 are a dilution series (1:10, 1:100, 1:1000, and 1:10000 respectively) of environmental sample E35.

CHAPTER 4 : DISCUSSION

4.1 Population structure is present despite high gene flow

Gene flow was inferred to be occurring in *Di. chodatii* based on both the ITS (ITS1 and ITS2) rDNA and β-actin gene sequences (Table 3.2), which was not a surprise since there was no support for isolation-by-distance (Table 3.1). However, although gene flow was inferred, one landscape hypothesis (recall Wind, Hydrology, In-Out-Bay, and Bay topography) for each gene was found to exhibit significant variation based on significant p-values in the AMOVAs (Table 3.2). For both of the ITS partitions, the Wind landscape hypothesis (Figure 2.5D) showed significant variation between populations and for the β-actin, the Hydrology landscape hypothesis (Figure 2.5C) showed significant variation. The Hydrology landscape hypothesis subdivided the lake based on the net flow of water due to topography (and therefore infers waster dispersal; Figure 3.17). The Wind landscape hypothesis assumed predominant westerly wind patterns across the surface of the lake (and therefore infers the potential for wind dispersal). Based on this, it would seem that the significant distribution of β-actin genetic variation is explained by water dispersal while the ITS partitions are explained by wind dispersal or internal evolutionary changes such as drift as a result of the tandem repeat nature of the ITS rDNA and the concept of concerted evolution in this region.

The conflicting modes of dispersal inferred by the spatial distribution of genetic variation and population structure can be explained. The ITS region of the rDNA and β-actin genes may exhibit different rates of evolution and the possibility for concerted evolution in the ITS (Liao 1999). The ITS2 was found to be the most variable of the gene regions examined due to a high frequency of SNPs and indels. If the β-actin is truly more conserved, perhaps not enough variation existed to be detected within the Wind landscape hypothesis, leading to the difference

in significant population structures between the ITS and β-actin haplotype networks. Using more variable DNA markers, such as microsatellites or mtDNA, may help to reveal more fine-scale variation between the samples, allowing for more population structure to be detected (Wongsawad and Peerapornpisal 2014). Additionally, increasing the sampling size (either by sampling more thalli within each population of each landscape hypothesis or by increasing sequencing success) may help to resolve more unique haplotypes into more dominant haplotype clusters, or by reducing the number of unique haplotypes by increasing the frequency of detection of those haplotypes.

Regardless of why each gene showed significant genetic variation in different landscape hypotheses, population structure was present between the subdivided populations. In the ITS1, there were significant differences between the Outflow and the other populations in the landscape hypothesis (Mistik Creek, Twin Creek, and Wind; Table 3.3). In all population comparisons, there were two shared haplotypes, with the rest of the haplotypes present in each population being unique (Tables 3.4). The same situation also occurred between significant pairwise population comparisons in the ITS2 (Tables 3.5, 3.6), and in the β-actin (Tables 3.7, 3.8). In all cases, dominant haplotypes were moving throughout the lake (Figures 3.14-3.16). The significant population structure despite gene flow may be a result of the high presence of unique haplotypes among the populations, which may be the result of several factors. If unique haplotypes were not shared between populations, more distinct population structure would be observed even if dominant haplotypes were being shared, differentiating the populations.

Run-off from the surrounding bedrock cliffs may be bringing in new haplotypes, which could explain the abundance of unique haplotypes (Figure 3.17). Additionally, animal vectors, such as water fowl and fishes, as well as insects may be introducing new haplotypes from nearby

lakes, bogs, or water sources. Kristiansen (1996) noted that many freshwater and terrestrial algae are introduced to new habitats via the use of animal or wind vectors. Furthermore, human activity, such as boating and fishing, may transport and introduce new haplotypes between lakes and streams. If ascospores from *De. luridum* are released during an exposed state and carried by wind, the abundance of *Di. chodatii* that may be in the lake would result in a wide variety of haplotypes being preserved in the lake due to the lichenised state. Preservation of haplotypes is important because clonal dispersal (from fragmentation) would not be enough to alone explain the high genetic variation observed, indicating that immigration of non-local haplotypes must be occurring (Wagner et al. 2006). Also, barriers to gene flow, such as islands and rocks or aquatic vegetation, may trap perspective *Di. chodatii* in various areas of the lake (Werth et al. 2014), leading to unique populations. This may be especially prominent in the southwestern bay if water currents bring in algae but backcurrents do not exist to allow the algae to return to the main hydrological flow (Figure 3.17). Having complete bathymetric data, as well as water current speed and depth and wind speed and direction, would allow for complete understanding of geological processes occurring within Payuk Lake in order to better understand barriers to gene flow and dispersal.

Lastly, spatial scale and sampling may contribute to the high presence of unique haplotypes and spatial variation of *Di. chodatii* within the lake. If the spatial scale is too large, complete genetic variation may be underestimated as sampling may not have been sufficient at the population level (Werth et al. 2011). Again, increasing sampling size may help to ensure all of the genetic variation in *Di. chodatii* is accounted for in order to see true population structure within Payuk Lake.

4.2 Total algal genetic variation was higher than expected

Rarefaction is used to detect the cumulative allelic diversity within a population, where increasing sample sizes beyond a sample size threshold is unlikely to add additional alleles (Werth 2011). Werth (2011) suggests that the sampling size should be high enough to account for the variation, with about 20 individuals needed per population to detect all of the genetic variation present within the site. In the case of this study, 102 *Dermatocarpon luridum* thalli were sampled within Payuk Lake (treating Payuk Lake as a single "population" according to the definition of Werth (2011)); however maximum genetic diversity (a plateau in the rarefaction curve) was not obtained in any of the ITS markers (ITS1 and ITS2; Figures 3.11 and 3.12, respectively), nor the β-actin (Figure 3.13).

One explanation may be due to the nature of the organism. *Diplosphaera chodatii* is a haploid organism, which would result in having single copy actin genes present within the DNA (not accounting for tandem repeats in the ITS), thus requiring twice as intensive sampling as would be required for diploid organisms (Werth 2011). Without a second gene copy to mask mutations, single copy genes would be potentially more variable than multi-copy genes if they were non-deleterious changes and therefore it is possibly that not all of the variation was detected in the ITS rDNA and β-actin gene regions, so more exhaustive sampling would be required to reach a plateau of allelic diversity. One way to alleviate this would be to use more variable, multi-locus markers, such as microsatellites (Werth 2011). Microsatellite markers (ISSR) can identify more complex patterns in haploid genomes than single locus genetic markers such as the ITS or β-actin. Microsatellite markers result in multiple banding patterns (Wongsawad and Peerapornpisal 2014), and the combination of bands would be a unique haplotype (and therefore cover more variation within a single haplotype) instead of the definition

of haplotype used in this study (i.e. a single base pair change resulting in a different DNA sequence from the first assessed sequence). Since more of the genetic variation may be contained within a single banding pattern of microsatellites, it could be faster to reach maximum allelic diversity with a smaller sample size needed compared to a single copy gene β-actin gene or genes with tandem repeats such as the rDNA.

Sequencing success can also affect the final sample size of sequences obtained from specimens collected. Although 102 lichen thalli were collected, only 79 thalli were successfully sequenced using the ITS rDNA (ITS1 and ITS2; 77% success), and 51 thalli were successfully sequenced using the β-actin gene marker (50% success), thus resulting in a smaller effective sample size. Difficulty in sequencing these gene regions may be due to sequencing miscalls or errors introduced in PCR amplification (Ewing and Green 1998). The steps needed to successfully sequence DNA can damage the sample (Chen et al. 2017), especially during the sample preparation (PCR, purification, and cycle-sequencing). Chen et al. (2017) reported that up to 41% of 1000 Genome Projects contained damaged DNA reads (from oxidation and G to T transversions), and that a third of DNA variants (haplotypes) could be the result of damaged DNA reads. True sequence variants would have a base-pair substitution on both strands rather than just one as would be present in DNA damage through amplification and/or sequencing. Using DNA repair enzymes prior to sequencing or increasing the length of sequence reads could lessen the effects of DNA damage since smaller fragments tend to be more easily damaged than longer DNA fragments (Chen et al. 2017).

Noise in the phylogenetic signal of the DNA sequence alignment could also cause discrepancies in effective sample sizes. Many nucleotide substitutions can cause the apparent distances between sequences to be greater than the actual genetic distances, resulting in apparent

saturation (Phillipe et al. 2011), which may suggest that there are many more haplotypes than there are actually present. Third codon positions in protein coding genes would saturate a lot faster than first or second codon positions in protein coding (β-actin) genes (Phillipe et al. 2011), resulting in many more apparent haplotypes present. Compensatory substitutions in the secondary structure of the ITS rDNA may also increase the number of apparent haplotypes.

4.3 Free-living *Diplosphaera chodatii* may contribute to high levels of genetic variation

While DNA damage and choice of markers may influence the amount of genetic variation detected, external sources of genetic variation may also be present. Additional free-living algal haplotypes may be travelling in the water and may cause an influx of diversity during the spring thaw and runoff. Deryck et al. (2006) observed that additional haplotypes in a nematode species increased as they sampled downstream, suggesting that tributaries may be adding genetic variation from other sources connected in the same watershed. In Payuk Lake, there are two inflow sources: the large Mistik Creek on the northern shore and the smaller Twin Creek on the southeastern shore (Figure 3.17). These two inflows converge within Payuk Lake and water flows out of the lake as a single outflow source on the southwestern portion (Figure 3.17), which could result in mixing of haplotypes brought in from both source and the subsequent transport of haplotypes out of the lake. Fontaine et al. (2013) showed that the haplotype numbers did increase along the Mistik Creek chain (see Figure 2.2), suggesting a downstream movement of haplotypes in the watershed into Payuk Lake.

Along with movement of alleles, seasonal effects on genetic variation can also occur. Buxton et al. (2017) found that adult and juvenile larvae of newts exhibited seasonal variation based on their life stage cycles, where increases occurred due to the influx of gametes during breeding season as well as peak larval abundance. Due to the steep cliffs and heavy snow fall

surrounding Payuk Lake (Figure 3.17), water run-off potential would be great. During the spring thaw, surface run-off could add additional species of terrestrial algae not normally found within the lake (which may or may not survive), resulting in an increased number of species and haplotypes, especially if free-living *Diplosphaera chodatii* was carried into the lake from the cliff surfaces. However, due to the slow growth of the lichen thallus, it is unlikely that the free-living *Di. chodatii* would be incorporated that quickly into the thallus, suggesting that free-living *Di. chodatii* may not contribute to much of the variation seen within lichenised samples.

Most lichen photobionts are believed to be facultatively symbiotic, with short-lived or full free-living states (Friedl and Büdel 2008). *Diplosphaera chodatii* has been observed to occur free-living in the soil (Flechtner et al. 1998; Lukesova and Hoffmann 1996), on wood (Handa et al. 2001), and in extreme habitats such as deserts (Fletchtner et al. 2008), but the ability for the free-living strain to lichenise has not been examined. In this study, *Di. chodatii* was successfully cultured from rock scrapings around Payuk Lake (Table 3.10; Figure 3.18). Furthermore, PCR using *Diplosphaera*-specific primers, revealed a band of the expected size suggesting the presence of DNA from the environmental source was the same as that of the lichenised source (Figure 3.19).

If free-living *Di. chodatii* was present on the *Dermatocarpon luridum* thalli, and detected using algal specific markers, it could have overestimated the level of genetic variation observed in lichenised *Di. chodatii* around Payuk Lake. Due to the availability of small protected spaces in between thallus lobes, Muggia et al. (2013) suggested that lichen thalli could provide protected niches for other photobionts or algal species to inhabitant. Therefore the potential for free-living *Di. chodatii* to be present superficially on the thallus is likely, which is further supported by the cultured algae from this study where a diversity of species were reported in culture (Table 3.10;

Figure 3.18). Although the *De. luridum* thalli were washed prior to photobiont extraction, superficial algae hiding in the spaces between the narrow thallus lobes and holdfasts would have been present in the crushed thallus. Given the optimal conditions of enriched growth media (i.e. BBM), it is likely that these algae would grow in culture (Fontaine et al. 2012; Grube and Muggia 2010). It is possible that superficial algae were present in the *De. luridum* photobiont isolates, where many of the cultures contained both the photobiont *Di. chodatii* and other species of algae (Table 3.11). However, unless there was a high biomass of free-living *Di. chodatii* nestled within thallus niches, the algal specific markers would most likely pick up the DNA of the lichenised photobiont. Thus the thallus DNA extracted in this study may truly represent that of the photobiont, while free-living *Di. chodatii* may not have contributed to much of the DNA extracted and hence the genetic variation observed.

Photobiont switching among lichen fungal partners or thalli may also have an effect on the level of algal genetic variation reported. Piercey-Normore and DePriest (2001) reported that photobiont switching within the Cladoniaceae occurred, with mycobiont partners exchanging or "stealing" photobionts of one genotype with photobionts of another genotype, either from the environment or nearby lichen thalli. It is unknown whether algal switching occurs within the Verrucariaceae, but if it does, then *De. luridum* thalli could potentially be incorporating (if newly establishing the association through ascospores), or stealing photobionts from nearby thalli, either from other *De. luridum* thalli, fragments, or associated species such as *Staurothele fissa* or *De. miniatum* (Fontaine et al. 2014; Thüs et al. 2011), which have *Diplosphaera* or *Stichococcus* photobionts (Aptroot and Seaward 2003; Thüs et al. 2011). The potential to incorporate free-living *Di. chodatii* into the thallus may also increase the available haplotypes reported for lichenised *Di. chodatii* in Payuk Lake. However, the limited capacity of photobionts to adapt to

changing environments (due to the lack of sexual reproduction and therefore recombination), may result in genetically similar lichenised and free-living *Diplosphaera* (Hill 2009) or genetically different strains that form compatible associations with the fungal partner. Parapatric speciation with the barrier of a thallus (and genetic compatibility) rather than geography, could be occurring (if algal switching was not taking place and the free-living populations were evolving at different rates than the lichenised populations) or truly allopatric speciation (if terrestrial *Di. chodatii* remained on the cliffs or at a distance away from the shore due to run-off, preventing the two populations from mixing), resulting in genetically different strains of free-living and lichenised algal cells (Hill 2009). The presence of free-living *Di. chodatii* has implications in the potential establishment of semi-aquatic lichens, since other species such as *Staurothele fissa*, *Dermatocarpon miniatum*, and others are believed to associate with this alga as well (Thüs et al. 2011). Dispersed fungal ascospores of any of these species landing on the rock surface would have a pool of free-living algae from which to choose as a photobiont in developing symbiotic thalli.

4.4 Phylogenetic incongruence may be a result of high genetic variation

Although computationally intensive, Maximum Likelihood (ML) is often used when analysing DNA sequence alignments for phylogenetic hypotheses due to its robustness in variance when dealing with small or varying sample sizes (Will 2012). When analysing multiple sequence alignments using ML, the best models can be determined based on the output values. The ML algorithm tries to maximise the likelihood that the samples will fall within the same clade after each permutation, so a higher logLikelihood value (closer to zero) indicates a better model (Will 2012). Higher numbers of substitutions within the DNA sequences may make them less likely to fall within the same clade after each permutation. The shared branch length (sbl)

indicates the number of substitutions, where larger sbl values mean more substitutions compared to models with smaller sbl values (Will 2012).

The ITS rDNA phylogeny exhibited the lowest logLikelihood value (logL = -3433.71) of all the phylogenies produced. It also had the longest sbl of the two markers examined, as well as the combined ITS/β-actin phylogeny, indicating that there were more substitutions and lower resolution in the model (Figure 3.1) compared to the β-actin or combined phylogenies (Figures 3.5 and 3.7, respectively). Skaloud and Peksa (2010) also found that the ITS rDNA phylogeny showed low resolution, and like this study, they split the ITS rDNA into two partitions: ITS1 and ITS2 regions. Splitting the ITS rDNA into partitions yielded better resolution in the phylogenies when compared to the full ITS rDNA gene region. The findings of Skaloud and Peksa (2010) support the findings of this study, where each of the separate ITS1 and ITS2 phylogenies showed higher logLikelihood values (-977.59 and -2036.98, respectively). The ITS2 phylogeny had a higher sbl length (1.2677250) than the ITS rDNA or ITS1, indicating more substitutions present (which was not unexpected given the high variation in the indel regions of ITS2 (Figure 3.2)). The best phylogeny was the β-actin gene because it had the highest logLikelihood value, as well as the lowest sbl value, indicating lower genetic variation and stronger clade resolution compared to the full ITS, the partitioned ITS rDNA (ITS1 and ITS2), and the combined phylogenies (ITS/β-actin). Skaloud and Peksa (2010) also showed that in lichen symbionts, actin markers exhibited better resolved phylogenies with higher bootstrap clade support compared to the ITS rDNA.

Since the combined ITS/β-actin and the ITS1 + ITS2 rDNA (full ITS) ML trees exhibited low resolution, subsequent analyses were performed on the partitioned ITS1 and ITS2 gene regions, and β-actin gene alone. While there were some similarities in the topology of the

combined phylogeny (Figure 3.7) with the ITS1 and β-actin phylogenies (Figures 3.3 and 3.5, respectively), it was interesting to note that the ITS2 topology (Figure 3.4) did not match any topology. This incongruency could be explained by the ITS1 and β-actin phylogenies exhibiting moderate support in their respective clades (bootstraps of > 60 -- 80% on average), but the ITS2 phylogeny had low support (> 50 – 70% on average). The addition of a more variable gene region to the concatenated ITS1, ITS2, and β-actin phylogenies could cause non-phylogenetic signal (combinations of structured noise (undetected homoplasies) that would compete with the true phylogenetic signal of the gene regions), resulting in the incongruence (Phillipe et al. 2011). The highly variable indels in ITS2 (Figure 3.2) may have contributed too much noise, resulting in the low resolution of the clades. Noise can be reduced in concatenated gene sequences by using genes that are less subject to saturation, such as mitochondrial DNA genes or more conserved, transcribed non-protein coding genes (Phillipe et al. 2011).

Incongruence was also observed between the ITS1 and ITS2 phylogenies (Figures 3.3 and 3.4 respectively). Since the ITS1 and ITS2 regions within the nuclear rDNA gene region are generally thought to have coevolved (Hausner and Wang 2005; Nazar 2003) and contain relatively conserved and equal G-C content within species (Torres et al. 1990), it was expected that the topologies of the ITS partitions would be similar. The ITS1 and ITS2 regions share similar hairpin structures, which when transcribed help to place subunits of the ribosome together before being removed by endonucleases out of the ribosome (Hausner and Wang 2005). Beiggi and Piercey-Normore (2007) found that the ITS2 region was more conserved in secondary structure folding than the ITS1 in lichen photobionts, but this study found that the ITS2 region was potentially more variable due to the presence of two indel regions, though intron folding was not investigated. The ITS2 region contained seven more haplotypes (43

haplotypes total) in the samples than the ITS1 region (36 total). If the point mutations were compensatory within the ITS2 region indels (Coleman 2015; Coleman et al. 1998), the secondary structures of the hairpins (and therefore functionality) may not be affected, resulting in an incongruence between the phylogenies.

DePriest (2004) also found high genetic variation within group 1 introns, spliceosomal introns, and other mobile elements. Such variation could be a result of vertical or horizontal gene transfer or mobility of the elements. Vertical gene transfer (gene flow from parent to offspring) may introduce changes as a result of point or other types of mutations or gene duplications causing paralogs (Tunjíc and Korać 2013). Lichen photobionts are known to adapt to the environment almost exclusively due to mutations since recombination is lacking due to the limitation of sexual reproduction within the thallus (Dal Grande et al. 2012; Tunjíc and Korać 2013). However, in a free-living state, sexual reproduction of lichen photobionts is possible, allowing for genetic recombination, which would also increase genetic variation. Both recombination and mutations would facilitate genetic variation, allowing for speciation or evolutionary divergence if populations became isolated. Additionally, paralogs may overestimate diversity due the higher frequency of mutations, causing mismatch in topologies (Lindner and Banik 2011; Fontaine et al. 2012).

In contrast, horizontal gene transfer occurs between lineages of two different species (Tunjíc and Korać 2013). Operational genes (such as housekeeping genes regions like the ITS rDNA) have been postulated to undergo horizontal gene transfer (Tunjíc and Korać 2013). Due to the close proximity of the algal and fungal partners in the lichen association, horizontal gene transfer has been hypothesised to occur (Tunjíc and Korać 2013). This could cause increased or new genetic variation in a population if fungal ITS sequences were added into the photobiont

DNA. The presence of variation in the two indels in the ITS2 may be of fungal origin if horizontal gene transfer occurred between the fungus, *De. luridum* and its photobiont. BLAST searching of the sequences within the indels to ITS2 sequences in the mycobiont may reveal if there are similarities between the two organisms, which would help infer if horizontal gene transfer has occurred.

Incongruence between the ITS phylogenies and the β-actin phylogeny may be a result of different evolutionary trajectories of the genes, as well as horizontal gene transfer from the preceding group I introns of the 18S rDNA. . Since the ITS regions are surrounded by highly conserved ribosomal subunit gene regions (18S, 5.8S, and 28S; Coleman 2015; Hausner and Wang 2005), portions adjacent to the conserved ribosomal units of the gene region would undergo little divergence. Low divergence may be a result of concerted evolution, where tandem repeating gene regions (such as the rDNA gene region and associated ITSs) often retain the same function and variability (Liao 1999). In contrast, protein coding genes, such as β-actin have a higher chance of divergence since every codon within a protein coding sequence can evolve independently and at different rates than the rest in the sequence (Skaloud and Peska 2010). Single-copy protein genes, such as the β-actin gene, do not undergo concerted evolution (though multicopy protein-coding genes can), which may result in potentially higher divergence rates compared to the ITS region (Liao 1999). The difference divergence rates between the tandemly repeating gene regions and single-copy protein coding genes could result in different phylogenetic signals, causing incongruence between the gene phylogenies.

4.5 Haplotype networks and phylogenies did not correspond to geographic location

While the topologies of the ITS1, ITS2, and β-actin phylogenies were incongruent, the most dominant haplotypes clustered together in all of the ML phylogenies. Furthermore, the

resolution into broad clades was also shared with resolution into dominant haplotype networks. The clades of the ML trees and haplotype networks demonstrate the association between genealogical relationships and genetic relatedness. Both methods use DNA sequence variation to construct relationships among the species being examined (Mardulyn 2012). However, there are key differences between the two methods. Phylogenies show the relationship of evolutionary changes that have diverged from a common ancestor based on how likely certain types of transversions and transitions (calculated with the Kimura 2 parameter) occur using the support of robust statistical permutations (Clement et al. 2000). Phylogenetic analyses, such as ML, assume that ancestral haplotypes will not be present in the population, since they have diverged over a long period of time. In contrast, in a small scale study long-term divergence may not have occurred (or been detected) and so ancestral haplotypes may be the most common (Clement et al. 2000). Haplotype networks can detect genetic similarities between individuals in a population, without being concerned about ancestral lineages (Clement et al. 2000). Haplotype networks are used most often to assess gene flow since they measure the association (or how similar samples are genetically based on single nucleotide polymorphisms (SNPs)), and can be a true measure of genetic relatedness over a landscape (Teacher and Griffiths 2011). The larger number of nodes between samples in the network, suggests that more recombination (through SNPs, genetic drift, horizontal gene transfer, etc) has occurred (Clement et al. 2000; Mardulyn 2012). Phylogenies would not be able to detect these small scale changes in genetic sequences since mutations are assumed to be linear, with one change leading to another (Clement et al. 2000; Ruda 2011). This could be why the largest clades within the ITS1, ITS2, and β-actin phylogenies were unresolved, containing the dominant haplotypes, but not in distinct groups. The ML phylogenies of the ITS1, ITS2, and β-actin showed that the samples investigated belonged to the same species (based on

previously known species being incorporated into the phylogeny) due to common changes from a common ancestor, while the haplotype networks would provide fine detail changes in the genetic structure between them.

While the phylogenies and haplotype networks of the ITS1, ITS2, and β-actin were similar, samples did not cluster based on location within Payuk Lake. For example, samples that fell within N1 were found in all areas around Payuk Lake (Figures 3.14, 3.15, and 3.16), rather in distinct bays or inflow sources. In all of landscape hypotheses (Wind, Hydrology, In-Out-Bay, and Bay Topography), high gene flow was found in the ITS1, ITS2, and β-actin genes using all three distance measures (Euclidean, shoreline, and hydrological network; Table 3.1). High gene flow has been found to reduce algal population structure in lichen thalli growing adjacent to one another (Doering and Piercey-Normore 2009), which is similar to this study. Samples in specific locations around the lake may not have clustered into distinct groups within the phylogenetic trees or haplotype networks because there was high gene flow of the dominant haplotypes between geographically close thalli, thus reducing population structure resulting in low resolution within the trees and networks.

High gene flow may be a result of dispersal of *Di. chodatii* within Payuk Lake. Freshwater and terrestrial algae are most commonly dispersed by wind or water (Kristiansen 1996). Wind dispersal would result in a broader, more scattered dispersal pattern than water dispersal since the organisms would not be confined to the stream channel. In lichens, species that utilise wind dispersal would be expected to have smaller propagule sizes since the lighter, smaller propagules (such as soredia) could be potentially carried further that larger, heavier thallus fragments (Werth et al. 2014). Marshall (1996) suggested that codispersal in soredia is more abundant than ascospores in some Antarctic lichens, which rely heavily on wind dispersal

in this extreme environment. Terrestrial algae, which may include *Di. chodatii*, also commonly utilise wind dispersal (Broady 1996). Long distance dispersal in the atmosphere could carry ascospores or algal cells hundreds to thousands of kilometers away (Kristiansen 1996; Revill et al. 1967), dispersed as coenobia (Tormo et al. 2001). However, *De. luridum* does not produce soredia (Heiðmarsson 2000; Amtoft et al. 2008; Gueidan et al. 2009), so codispersal via wind of symbiotic propagules may not be a realistic method since only the heavy fragments of thallus lobes could serve as vegetative propagules, though they could be transported via animal vectors if they were picked up from the water. Yet some members of the Verrucariaceae have been known to codisperse both the mycobiont ascospores with the photobiont partner where some algae have been found within the perithecia along with the ascospores (Thüs et al. 2011; Gueidan et al. 2009). This has been seen in species of *Verrucaria*, *Staurothele*, and *Endocarpon*, but has not been observed in *Dermatocarpon* (Thüs et al. 2011; Gueidan et al. 2009). Microscopic examination of the perithecia of *De. luridum* would be needed to see if the photobiont was present within the hymenial layer (and therefore have the potential to codisperse during forceful expulsion of the ascospores).

In lichens, fragmentation is probably the most common form of dispersal (Thomson 1971; Tunjíc and Korać 2013). Water dispersal in the spring runoff carries ice-scoured lichen fragments downstream (Elridge 1996; Thomson 1971); however, the establishment of new thalli requires that the fragments be deposited in suitable habitats, which may be difficult due to currents, substrata surface properties, and other environmental characteristics (Armstrong 1981). If algae in the thallus fragments were water dispersed, it would be expected that genetic variation would follow hydrological patterns, or be uniform throughout the water system (Tunjíc and Korać 2013). In this study, haplotypes that were found in both the ITS1/ITS2 and β-actin were

present in both the inflow creeks as well as the outflow creek (Figures 3.14, 3.15, and 3.16). Furthermore, haplotypes that were found in one creek but not the other (i.e. Mistik Creek but not Twin Creek and vice-versa) also occurred in the outflow based on the haplotype networks, suggesting that some transport of alleles may be occurring within the lake. The interpretation of dispersal within the lake is also supported by Fontaine et al. (2013), who found that haplotypes of *Di. chodatii* accumulated downstream from Naosap Lake at the source of Mistik Creek where it flows into Payuk Lake near the end of the lake chain.

In the case of *Di. chodatii*, dispersal may utilise both types of vectors, wind and water. *Lasallia pustulata* (L.) Mérat, a peltate lichen that occurs in similar habitats as *De. luridum*, since it may grow on rocky outcrops near coasts and flowing streams (Hestmark et al. 2016), as well as boulders in open heathland, may employ water dispersal for asexual fragments and wind dispersal for sexual ascospores (Hestmark 1992), which is important because life history strategies are known to shape population structure, such as in *Umbilicaria* spp. (Cao et al. 2015). Since haplotypes that were found in both Mistik Creek and Twin Creek were also found in the outflow, it suggests that the photobiont is being carried downstream, possibly through fragmentation. Payuk Lake is a typical northern boreal lake that experiences annual freeze-thaw cycles, which could shred the thalli along the shore into pieces to be carried downstream. Furthermore, free-living *Di. chodatii* may be found on the surrounding cliffs, and the annual spring thaw could result in it being carried from the top of the cliffs into the water system. However, wind dispersal may also be occurring. Fontaine et al. (2013) found that there were few shared haplotypes of Payuk Lake samples (in Canada) with *Di. chodatii* samples from Austria. Furthermore, it was found in this study that there were related haplotypes between Payuk Lake and Whiteshell Provincial Park (some 800 km southeast of Payuk Lake), which are not

connected by the same water system. Since the genetic similarity may be part of the hereditary history of *Di. chodatii*, which may have not yet diverged (Tunjíc and Korać 2013), it seems unlikely that the two populations exhibited coevolution, suggesting that wind dispersal, though limited, may be occurring. The closely related *Stichococcus* has been known to be transported via wind (Kristiansen 1996), so it is possible that *Diplosphaera* could also utilise wind as a dispersal vector. Lastly, long-distance dispersal may also be occurring via passive dispersal from birds, such as ducks, into the lake (Revill et al. 1967) and insects (van Overeem 1937), which can then be further facilitated via wind or water.

However, at local scales, size or dispersal vector may not be as important as other factors, such as topography, which may provide barriers to long distance dispersal (Werth et al. 2014). Payuk Lake contains many islands, which separate the two inflow channels (Figure 2.2; Figure 3.17). These islands contained unique ITS1 and ITS2 haplotypes (Figures 3.14 and 3.15)), which may have been transported there by the wind, blocking them from entering the Twin Creek channel. Also, spatial scale plays a large role in the patterns of genetic variation and inference of gene flow. Martiny et al. (2011) found that a spatial scale that is too large may prevent the detection of dispersal barriers at local scales in microorganisms, which would result in apparent high levels of gene flow. Since the whole lake was examined as the spatial extent for genetic variation in *Di. chodatii*, it may have been too large an area to detect smaller genetic variation within the species. Subdividing the lake into more locally defined populations, coupled with more extensive sampling within those populations using more gene regions containing suitable variation, may help to reveal more refined population structure. Additionally, the use of more genetic markers may provide a broader sampling of genetic variation, which can be assessed at various spatial scales.

CHAPTER 5 : CONCLUSIONS AND FUTURE DIRECTIONS

5.1 Conclusions

This thesis provides evidence to support water dispersal and some wind dispersal for *Di. chodatii* in Payuk Lake using spatial analyses and population genetics. This study is the first time, to my knowledge, that dispersal has been examined for photobionts using these GIS and spatial modelling methods. Landscape genetics, along with methods of isolation by distance, have been used to assess gene flow in lichen symbionts, but the use of modelling geological features, such as hydrology and net flow accumulation, as well as defining new landscape specific distance measures (shoreline and flow network), have not been used to infer dispersal based on correspondence to spatial patterns in genetic variation, though inference of dispersal has been done using the spatial distribution of haplotypes and Euclidean distances alone (Walser 2004). These types of landscape analyses help to paint a more realistic picture since they take into account physical barriers to gene flow and dispersal that simple isolation by distance measures cannot account for. These findings also have implications for risk assessment of this species and other species in the same ecological niche in this locality as well as more broadly on a global scale.

The first objective assessed the spatial distribution of genetic variation in *Diplosphaera chodatii*, in which it was hypothesised that populations closer together would be genetically more similar than populations further apart, or isolation by distance. Mantel's test revealed that gene flow was occurring between samples of *Di. chodatii* within Payuk Lake, though at a finer scale there was population structure due to the abundance of unique haplotypes found within the inflows, middle, and outflow of the lake. Rarefaction showed that the total genetic variation present within the partitioned ITS1 and ITS2 rDNA genes, as well as the β-actin gene, was

higher than expected since a plateau was not achieved. The predicted higher abundance of haplotypes present in the three genes may be a result of low sequencing success making the effective sample size smaller than the number of thalli which were actually collected, incomplete primer binding or other mismatch issues with the markers overestimating the variation present, or from an ecological perspective, the introduction of immigrant haplotypes from free-living *Di. chodatii* that were potentially recently lichenised or found on the lichen thallus. The measure of distance throughout the lake did not take into account distance away from the shore line, which is where runoff may introduce these immigrant haplotypes into the lake system.

The second objective compared hydrological movement and other models with haplotype variation in *Di. chodatii* since it was expected that haplotype numbers around Payuk Lake would correspond with net hydrological flow or inflow sources if the alga was dispersed by water currents. Dispersal by water was supported by the maximum likelihood phylogenies and haplotype networks of the ITS1, ITS2, and β-actin genes from *Di. chodatii* samples collected within Payuk Lake, and further upstream. However, they did not correspond to geographical location suggesting that the effectiveness of the dispersal vectors, water and wind, was extensive within the lake, and the geographic area of the lake was too small to support isolation by distance. Incongruence between the phylogenies and haplotype networks is difficult to explain but may be the result of evolutionary divergence of the two genes or additional substitutions in the DNA sequences resulting in a larger number of haplotypes. Furthermore, it was found that *Di. chodatii* may utilise multiple modes of dispersal since the Wind landscape hypothesis (based on dominant wind directions) exhibited the most genetic variation in the ITS1 and ITS2 rDNA gene regions while the Hydrology landscape hypothesis supported the prediction of water dispersal (based on β-actin), since haplotypes found in the inflows were also present in the

outflow. Furthermore, haplotypes found farther upstream (Fontaine et al. 2013) were also identical to haplotypes found within Payuk Lake, suggesting long distance transport may be facilitated through Mistik Creek. Dispersal by water would suggest that algal populations would be structured by lake and even more structured by watershed, which is seen in populations of other aquatic algae and protistan organisms.

The last objective isolated and cultured the lichen alga and the algae in the immediate vicinity on rocks to determine whether *Di. chodatii* was available in a free-living form for potential switching between free-living and lichenised forms. Free-living *Di. chodatii* was found in Payuk Lake based on microscopic examination of cultured rock scraping samples, and further evidence was provided by the amplification of a discrete band for the ITS rDNA using *Diplosphaera*-specific primers in PCR. Six other green algal taxa, and one cyanobacterium, were also found within the rock scraping samples, as well as the lichenised algal samples, suggesting that "epiphytic" algae may exist within micro-niches of the lichen thallus and on the rock in the vicinity of the lichen. The presence of free-living *Di. chodatii* on the rock around the lichen thallus has implications in the potential establishment of this and other semi-aquatic lichens. Since other lichen-forming fungal species such as *Staurothele fissa*, *Dermatocarpon miniatum*, are believed to associate with this alga, the dispersed fungal spores landing on the rock surface have a pool of free-living algae from which to choose as a photobiont in developing symbiotic thalli. Furthermore, if photobiont switching does occur in *De. luridum*, switching haplotypes from the photobiont with those of free-living *Di. chodatii* may allow for increased adaptation to changing microhabitat and water conditions due to climate change or increased human activity.

5.2 Future Directions

While this study was extensive, the research could benefit from some improvements. Further sequencing of the ITS rDNA and β-actin genes, as well as the use of additional multi-locus markers and further assessment of population structure, may help to obtain greater genetic variation present within the lake. Many unique haplotypes found may actually not be unique at all but were not sampled enough to group them into dominant haplotype networks. Also, although free-living *Di. chodatii* was present, the amount of genetic variation that was contributed to the gene pool was not quantified, so the role of free-living *Di. chodatii* within the population still remains undetermined. Lastly, sampling of the water column, as well as obtaining bathymetric, hydrological, and wind pattern data for Payuk Lake would further clarify the type of dispersal exhibited by *Di. chodatii*.

More broadly, the methods and results of this study have the potential to be used to understand other lichens and organisms within aquatic systems. For example, assessment of the genetic spatial variation of the mycobiont, *De. luridum*, would allow the investigation of whether it displays the same spatial patterns in genetic variation as the photobiont. Investigation into spatial variation may help to elucidate whether these two symbionts undergo coevolution, which would be important for inhabiting such ecologically challenging semi-aquatic habitats. Furthermore, the spatial techniques and modelling used in this study could be applied to the study of other co-occurring lichens, such as the threatened *Leptogium rivulare*, as well other aquatic and semi-aquatic lichens. On a larger scale, these methods could also be applied to the study of dispersal and movement of fishes, vegetation, and other aquatic organisms since barriers to gene flow and dispersal can be accounted for in the modelling of net flow within a hydrological system.

Since water can carry new sources of genetic variation through the fragmentation of this semi-aquatic lichen from further upstream, it is important that conservation efforts focus on protecting streams and waterways in which these lichens occur. Payuk Lake was seen to have a high level of genetic variation in *Di. chodatii* populations, and may be able to support genetically unique populations of lichen fungi that associate with this alga, as well as rare or threatened lichens that are known to co-occur within the same habitat. Discovery of new genetic diversity in the same and other species is especially important with regards to climate change. Increasing precipitation could result in higher than normal water levels, which may kill *De. luridum* (and other semi-aquatic and terrestrial lichens occurring near the water) since it is not truly aquatic. In contrast, extreme dry spells could result in lower water levels and long term desiccation, which could also prevent the semi-aquatic lichens from thriving and establishing new populations through dispersal, especially if *De. luridum* and its photobiont disperses by water. The lichen appears to need fluctuating water levels throughout the year where water levels tend to be high in the spring and lower in the summer and fall. Implementation of protective measures for this lake and those further upstream would conserve this unique ecosystem so that it may continue to support lichens, and other sensitive organisms.

This study helped to understand the population structure and method of dispersal of *Di. chodatii* in a northern lake in Manitoba using indirect inferences from patterns in genetic variation and microscopic examination. The fungus *De. luridum*, which associates with *Di. chodatii*, may also be important as an indicator of environmental change in the water system and the niche at the edge of the water for less sensitive lichen species, endangered or threatened species, and the microbial populations that occur in the area. The monitoring of *De. luridum* populations may also provide an indication of the health of the ecosystem in the waterway. By

understanding how dispersal, and therefore potential establishment, occurs within this semi-aquatic lichen, other co-occurring sensitive species such as *Leptogium rivulare* can also be understood and its habitat conserved since barriers to dispersal can be identified.

LITERATURE CITED

Ahmadjian, V. 1993. The Lichen Symbiosis. 2nd edition. Wiley.

Akaike, H. 1974. A new look at the statistical model identification. IEEE Trans. Automat. Contr. **19**(6): 716–723. doi:10.1109/TAC.1974.1100705.

Amtoft, A., Lutzoni, F., and Miadlikowska, J. 2008. *Dermatocarpon* (Verrucariaceae) in the Ozark Highlands, North America. Bryologist **111**(1): 1–40. doi:10.1639/0007-2745(2008)111[1:DVITOH]2.0.CO;2.

Aptroot, A., and Seaward, M.R.D. 2003. Freshwater lichens. Fungal Dviersity Res. Ser. **10**: 101–110.

Armstrong, R.A. 1981. Field experiments on the dispersal, establishment and colonization of lichens on a slate rock surface. Environ. Exp. Bot. **21**(1): 115–120. doi:10.1016/0098-8472(81)90016-2.

Armstrong, R.A. 1987. Dispersal in a population of the lichen *Hypogymnia physodes*. Environ. Exp. Bot. **27**(3): 357–363. doi:10.1016/0098-8472(87)90046-3.

Bailey, R.H. 1967. Dispersal of lichen soredia in water trickles. Rev. Bryol. Lichenol. **35**: 314–315.

Beck, A. 1999. Photobiont inventory of a lichen community growing on heavy-metal-rich rock. Lichenol. **31**(5): 501–510. doi:10.1006/lich.1999.0232.

Beck, A., Friedl, T., and Rambold, G. 1998. Selectivity of photobiont choice in a defined lichen community: inferences from cultural and molecular studies. New Phytol. **139**(4): 709–720. doi:10.1046/j.1469-8137.1998.00231.x.

Beck, A., Kasalicky, T., and Rambold, G. 2002. Myco-photobiontal selection in a Mediterranean cryptogam community with *Fulgensia fulgida*. New Phytol. **153**(2): 317–326. doi:10.1046/j.0028-646X.2001.00315.x.

Beckett, R., Minibayeva, F. V., and Liers, C. 2012. Occurrence of high tyrosinase activity in the non-Peltigeralean lichen *Dermatocarpon miniatum* (L.) W. Mann. Lichenol. **44**(6): 827–832. doi:10.1017/S0024282912000394.

Beiggi, S., and Piercey-Normore, M.D. 2007. Evolution of ITS ribosomal RNA secondary structures in fungal and algal symbionts of selected species of *Cladonia* sect. *Cladonia* (Cladoniaceae, Ascomycotina). J. Mol. Evol. **64**(5): 528–542. doi:10.1007/s00239-006-0115-x.

Bhattacharya, D., and Ehlting, J. 1995. Actin coding regions: gene family evolution and use as a phylogenetic marker. Arch. für Protistenkd. **145**(3–4): 155–164. doi:10.1016/S0003-9365(11)80312-X.

Bialosuknia, M.W. 1909. Sur un nouveau genre de pleurococcacées. Bull. la Société Bot. Geneve, Série 2 **1**: 101–104.

Bischoff, H.W., and Bold, H.C. 1963. Some soil algae from enchanted rock and related algal

species. Phycol. Stud. IV **6318**: 1–95.

Bittencourt-Oliveira, M.D.C., Massola, N.S., Hernandez-Marine, M., Romo, S., and Moura, A.D.N. 2007. Taxonomic investigation using DNA fingerprinting in *Geitlerinema* species (Oscillatoriales, Cyanobacteria). Phycol. Res. **55**(3): 214–221. doi:10.1111/j.1440-1835.2007.00464.x.

Branquinho, C., Matos, P., Vieira, A.R., and Ramos, M.M.P. 2011. The relative impact of lichen symbiotic partners to repeated copper uptake. Environ. Exp. Bot. **72**(1): 84–92. Elsevier B.V. doi:10.1016/j.envexpbot.2010.09.016.

Broady, P.A. 1996. Diversity, distribution and dispersal of Antarctic terrestrial algae. Biodivers. Conserv. **5**(11): 1307–1335. doi:10.1007/BF00051981.

Brodo, I.M., and Sloan, N.A. 2004. Lichen zonation on coastal rocks in Gwaii Haanas National Park Reserve, Haida Gwaii (Queen Charlotte Islands), British Columbia. Can. Field-Naturalist **118**(3): 405–424.

Buxton, A.S., Groombridge, J.J., Zakaria, N.B., and Griffiths, R.A. 2017. Seasonal variation in environmental DNA in relation to population size and environmental factors. Sci. Rep. **7**(April): 46294. Nature Publishing Group. doi:10.1038/srep46294.

del Campo, E.M., Casano, L.M., Gasulla, F., and Barreno, E. 2010. Suitability of chloroplast LSU rDNA and its diverse group I introns for species recognition and phylogenetic analyses of lichen-forming *Trebouxia* algae. Mol. Phylogenet. Evol. **54**(2): 437–444. Elsevier Inc. doi:10.1016/j.ympev.2009.10.024.

Cao, S., Zhang, F., Liu, C., Hao, Z., Tian, Y., Zhu, L., and Zhou, Q. 2015. Distribution patterns of haplotypes for symbionts from *Umbilicaria esculenta* and *U. muehlenbergii* reflect the importance of reproductive strategy in shaping population genetic structure. BMC Microbiol. **15**(1): 212. BMC Microbiology. doi:10.1186/s12866-015-0527-0.

Carey, S.K., and Woo, M-K. 1999. Hhydrology of two slopes in subarctic Yukon, Canada. Hydrol. Proc. **13**(16): 2549–2562. doi: 10.1002/(SICI)1099-1085(199911)13:16<2549::AID-HYP938>3.0.CO;2-H.

Chase, M.W., Salamin, N., Wilkinson, M., Dunwell, J.M., Kesanakurthi, R.P., Haidar, N., and Savolainen, V. 2005. Land plants and DNA barcodes: short-term and long-term goals. Philos. Trans. R. Soc. B Biol. Sci. **360**(1462): 1889–1895. doi:10.1098/rstb.2005.1720.

Chen, L., Liu, P., Evans, T.C., and Ettwiller, L.M. 2017. DNA damage is a major cause of sequencing errors, directly confounding variant identification. Science. **355**: 752–756. doi:10.1101/070334.

Chodat, R. 1913. Monographies d'algues en culture pure. Matériaux pour la Flore Cryptogam. Suisse **4**: 1–266.

Clement, M., Posada, D., and Crandall, K.A. 2000. TCS: A computer program to estimate gene genealogies. Mol. Ecol. **9**(10): 1657–1659. doi:10.1046/j.1365-294X.2000.01020.x.

Coleman, A.W. 2015. Nuclear rRNA transript processing versus interal transcribed spacer secondary structure. Trends Genet. **31**(3): 157–163. doi: 10.1016/j.tig.2015.01.002.

Coleman, A.W. 2003. ITS2 is a double-edged tool for eukaryote evolutionary comparisons. Trends Genet. **19**(7): 370–375. doi:10.1016/S0168-9525(03)00118-5.

Coleman, A.W., and Mai, J.C. 1997. Ribosomal DNA and ITS-2 sequence comparisons as a tool for predicting genetic relatedness. J. Mol. Evol. **45**(2): 168–177. doi:10.1007/PL00006217.

Coleman, A.W., Maria Preparata, R., Mehrotra, B., and Mai, J.C. 1998. Derivation of the secondary structure of the ITS-1 transcript in Volvocales and its taxonomic correlations. Protist **149**(2): 135–46. Elsevier. doi:10.1016/S1434-4610(98)70018-5.

Coppins, B.J. 1983. A taxonomic study of the lichen genus *Micarea* in Europe. Bull. Br. Museum (Nat. Hist.) **11**(2): 17–214.

Cordeiro, L.M.C., Reis, R.A., Cruz, L.M., Stocker-Wörgötter, E., Grube, M., and Iacomini, M. 2005. Molecular studies of photobionts of selected lichens from the coastal vegetation of Brazil. FEMS Microbiol. Ecol. **54**(3): 381–390. doi:10.1016/j.femsec.2005.05.003.

COSEWIC. 2004. COSEWIC assessment and status report on the flooded jellyskin *Leptogium rivulare* in Canda. Committee on the Status of Endangered Wildlife in Canada. Ottawa. vi + 30pp. [online]. Available at www.sararegistry.gc.ca/status/status_e.cfm. Accessed 14 November 2014.

Dal Grande, F., Alors, D., Divakar, P.K., Bálint, M., Crespo, A., and Schmitt, I. 2014a. Insights into intrathalline genetic diversity of the cosmopolitan lichen symbiotic green alga *Trebouxia decolorans* Ahmadjian using microsatellite markers. Mol. Phylogenet. Evol. **72**(1). doi:10.1016/j.ympev.2013.12.010.

Dal Grande, F., Beck, A., Cornejo, C., Singh, G., Cheenacharoen, S., Nelsen, M.P., and Scheidegger, C. 2014b. Molecular phylogeny and symbiotic selectivity of the green algal genus *Dictyochloropsis* s.l. (Trebouxiophyceae): a polyphyletic and widespread group forming photobiont-mediated guilds in the lichen family Lobariaceae. New Phytol. **202**(2): 455–470. doi:10.1111/nph.12678.

Dal Grande, F., Widmer, I., Beck, A., and Scheidegger, C. 2010. Microsatellite markers for *Dictyochloropsis reticulata* (Trebouxiophyceae), the symbiotic alga of the lichen *Lobaria pulmonaria* (L.). Conserv. Genet. **11**(3): 1147–1149. doi:10.1007/s10592-009-9904-2.

Dal Grande, F., Widmer, I., Wagner, H.H., and Scheidegger, C. 2012. Vertical and horizontal photobiont tramission within populations of a lichen symbiosis. Mol. Ecol. **21**: 3159–3172.

Dale, M.R.T., and Fortin, M-J. 2014. Spatial analysis: A guide for ecologists, 2nd edition. Cambride University Press, Cambridge.

Davis, W.C., Gries, C., and Nash, T.H. 2000. The ecophysiological response of the aquatic lichen *Hydrothyria venosa* to nitrates in terms of with and photosythesis over long periods of time. Bibl. Lichenol. **75**: 201–208.

Davis, W.C., Gries, C., and Nash, T.H. 2003. The influence of temperature on the weight and net photosynthesis of the aquatic lichen *Peltigera hydrothyria* over long periods of time. Bibl. Lichenol. **86**: 233–242..

Deduke, C., Timsina, B., and Piercey-Normore, M.D. 2012. Effect of environmental change on

secondary metabolite production in lichen-forming fungi. *In* International Perspectives on Global Environmental Change. *Edited by* S.S. Young and S.E. Silvern. InTech Open, . doi:10.5772/26954.

Dennis, W.M., Collier, P.A., DePriest, P., and Morgan, E.L. 1981. Habitat notes on the aquatic lichen *Hydrotheria venosa* Russell in Tennessee. Bryologist **84**(3): 402. doi:10.2307/3242862.

Depriest, P.T. 2004. Early molecular investigations of lichen-forming symbionts: 1986-2001. Annu. Rev. Microbiol. **58**: 273–301. doi:10.1146/annurev.micro.58.030603.123730.

Derycke, S., Backeljau, T., Vlaeminck, C., Vierstraete, A., Vanfleteren, J., Vincx, M., and Moens, T. 2006. Seasonal dynamics of population genetic structure in cryptic taxa of the *Pellioditis marina* complex (Nematoda: Rhabditida). Genetica **128**(1–3): 307–321. doi:10.1007/s10709-006-6944-0.

Doering, M., and Piercey-Normore, M.D. 2009. Genetically divergent algae shape an epiphytic lichen community on Jack Pine in Manitoba. Lichenol. **41**(1): 69–80. doi:10.1017/S0024282909008111.

Eldridge, D.J. 1996. Dispersal of microphytes by water erosion in an Australian semi-arid woodland. Lichenol. **28**(1) 97–100.

Elshobary, M.E., Osman, M.E.H., Abushady, A.M., and Piercey-Normore, M.D. 2015. Comparison of lichen-forming cyanobacterial and green algal photobionts with free-living algae. Cryptogam. Algol. **36**(1): 81–100. doi:10.7872/crya.v36.iss1.2015.81.

ESRI. 2013. ArcGIS Desktop: Release 10.2. Redlands, CA: Environmental Systems Research Institute.

Esslinger, T. 2011. A cumulative checklist for the lichen-forming, lichenicolous and allied fungi of the continental United States and Canada [online]. Available from http://www.ndsu.edu/pubweb/~esslinge/chcklst/chcklst7.htm [accessed 1 June 2015].

Ettl, H., and Gärtner, G. 1995. Syllabus der Boden-, Luft- und Flechtenalgen. Gustav Fischer Verlag, Stuttgart, Germany.

Ewing, B., and Green, P. 1998. Base-calling of automated sequencer traces using Phred. II. Error probabilities. Genome Res. **8**: 186–194. doi:10.1101/gr.8.3.175.

Excoffier, L., Smouse, P.E., and Quattro, J.M. 1992. Analysis of molecular variance inferred from metric distances among DNA haplotypes: Application to human mitochondrial DNA restriction data. Genetics **131**(2): 479–491. doi:10.1007/s00424-009-0730-7.

Fernández-Mendoza, F., Domaschke, S., García, M.A., Jordan, P., Martín, M.P., and Printzen, C. 2011. Population structure of mycobionts and photobionts of the widespread lichen *Cetraria aculeata*. Mol. Ecol. **20**(6): 1208–1232. doi:10.1111/j.1365-294X.2010.04993.x.

Flechtner, V.R., Johansen, J.., and Clark, W.. 1998. Algal composition of microbiotic crusts from the central desert of Baja California, Mexico. Gt. Basin Nat. **58**(4): 95–311.

Flechtner, V.R., Johansen, J.R., and Belnap, J. 2008. The Biological soil crusts of the San

Nicolas Island: enigmatic algae from a geographically isolated ecosystem. West. North Am. Nat. **68**(4): 405–436. doi:10.3398/1527-0904-68.4.405.

Fletcher, A. 1973. The ecology of marine (littoral) lichens on some rocky shores of Anglesey. Lichenol. **5**(5–6): 368–400. doi:10.1017/S0024282973000459.

Fontaine, K.M. 2013. An investigation of the symbiotic association between the sub-aquatic fungus *Dermatocarpon luridum* var. *luridum* and its green algal photobiont. M.Sc. thesis, Department of Biological Sciences. Univesity of Manitoba, WInnipeg, Manitoba.

Fontaine, K.M., Beck, A., Stocker-Wörgötter, E., and Piercey-Normore, M.D. 2012. Photobiont relationships and phylogenetic history of *Dermatocarpon luridum* var. *luridum* and related *Dermatocarpon* species. Plants **1**(2): 39–60. doi:10.3390/plants1020039.

Fontaine, K.M., Booth, T., Deduke, C., and Piercey-Normore, M.D. 2014. Notes on the species assemblage of the lichen *Dermatocarpon luridum* in Northwestern Manitoba, Canada. Evansia **31**(2): 69–74. doi:10.1639/079.031.0201.

Fontaine, K.M., Stocker-Wörgötter, E., Booth, T., and Piercey-Normore, M.D. 2013. Genetic diversity of the lichen-forming alga, *Diplosphaera chodatii*, in North America and Europe. Lichenol. **45**(6): 799–813. doi:10.1017/S0024282913000510.

Francisco de Oliveira, P.M., Timsina, B., and Piercey-Normore, M.D. 2012. Diversity of *Ramalina sinensis* and its photobiont in local populations. Lichenol. **44**(5): 649–660. doi:10.1017/S0024282912000217.

Friedl, T., Besendahl, A., Pfeiffer, P., and Bhattacharya, D. 2000. The distribution of group I introns in lichen algae suggests that lichenization facilitates intron lateral transfer. Mol. Phylogenet. Evol. **14**(3): 342–352. doi:10.1006/mpev.1999.0711.

Friedl, T., and Büdel, B. 2008. Photobionts. *In* Lichen Biology, 2nd edition. *Edited by* T.H. Nash III. Cambridge University Press, Cambridge. pp. 9–26.

Friedl, T., and O'Kelly, C.J. 2002. Phylogenetic relationships of green algae assigned to the genus *Planophila* (Chlorophyta): evidence from 18S rDNA sequence data and ultrastructure. Eur. J. Phycol. **37**(3): S0967026202003712. doi:10.1017/S0967026202003712.

Fröberg, L., Berg, C.O., Baur, A., and Baur, B. 2001. Viability of lichen photobionts after passing through the digestive tract of a land snail. Lichenol. **33**(6): 543–545. doi:10.1006/lich.2001.0355.

Gasulla, F., Guéra, A., and Barreno, E. 2010. A simple and rapid method for isolating lichen photobionts. Symbiosis **51**(2): 175–179. doi:10.1007/s13199-010-0064-4.

Gilbert, O.L. 1996. The lichen vegetation of chalk and limestone streams in Britain. Lichenol. **28**(2): 145–159. doi:10.1006/lich.1996.0013.

Gilbert, O.L. 2000. The lichen vegetation of lake margins in Britain. Lichenol. **32**(4): 365–386. doi:10.1006/lich.2000.0270.

Gilbert, O.L., and Giavarini, V.J. 1997. The lichen vegetation of acid watercourses in England.

Lichenol. **29**(4): 347–367. doi:10.1017/S0024282997000418.

Glavich, D.A. 2009. Distribution, rarity and habitats of three aquatic lichens on federal land in the U.S. Pacific Northwest. Bryologist **112**(1): 54–72. doi:10.1639/0007-2745-112.1.54.

Gontcharov, A.A., Marin, B., and Melkonian, M. 2004. Are combined analyses better than single gene phylogenies? A case study using SSU rDNA and *rbc*L sequence comparisons in the Zygnematophyceae (Streptophyta). Mol. Biol. Evol. **21**(3): 612–624. doi: 10.1093/molbev/msh052.

Grube, M., and Muggia, L. 2010. Identifying algal symbionts in lichen symbioses. *In* Tools for identifying biodiversity: progress and problems. *Edited by* L.. Nimis, P. L.; Vignes. pp. 295–299.

Gueidan, C., Savić, S., Thüs, H., Roux, C., Keller, C., Tibell, L., Prieto, M., Heissmarsson, S., Breuss, O., Orange, A., Fröberg, L., Wynns, A.A., Navarro-Rosinés, P., Krzewicka, B., Pykälä, J., Grube, M., and Lutzoni, F. 2009. Generic classification of the Verrucariaceae (Ascomycota) based on molecular and morphological evidence : recent progress and remaining challenges. Taxon **58**(1): 184–208.

Guiry, M.D. 2012. How many species of algae are there? J. Phycol. **48**(5): 1057–1063. doi:10.1111/j.1529-8817.2012.01222.x.

Guzow-Krzeminska, B. 2006. Photobiont flexibility in the lichen *Protoparmeliopsis muralis* as revealed by ITS rDNA analyses. Lichenol. **38**(5): 469–476. doi:10.1017/S0024282906005068.

Hachułka, M. 2013. Freshwater lichens on submerged stones and alder roots in the Polish lowlands. Acta Mycol. **46**(2): 233–244. doi:10.5586/am.2011.016.

Hale, M.E. 1974. The Biology of Lichens, 2nd edition. Edward Arnold, London.

Hall, J.D., Fucikova, K., Lo, C., Lewis, L.A., and Karol, K.G. 2010. An assessment of proposed DNA barcodes in freshwater green algae. Cryptogam. Algol. **31**(4): 529–555.

Handa, S., Nakahara, M., Nakano, T., Itskovich, V.B., and Masuda, Y. 2001. Aerial algae from southwestern area of Lake Baikal. Hikobia **13**(3): 463–472.

Hanyuda, T., Arai, S., and Ueda, K. 2000. Variability in the rbcL introns of Caulerpalean algae (Chlorophyta, Ulvophyceae). J. Plant Res. **113**(4): 403–413. doi:10.1007/PL00013948.

Harada, H. 1993. A taxonomic study on *Dermatocarpon* and its allied genera (Lichens, Verucariaceae) in Japan. Nat. Hist. Res **2**(March): 113–152.

Hausner, G., and Wang, X. 2005. Unusual compact rDNA gene arrangements within some members of the Ascomycota: evidence for molecular co-evolution between ITS1 and ITS2. Genome **48**(4): 648–660. doi:10.1139/g05-037.

Hawksworth, D.L. 2000. Freshwater and marine lichen-forming fungi. Fungal Divers. **5**: 1–7.

Hawksworth, D.L., and Hill, D.J. 1984. The lichen-forming fungi. Chapman & Hall.

Heering, W. 1914. Ulotrichales, Mikrosporales, Oedogoniales. *In* Die Susswasserflora

Deutschlands Osterreichs und der Schweiz, Heft 6, Chlorophyceae. *Edited by* A. Pascher. G. Fisher, Jena. pp. 51–53.

Heiđmarsson, S. 1996. Pruina as a taxonomic character in the lichen genus *Dermatocarpon*. Bryologist **99**(3): 315–320.

Heiđmarsson, S. 1998. Species delimitation in four long-spored species of *Dermatocarpon* in the Nordic countries. Ann. Bot. Fenn. **35**(April): 59–70.

Heiđmarsson, S. 2000. The genus *Dermatocarpon* (Verrucariales, lichenized Ascomycotina) in the Nordic countries. Nord. J. Bot. **20**(5): 605–639. doi:10.1111/j.1756-1051.2000.tb01612.x.

Heiđmarsson, S. 2003. Molecular study of *Dermatocarpon miniatum* (Verrucariales) and allied taxa. Mycol. Res. **107**(4): 459–468. doi:10.1017/S0953756203007652.

Helms, G. 2001. Identification of photobionts from the lichen family Physciaceae using algal-specific ITS rDNA sequencing. Lichenol. **33**(1): 73–86. doi:10.1006/lich.2000.0298.

Hestmark, G. 1992. Sex, size, competition and escape-strategies of reproduction and dispersal in *Lasallia pustulata* (Umbilicariaceae, Ascomycetes). Oecologia **92**(3): 305–312. doi:10.1007/BF00317455.

Hestmark, G., Lutzoni, F., and Miadlikowska, J. 2016. Photobiont associations in co-occurring umbilicate lichens with contrasting modes of reproduction in coastal Norway. Lichenol. **48**(5): 545–557. doi:10.1017/S0024282916000232.

Hill, D.J. 2009. Asymmetric co-evolution in the lichen symbiosis caused by a limited capacity for adaptation in the photobiont. Bot. Rev. **75**(3): 326–338. doi:10.1007/s12229-009-9028-x.

Hill, D.J., and Ahmadjian, V. 1972. Relationship between carbohydrate movement and the symbiosis in lichens with green algae. Planta **103**(3): 267–277. doi:10.1007/BF00386850.

Hirose, N., Nishimura, K., Inoue-Sakamoto, M., and Masuda, M. 2013. Ribosomal internal transcribed spacer of *Prototheca wickerhamii* has characteristic structure useful for identification and genotyping. PLoS One **8**(11): e81223. doi:10.1371/journal.pone.0081223.

Hodkinson, B.P., Moncada, B., and Lücking, R. 2014. Lepidostromatales, a new order of lichenized fungi (Basidiomycota, Agaricomycetes), with two new genera, *Ertzia* and *Sulzbacheromyces*, and one new species, *Lepidostroma winklerianum*. Fungal Divers. **64**(1): 165–179. doi:10.1007/s13225-013-0267-0.

van den Hoek, C., Mann, D.G., and Jahns, H.M. 1995. Algae: An introuction to phycology. Cambridge University Press.

Holderegger, R., and Wagner, H.H. 2006. A brief guide to landscape genetics. Landsc. Ecol. **21**(6): 793–796. doi:10.1007/s10980-005-6058-6.

Holzinger, A. 2009. Desiccation tolerant green algae: implications of physiological adaptation and structural requirements. *In* Algae: nutrition, pollution control and energy sources. *Edited by* K.. Hagen. Nova Science, New York. pp. 41–56.

Holzinger, A., Lütz, C., and Karsten, U. 2011. Desiccation stress causes structural and ultrastructural alterations in the aeroterrestrial green alga *Klebsormidium crenulatum* (Klebsormidiophyceae, Streptophyta) isolated from an alpine soil crust. J. Phycol. **47**(3): 591–602. doi:10.1111/j.1529-8817.2011.00980.x.

Honegger, R. 2008a. Mycobionts. *In* Lichen Biology, 2nd edition. *Edited by* T.H. Nash III. Cambridge University Press, Cambridge. pp. 27–39.

Honegger, R. 2008b. Morphogenesis. *In* Lichen Biology, 2nd edition. *Edited by* T.H. Nash III. Cambridge University Press, Cambridge. pp. 69–93.

Honegger, R., and Scherrer, S. 2008. Sexual reproduction in lichen-forming ascomycetes. *In* Lichen Biology, 2nd edition. *Edited by* T. Nash III. Cambridge University Press, Cambridge. pp. 94–103.

Honegger, R., Zippler, U., Gansner, H., and Scherrer, S. 2004. Mating systems in the genus *Xanthoria* (lichen-forming ascomycetes). Mycol. Res. **108**(5): 480–488. doi:10.1017/S0953756204009682.

Hur, J.-S., Harada, H., Oh, S.-O., Lim, K.-M., Wang, L.-S., Lee, S.M., Kim, G.-H., and Koh, Y.J. 2004. Taxonomic studies on *Dermatocarpon* (lichenized Ascomycota) and its allied fungi in South Korea. Korean J. Mycol. **32**(2): 66–70. doi:10.4489/KJM.2004.32.2.066.

Jacobs, J.B., and Ahmadjian, V. 1973. The ultrastructure of lichens V. *Hydrothyria venosa*, a freshwater lichen. New Phytol. **72**(1): 155–160. doi:10.1111/j.1469-8137.1973.tb02020.x.

John, D.M. 2003. Filamentous and plantlike green algae. *In* Freshwater Algae of North America: Ecology and Classification. *Edited by* J.D. Wehr and R.. Sheath. Academic Press Inc, Elsevier. pp. 311–352.

Karbovska, V.M., and Kostikov, I.Y. 2012. *Chlorella sphaerica* and its position in the genus *Diplosphaera* (Chlorophyta, Trebouxiophyceae). Visnyk Dnipropetr. Univ. Biol. Ecol. **20**(1): 34–42. doi:10.15421/011205.

Keller, C. 2005. Artificial substrata colonized by freshwater lichens. Lichenol. **37**(4): 357–362. doi:10.1017/S0024282905014672.

Kristiansen, J. 1996. 16. Dispersal of freshwater algae — a review. Hydrobiologia **336**(1–3): 151–157. doi:10.1007/BF00010829.

Kroken, S., and Taylor, J.W. 2000. Phylogenetic species, reproductive mode, and specificity of the green alga *Trebouxia* forming lichens with the fungal genus *Letharia*. Bryologist **103**(4): 645–660. doi:10.1639/0007-2745(2000)103[0645:PSRMAS]2.0.CO;2.

Kulichová, J., Škaloud, P., and Neustupa, J. 2014. Molecular diversity of green corticolous microalgae from two sub-Mediterranean European localities. Eur. J. Phycol. **49**(3): 345–355. doi:10.1080/09670262.2014.945190.

Kulikova, N.N., Suturin, A.N., Saibatalova, E. V., Boiko, S.M., Vodneva, E.N., Timoshkin, O.A., and Lishtva, A. V. 2011. Geologic and biogeochemical role of crustose aquatic lichens in Lake Baikal. Geochemistry Int. **49**(1): 66–75. doi:10.1134/S0016702910111023.

Lee, R.E. 2008. Phycology. 4th edition. Cambridge University Press, Cambridge.

Leliaert, F., Smith, D.R., Moreau, H., Herron, M.D., Verbruggen, H., Delwiche, C.F., and De Clerck, O. 2012. Phylogeny and molecular evolution of the green algae. CRC. Crit. Rev. Plant Sci. **31**(1): 1–46. doi:10.1080/07352689.2011.615705.

Liao, D. 1999. Concerted evolution: Molecular mechanism and biological implications. Am. J. Hum. Genet. **64**: 24–30.

Linblom, L. 2009. Sample size and haplotype richness in population samples of the lichen-forming ascomycete *Xanthoria parietina*. Lichenol. **41**(5): 529–535. doi:10.1017/S0024282909008743.

Lindner, D.L., and Banik, M.T. 2011. Intragenomic variation in the ITS rDNA region obscures phylogenetic relationships and inflates estimates of operational taxonomic units in genus *Laetiporus*. Mycologia **103**(4): 731–740. doi:10.3852/10-331.

Lukešová, A., and Hoffmann, L. 1996. Soil algae from acid rain impacted forest areas of the Krušnéhory Mts. 1. Algal communities. Vegetatio **125**(2): 123–136. doi:10.1007/BF00044646.

Lüttge, U., and Büdel, B. 2010. Resurrection kinetics of photosynthesis in desiccation-tolerant terrestrial green algae (Chlorophyta) on tree bark. Plant Biol. **12**(3): 437–444. doi:10.1111/j.1438-8677.2009.00249.x.

Mai, J.C., and Coleman, A.W. 1997. The internal transcribed spacer 2 exhibits a common secondary structure in green algae and flowering plants. J. Mol. Evol. **44**(3): 258–271. doi:10.1007/PL00006143.

Manel, S., and Holderegger, R. 2013. Ten years of landscape genetics. Trends Ecol. Evol. **28**(10): 614–621. doi:10.1016/j.tree.2013.05.012.

Mantel, N. 1967. The detection of disease clustering and a generalized regression approach. Cancer Res. **27**(2): 209–20.

Mardulyn, P. 2012. Trees and/or networks to display intraspecific DNA sequence variation? Mol. Ecol. **21**(14): 3385–3390. doi: 10.1111/j.1365-294X.2012.05622.x.

Marshall, W.A. 1996. Aerial dispersal of lichen soredia in the maritime Antarctic. New Phytol. **134**(3): 523–530. doi:10.1111/j.1469-8137.1996.tb04370.x.

Martiny, J.B.H., Eisen, J.A., Penn, K., Allison, S.D., and Horner-Devine, M.C. 2011. Drivers of bacterial -diversity depend on spatial scale. Proc. Natl. Acad. Sci. **108**(19): 7850–7854. doi:10.1073/pnas.1016308108.

McCarthy, P.M., and Healey, J.A. 1978. Dispersal of lichen propagules by slugs. Lichenol. **10**: 131–132.

McLeod, J.A. 1943. Report on a biological investigation of Payuk Lake and Payuk rapids. Department of Mines and Natural Resources: Game and Fisheries Branch, Winnipeg.

Meier, F.A., Scherrer, S., and Honegger, R. 2002. Faecal pellets of lichenivorous mites contain viable cells of the lichen-forming ascomycete *Xanthoria parietina* and its green algal

photobiont, *Trebouxia arboricola*. Biol. J. Linn. Soc. **76**(2): 259–268. doi:10.1046/j.1095-8312.2002.00065.x.

Millot, M., Di Meo, F., Tomasi, S., Boustie, J., and Trouillas, P. 2012. Photoprotective capacities of lichen metabolites: A joint theoretical and experimental study. J. Photochem. Photobiol. B Biol. **111**: 17–26. Elsevier B.V. doi:10.1016/j.jphotobiol.2012.03.005.

Moncalvo, J.M., and Buchanan, P.K. 2008. Molecular evidence for long distance dispersal across the Southern Hemisphere in the *Ganoderma applanatum-australe* species complex (Basidiomycota). Mycol. Res. **112**(4): 425–436. doi:10.1016/j.mycres.2007.12.001.

Monnet, F., Bordas, F., Deluchat, V., Chatenet, P., Botineau, M., and Baudu, M. 2005. Use of the aquatic lichen *Dermatocarpon luridum* as bioindicator of copper pollution: Accumulation and cellular distribution tests. Environ. Pollut. **138**(3): 455–461. doi:10.1016/j.envpol.2005.04.019.

Muggia, L., Vancurova, L., Škaloud, P., Peksa, O., Wedin, M., and Grube, M. 2013. The symbiotic playground of lichen thalli - a highly flexible photobiont association in rock-inhabiting lichens. FEMS Microbiol. Ecol. **85**(2): 313–323. doi:10.1111/1574-6941.12120.

Mukhtar, A., Garty, J., and Galun, M. 1994. Does the lichen algal *Trebouxia* occur free-living in nature: further immunological evidence. Symbiosis. **17**(2-3): 247–253.

Muñoz, J., Felicísimo, Á.M., Cabezas, F., Burgaz, A.R., and Martínez, I. 2004. Wind as a long-distance dispersal vehicle in the southern hemisphere. Science. **304**(May): 1144–1147. doi:10.1126/science.1095210.

Murtagh, G.J., Dyer, P.S., McClure, P.C., and Crittenden, P.D. 1999. Use of randomly amplified polymorphic DNA markers as a tool to study variation in lichen-forming fungi. Lichenol. **31**(3): 257–267. doi:10.1017/S0024282999000365.

Nakamura, Y., Leppert, M., O'Connell, P., Wolff, R., Holm, T., Culver, M., Martin, C., Fujimoto, E., Hoff, M., and Kumlin, E. 1987. Variable number of tandem repeat (VNTR) markers for human gene mapping. Science **235**(4796): 1616–22.

Nascimbene, J., and Nimis, P.L. 2006. Freshwater lichens of the Italian Alps : a review. Ann. Limnol. - Int. J. Limnol. **42**(1): 27–32. doi:10.1051/limn/2006003.

Nascimbene, J., Nimis, P.L., and Thüs, H. 2013. Lichens as bioindicators in freshwater ecosystems - challenges and perspectives. Ann. Di Bot. **3**: 45–50.

Nascimbene, J., Thüs, H., Marini, L., and Nimis, P.L. 2007. Freshwater lichens in springs of the eastern Italian Alps: floristics, ecology and potential for bioindication. Ann. Limnol. - Int. J. Limnol. **43**(4): 285–292. doi:10.1051/limn:2007006.

Nascimbene, J., Thüs, H., Marini, L., and Nimis, P.L. 2009. Early colonization of stone by freshwater lichens of restored habitats: A case study in northern Italy. Sci. Total Environ. **407**(18): 5001–5006. Elsevier B.V. doi:10.1016/j.scitotenv.2009.06.012.

Nash III, T.H. 2008. Introduction. *In* Lichen Biology, 2nd edition. *Edited by* T.H. Nash III.

Cambridge University Press, Cambridge. pp. 1–8.

Nazar, R.N. 2003. Ribosome biogenesis in yeast: rRNA processing and quality control. *In* Applied mycology and biotechnology. Vol. 3. Fungal genomics and bioinformatics. *Edited by* D.K. Arora and G.G. Khachatourians. Elsevier Inc. Science & Technology / Academic Press, San Diego, Calif. pp. 161–183.

Nelsen, M.P., and Gargas, A. 2006. Actin type I introns offer potential for increasing phylogenetic resolution in *Asterochloris* (Chlorophyta: Trebouxiophyceae). Lichenol. **38**(5): 435–440. doi:10.1017/S0024282906005779.

Nelsen, M.P., Plata, E.R., Andrew, C.J., Lücking, R., and Lumbsch, H.T. 2011. Phylogenetic diversity of trentepohlialean algae associated with lichen-forming fungi. J. Phycol. **47**(2): 282–290. doi:10.1111/j.1529-8817.2011.00962.x.

Neustupa, J., Eliáš, M., and Šejnohová, L. 2007. A taxonomic study of two *Stichococcus* species (Trebouxiophyceae, Chlorophyta) with a starch-enveloped pyrenoid. Nov. Hedwigia **84**(1–2): 51–63. doi:10.1127/0029-5035/2007/0084-0051.

Nguyen, T., Chollet-Krugler, M., Lohézic-Le Dévéhat, F., Rouaud, I., and Boustie, J. 2015. Mycosporine-like compounds in chlorolichens: Isolation from *Dermatocarpon luridum* and *Dermatocarpon miniatum*, and their photoprotective properties. Planta Medica Lett. **2**(1): e1–e5. doi:10.1055/s-0034-1396321.

Nozaki, H., Itoh, M., Sano, R., Uchida, H., Watanabe, M.M., and Kuroiwa, T. 1995. Phylogenetic relationships within the colonial Volvocales (Chlorophyta) inferred from rbcL gene sequence data. J. Phycol. **31**(6): 970–979. doi:10.1111/j.0022-3646.1995.00970.x.

Nyati, S., Beck, A., and Honegger, R. 2007. Fine structure and phylogeny of green algal photobionts in the microfilamentous genus *Psoroglaena* (Verrucariaceae, lichen-forming Ascomycetes). Plant Biol. **9**(3): 390–399. doi:10.1055/s-2006-924654.

Nyati, S., Scherrer, S., Werth, S., and Honegger, R. 2014. Green-algal photobiont diversity (*Trebouxia* spp.) in representatives of Teloschistaceae (Lecanoromycetes, lichen-forming ascomycetes). Lichenol. **46**(2): 189–212. doi:10.1017/S0024282913000819.

Nyati, S., Werth, S., and Honegger, R. 2013. Genetic diversity of sterile cultured *Trebouxia* photobionts associated with the lichen-forming fungus *Xanthoria parietina* visualized with RAPD-PCR fingerprinting techniques. Lichenol. **45**(6): 825–840. doi:10.1017/S0024282913000546.

Opanowicz, M., and Grube, M. 2004. Photobiont genetic variation in *Flavocetraria nivalis* from Poland (Parmeliaceae, lichenized Ascomycota). Lichenol. **36**(2): 125–131. doi:10.1017/S0024282904013763.

Oppermann, B., Karlovsky, P., and Reisser, W. 1997. M13 DNA fingerprinting in unicellular and filamentous green algae. Eur. J. Phycol. **32**(2): 103–110. doi:10.1017/S0967026297001157.

Overeem, M.A. van. 1937. On green organisms occurring in the lower troposphere. Trav. Bot. Neerl. **34**: 388–442.

Peakall, R., and Smouse, P.E. 2006. GenAlEx 6: Genetic analysis in Excel. Population genetic software for teaching and research. Mol. Ecol. Notes **6**(1): 288–295. doi:10.1111/j.1471-8286.2005.01155.x.

Peakall, R., and Smouse, P.E. 2012. GenAlEx 6.5 : genetic analysis in Excel. Population genetic software for teaching and research — an update. **28**(19): 2537–2539. doi:10.1093/bioinformatics/bts460.

Pentecost, A. 1977. A comparison of the lichens of two mountain streams in Gwynedd. Lichenol. **9**(2): 107–111. doi:10.1017/S0024282977000188.

Philippe, H., Brinkmann, H., Lavrov, D. V., Littlewood, D.T.J., Manuel, M., Wörheide, G., and Baurain, D. 2011. Resolving difficult phylogenetic questions: Why more sequences are not enough. PLoS Biol. **9**(3): e1000602. doi:10.1371/journal.pbio.1000602.

Piercey-Normore, M. 2009. Vegetatively reproducing fungi in three genera of the Parmeliaceae share divergent algal partners. Bryologist **112**(4): 773–785. doi:10.1639/0007-2745-112.4.773.

Piercey-Normore, M.D. 2004. Selection of algal genotypes by three species of lichen fungi in the genus *Cladonia*. Can. J. Bot. **82**(7): 947–961. doi:10.1139/b04-084.

Piercey-Normore, M.D. 2006. The lichen-forming ascomycete *Evernia mesomorpha* associates with multiple genotypes of *Trebouxia jamesii*. New Phytol. **169**(2): 331–44. doi:10.1111/j.1469-8137.2005.01576.x.

Piercey-Normore, M.D., and Depriest, P.T. 2001. Algal switching among lichen symbioses. Am. J. Bot. **88**(8): 1490–1498.

Pino-Bodas, R., Martín, M.P., Burgaz, A.R., and Lumbsch, H.T. 2013. Species delimitation in *Cladonia* (Ascomycota): a challenge to the DNA barcoding philosophy. Mol. Ecol. Resour. **13**(6): 1058–1068. doi:10.1111/1755-0998.12086.

Quantum GIS Development Team. 2017. QGIS 2.18.2 Las Palmas [software]. Available from qgis.org.

Rambout, A. 2016. FigTree v1.4.3 [software]. Available from http://tree.bio.ed.ac.uk/software/figtree/.

Rasmussen, U., and Svenning, M.M. 1998. Fingerprinting of cyanobacteria based on PCR with primers derived from short and long tandemly repeated repetitive sequences. Appl. Environ. Microbiol. **64**(1): 265–72. Available from http://www.ncbi.nlm.nih.gov/pubmed/16349487.

Reháková, H. 1968. Lisejníkoví rasy z rodu *Trebouxia*, *Diplosphaera* a *Myrmecia* (Flechtenalgen der Gattungen *Trebouxia*, *Diplosphaera* und *Myrmecia*). Ph.D. Thesis, Department of Katedra Bot.University of Karlova, Praha, Czech Republic.

Revill, D.L., Stewart, K.W., and Schlichting, H.E. 1967. Passive dispersal of viable algae and protozoa by certain craneflies and midges. Ecology **48**(6): 1023–1027. doi:10.2307/1934558.

Robba, L., Russel, S.J., Barker, G.L., and Brodie, J. 2006. Assessing the use of the mitochondrial

cox1 marker for use in DNA barcoding of red algae (Rhodophyta). Am. J. Bot. **93**(8): 1101–1108.

Robertson, J., and Piercey-Normore, M.D. 2007. Gene flow in symbionts of *Cladonia arbuscula*. Lichenol. **39**(1): 69–82. doi:10.1017/S0024282906005809.

Robinson, N.J., Robinson, P.J., Gupta, A., Bleasby, A.J., Whitton, B.A., and Morby, A.P. 1995. Singular over-representation of an octameric palindrome, HIP1, in DNA from many cyanobacteria. Nucleic Acids Res. **23**(5): 729–735. doi:10.1093/nar/23.5.729.

Rosentreter, R. 1984. The zonation of mosses and lichens along the Salmon River in Idaho. Northwest Sci. **58**(2): 108–117.

Rout, J., and Gaur, J.P. 1994. Composition and dynamics of epilithic algae in a forest stream at Shillong (India). Hydrobiologia **291**(1): 61–74. doi:10.1007/BF00024239.

Ruda, M. 2011. A study of phylogenetic trees versus networks to objectively identify haplogroups in mitochondrial DNA. M.Sc.thesis, Department of Bioinformatics. Rochester Institute of Technology, Rochester, NY.

Ryan, B.D. 1988a. Zonation of lichens on a rocky seashore on Fidalgo Island, Washington. Bryologist **91**(3): 167–180. doi:10.2307/3243214.

Ryan, B.D. 1988b. Marine and maritime lichens on serpentine rock on Fidalgo Island, Washington. Bryologist **91**(3): 186–190. doi:10.2307/3243217.

Santesson, R. 1939. Amphibious pyrenolichens I. Ark. för Bot. **29A**(10): 1–67.

Saunders, G.W., and Kucera, H. 2010. An evaluation of rbcL, tufA, UPA, LSU and ITS as DNA barcode markers for the marine green macroalgae. Cryptogam. Algol. **31**(4): 487–528.

Saunders, G.W., and McDevit, D.C. 2012. Methods for DNA barcoding photosynthetic protists emphasizing the macroalgae and diatoms. *In* DNA Barcodes: Methods and Protocols, Methods in Molecular Biology. *Edited by* W.J. Kress and D.L. Erickson. Springer Science+Business Media. pp. 379–393. doi:10.1007.978-1-61779-591-6_10.

Sherwood, A.R., Garbary, D.J., and Sheath, R.G. 2000. Assessing the phylogenetic position of the Prasiolales (Chlorophyta) using rbcL and 18S rRNA gene sequence data. Phycologia **39**(July): 139–146. doi:10.2216/i0031-8884-39-2-139.1.

Skaloud, P., and Peksa, O. 2010. Evolutionary inferences based on ITS rDNA and actin sequences reveal extensive diversity of the common lichen alga *Asterochloris* (Trebouxiophyceae, Chlorophyta). Mol. Phylogenet. Evol. **54**(1): 36–46. Elsevier Inc. doi:10.1016/j.ympev.2009.09.035.

Slatkin, M. 1993. Isolation by distance in equilibrium and non-equilibrium populations. Soc. Study Evol. **47**(1): 264–279.

Sonnenberg, R., Nolte, A.W., and Tautz, D. 2007. An evaluation of LSU rDNA D1-D2 sequences for their use in species identification. Front. Zool. **4**: 6. doi:10.1186/1742-9994-4-6.

Stocker-Wörgötter, E., and Türk, R. 1988. Licht- und elektronenmikroskopische Untersuchungen

von Entwicklungsstadien der Flechte *Endocarpon pusillum* unter Kulturbedingungen. Plant Syst. Evol. **158**(2–4): 313–328. doi:10.1007/BF00936353.

Stocker-Wörgötter, E., and Türk, R. 1989. The resynthesis of thalli of *Dermatocarpon miniatum* under laboratory conditions. Symbiosis **7**(1): 37–50.

Storfer, A., Murphy, M.A., Evans, J.S., Goldberg, C.S., Robinson, S., Spear, S.F., Dezzani, R., Delmelle, E., Vierling, L., and Waits, L.P. 2007. Putting the "landscape" in landscape genetics. Heredity (Edinb). **98**(3): 128–42. doi:10.1038/sj.hdy.6800917.

Storfer, A., Murphy, M.A., Spear, S.F., Holderegger, R., and Waits, L.P. 2010. Landscape genetics: Where are we now? Mol. Ecol. **19**(17): 3496–3514. doi:10.1111/j.1365-294X.2010.04691.x.

Tamura, K., Stecher, G., Peterson, D., Filipski, A., and Kumar, S. 2013. MEGA6: Molecular evolutionary genetics analysis version 6.0. Mol. Biol. Evol. **30**(12): 2725–2729. doi:10.1093/molbev/mst197.

Teacher, A.G.F., and Griffiths, D.J. 2011. HapStar: Automated haplotype network layout and visualization. Mol. Ecol. Resour. **11**(1): 151–153. doi:10.1111/j.1755-0998.2010.02890.x.

Templeton, A.R. 2006. Population genetics and microevolutionary theory. John Wiley & Sons, Inc, Hoboken, NJ.

Theroux, S., D'Andrea, W.J., Toney, J., Amaral-Zettler, L., and Huang, Y. 2010. Phylogenetic diversity and evolutionary relatedness of alkenone-producing haptophyte algae in lakes: Implications for continental paleotemperature reconstructions. Earth Planet. Sci. Lett. **300**(3–4): 311–320. Elsevier B.V. doi:10.1016/j.epsl.2010.10.009.

Thomson, J.W. 1972. Distribution patterns of American Arctic lichens. Can. J. Bot. **50**(5): 1135–1156. doi:10.1139/b72-138.

Thüs, H. 2002. Taxonomie, Verbreitung ond Ökologie silicoler Süβwasserflechten im auβeralpinen Mitteleuropa. Bibl. Lichenol. **83**: 1–214.

Thüs, H., Muggia, L., Pérez-Ortega, S., Favero-Longo, S.E., Joneson, S., O'Brien, H., Nelsen, M.P., Duque-Thüs, R., Grube, M., Friedl, T., Brodie, J., Andrew, C.J., Lücking, R., Lutzoni, F., and Gueidan, C. 2011. Revisiting photobiont diversity in the lichen family Verrucariaceae (Ascomycota). Eur. J. Phycol. **46**(4): 399–415. doi:10.1080/09670262.2011.629788.

Thüs, H., and Nascimbene, J. 2008. Contributions toward a new taxonomy of Central European freshwater species of the lichen genus *Thelidium* (Verrucariales, Ascomycota). Lichenol. **40**(6): 499–521. doi:10.1017/S0024282908007603.

Tormo, R., Recio, D., Silva, I., and Muñoz, A.F. 2001. A quantitative investigation of airborne algae and lichen soredia obtained from pollen traps in south-west Spain. Eur. J. Phycol. **36**(4): 385–390. doi:10.1080/09670260110001735538.

Torres, R.A., Ganal, M., and Hemleben, V. 1990. GC balance in the internal transcribed spacers ITS 1 and ITS 2 of nuclear ribosomal RNA genes. J. Mol. Evol. **30**: 170–181. doi:10.1007/BF02099943.

Tunjić, M., and Korać, P. 2013. Vertical and horizontal gene transfer in lichens. Period. Biol. **115**(3): 321–329.

Voytsekhovich, A.., Mikhailuk, T.I., and Daryenko, T. 2011a. Lichen photobionts. 1: biodiversity, ecophysiology and co-evolution with the mycobiont. Phycology **21**(1): 3–26.

Voytsekhovich, A., Dymytrova, L., and Nadyeina, O. 2011b. Photobiont composition of some taxa of the genera *Micarea* and *Placynthiella* (Lecanoromycetes , lichenized Ascomycota) from Ukraine. Folia Cryptogam. Est. **48**: 135–148.

Wagner, H.H., Holderegger, R., Werth, S., Gugerli, F., Hoebee, S.E., and Scheidegger, C. 2005. Variogram analysis of the spatial genetic structure of continuous populations using multilocus microsatellite data. Genetics **169**(3): 1739–52. doi:10.1534/genetics.104.036038.

Wagner, H.H., Werth, S., Kalwij, J.M., Bolli, J.C., and Scheidegger, C. 2006. Modelling forest recolonization by an epiphytic lichen using a landscape genetic approach. Landsc. Ecol. **21**(6): 849–865. doi:10.1007/s10980-005-5567-7.

Walser, J.C. 2004. Molecular evidence for limited dispersal of vegetative propagules in the epiphytic lichen *Lobaria pulmonaria*. Am. J. Bot. **91**(8): 1273–1276. doi:10.3732/ajb.91.8.1273.

Walser, J.C., Holderegger, R., Gugerli, F., Hoebee, S.E., and Scheidegger, C. 2005. Microsatellites reveal regional population differentiation and isolation in *Lobaria pulmonaria*, an epiphytic lichen. Mol. Ecol. **14**(2): 457–467. doi:10.1111/j.1365-294X.2004.02423.x.

Wang, Y.-Y., Liu, B., Zhang, X.-Y., Zhou, Q.-M., Zhang, T., Li, H., Yu, Y.-F., Zhang, X.-L., Hao, X.-Y., Wang, M., Wang, L., and Wei, J.-C. 2014. Genome characteristics reveal the impact of lichenization on lichen-forming fungus *Endocarpon pusillum* Hedwig (Verrucariales, Ascomycota). BMC Genomics **15**: 34. doi:10.1186/1471-2164-15-34.

Wehr, J.D., and Sheath, R.G. (*Editors*). 2003. Freshwater Algae of North America. Elsevier Science.

Werth, S. 2010. Population genetics of lichen-forming fungi – a review. Lichenol. **42**(5): 499–519. doi:10.1017/S0024282910000125.

Werth, S. 2011. Optimal sample sizes and allelic diversity in studies of the genetic variability of mycobiont and photobiont populations. Lichenol. **43**(1): 73–81. doi:10.1017/S0024282910000563.

Werth, S. 2012. Fungal-algal interactions in *Ramalina menziesii* and its associated epiphytic lichen community. Lichenol. **44**(4): 543–560. doi:10.1017/S0024282912000138.

Werth, S., Cheenacharoen, S., and Scheidegger, C. 2014. Propagule size is not a good predictor for regional population subdivision or fine-scale spatial structure in lichenized fungi. Fungal Biol. **118**(2): 126–138. Elsevier Ltd. doi:10.1016/j.funbio.2013.10.009.

Werth, S., Gugerli, F., Holderegger, R., Wagner, H.H., Csencsics, D., and Scheidegger, C. 2007. Landscape-level gene flow in *Lobaria pulmonaria*, an epiphytic lichen. Mol. Ecol. **16**(13): 2807–2815. doi:10.1111/j.1365-294X.2007.03344.x.

Werth, S., and Scheidegger, C. 2014. Gene flow within and between catchments in the threatened riparian plant *Myricaria germanica*. PLoS One **9**(6): e99400. doi:10.1371/journal.pone.0099400.

Werth, S., and Sork, V.L. 2008. Local genetic structure in a North American epiphytic lichen, *Ramalina menziesii* (Ramalinaceae). Am. J. Bot. **95**(5): 568–576. doi:10.3732/ajb.2007024.

Werth, S., and Sork, V.L. 2010. Identity and genetic structure of the photobiont of the epiphytic lichen *Ramalina menziesii* on three oak species in southern California. Am. J. Bot. **97**(5): 821–830. doi:10.3732/ajb.0900276.

Werth, S., Wagner, H.H., Gugerli, F., Holderegger, R., Csencsics, D., Kalwij, J.M., and Scheidegger, C. 2006a. Quantifying dispersal and establishment limitation in a population of an epiphytic lichen. Ecology **87**(8): 2037–2046. doi:10.1890/0012-9658(2006)87[2037:QDAELI]2.0.CO;2.

Werth, S., Wagner, H.H., Holderegger, R., Kalwij, J.M., and Scheidegger, C. 2006b. Effect of disturbances on the genetic diversity of an old-forest associated lichen. Mol. Ecol. **15**(4): 911–921. doi:10.1111/j.1365-294X.2006.02838.x.

White, T.J., Bruns, T., Lee, S., and Taylor, J.W. 1990. Amplification and direct sequencing of fungal ribosomal RNA genes for phylogenetics. *In* PCR Protocols: A Guide to Methods and Applications. *Edited by* M.A. Innis, D.H. Gelfand, J.J. Sninsky, and T.J. White. Academic Press Inc, New York. pp. 315–322.

Will, K. 2012. Principals of Phylogenetics [online]. University of California, Berkeley. Available from http://ib.berkeley.edu/courses/ib200a/lect/ib200a_lect11_Will_likelihood.pdf.

Woese, C.R., Kandler, O., and Wheelis, M.L. 1990. Towards a natural system of organisms: Proposal for the domains Archaea, Bacteria, and Eucarya. Proc. Natl. Acad. Sci. **87**: 4576–4579.

Wongsawad, P., and Peerapornpisal, Y. 2014. Molecular identification and phylogenetic relationship of green algae, *Spirogyra ellipsospora* (Chlorophyta) using ISSR and rbcL markers. Saudi J. Biol. Sci. **21**(5): 505–510. King Saud University. doi:10.1016/j.sjbs.2014.01.003.

Woodward, G., Perkins, D.M., and Brown, L.E. 2010. Climate change and freshwater ecosystems: impacts across multiple levels of organization. Philos. Trans. R. Soc. Lond. B. Biol. Sci. **365**(1549): 2093–106. doi:10.1098/rstb.2010.0055.

Wu, M., Comeron, J.M., Yoon, H.S., and Bhattacharya, D. 2009. Unexpected dynamic gene family evolution in algal actins. Mol. Biol. Evol. **26**(2): 249–253. doi:10.1093/molbev/msn263.

Yahr, R., Vilgalys, R., and DePriest, P.T. 2004. Strong fungal specificity and selectivity for algal symbionts in Florida scrub *Cladonia* lichens. Mol. Ecol. **13**(11): 3367–78. doi:10.1111/j.1365-294X.2004.02350.x.

Yahr, R., Vilgalys, R., and DePriest, P.T. 2006. Geographic variation in algal partners of *Cladonia subtenuis* (Cladoniaceae) highlights the dynamic nature of a lichen symbiosis. New Phytol. **171**(4): 847–860. doi:10.1111/j.1469-8137.2006.01792.x.

Yao, H., Song, J., Liu, C., Luo, K., Han, J., Li, Y., Pang, X., Xu, H., Zhu, Y., Xiao, P., and Chen, S. 2010. Use of ITS2 region as the universal DNA barcode for plants and animals. PLoS One **5**(10): e13102. doi:10.1371/journal.pone.0013102.

Zhang, T., and Wei, J. 2011. Survival analyses of symbionts isolated from *Endocarpon pusillum* Hedwig to desiccation and starvation stress. Sci. China Life Sci. **54**(5): 480–489. doi:10.1007/s11427-011-4164-z.

Zoschke, R., Liere, K., and Börner, T. 2007. From seedling to mature plant: *Arabidopsis* plastidial genome copy number, RNA accumulation and transcription are differentially regulated during leaf development. Plant J. **50**: 710–722. 10.1111/j.1365-313X.2007.03084.x.

Zuccarini, P., and Kampuš, S. 2011. Two aquatic macrophytes as bioindicators for medium-high copper concentrations in freshwaters. Plant Biosyst. - An Int. J. Deal. with all Asp. Plant Biol. **145**(2): 503–506. doi:10.1080/11263504.2010.547677.

APPENDIX A: ENVIRONMENTAL PARAMETERS COLLECTED AT COLLECTION SITES IN PAYUK LAKE

Table A1. Collection date, location, and substratum of 102 *Dermatocarpon luridum* thalli from Payuk Lake, Manitoba.

Sample Number	Date (m/d/y)	Latitude (°N)	Logitude (°W)	Colloquial Location	Lake Area	Height Above Water (cm)	Slope (0-90°)	Aspect (°)*	Geology
1	09-11-14	54.65020	-101.51223	Mistik Ck Bay	Lake	75	20	360	green granite
2	09-11-14	54.65020	-101.51223	Mistik Ck Bay	Lake	40	26.8	318	green granite
3	09-11-14	54.65020	-101.51223	Mistik Ck Bay	Lake	35	75	318	green granite
4	09-11-14	54.65099	-101.51040	Mistik Ck Bay	Lake	20	5.71	318	green granite
5	09-11-14	54.65099	-101.51040	Mistik Ck Bay	Lake	20	20	318	green granite
6	09-11-14	54.65099	-101.51040	Mistik Ck Bay	Lake	40	90	318	green granite
7	09-11-14	54.65200	-101.50655	Mistik Ck Inflow	Creek	40	45	336	green granite
8	09-11-14	54.65200	-101.50655	Mistik Ck Inflow	Creek	10	20	336	green granite
9	09-11-14	54.65200	-101.50655	Mistik Ck Inflow	Creek	20	90	336	green granite
10	09-11-14	54.65236	-101.50397	Mistik Ck Inflow	Creek	20	90	336	green granite
11	09-11-14	54.65236	-101.50397	Mistik Ck Inflow	Creek	30	90	336	green granite
12	09-11-14	54.65236	-101.50397	Mistik Ck Inflow	Creek	25	35	336	green granite
13	09-13-14	54.64952	-101.49782	Wayne's Bay	Lake	30	45	25	green granite
14	09-13-14	54.64952	-101.49782	Wayne's Bay	Lake	20	20	55	green granite
15	09-13-14	54.64952	-101.49782	Wayne's Bay	Lake	50	90	30	green granite
16	09-13-14	54.64869	-101.50079	Wayne's Bay	Lake	50	25	45	green granite
17	09-13-14	54.64869	-101.50079	Wayne's Bay	Lake	40	30	45	green granite
18	09-13-14	54.64869	-101.50079	Wayne's Bay	Lake	10	30	45	green granite
19	09-13-14	54.64816	-101.50269	Wayne's Bay	Lake	30	50	45	green granite
20	09-13-14	54.64816	-101.50269	Wayne's Bay	Lake	30	50	45	green granite
21	09-13-14	54.64816	-101.50269	Wayne's Bay	Lake	30	15	40	green granite
22	09-13-14	54.64606	-101.50195	Twin Ck Inflow	Creek	40	60	290	green granite
23	09-13-14	54.64606	-101.50195	Twin Ck Inflow	Creek	50	50	290	green granite
24	09-13-14	54.64606	-101.50195	Twin Ck Inflow	Creek	60	90	290	green granite
25	09-13-14	54.64558	-101.50225	Twin Ck Inflow	Creek	40	15	350	green granite
26	09-13-14	54.64558	-101.50225	Twin Ck Inflow	Creek	30	45	350	green granite

Table A1. Continued.

Sample Number	Date (m/d/y)	Latitude (°N)	Logitude (°W)	Colloquial Location	Lake Area	Height Above Water (cm)	Slope (0-90°)	Aspect (°)*	Geology
27	09-13-14	54.64558	-101.50225	Twin Ck Inflow	Creek	20	45	350	green granite
28	09-13-14	54.64500	-101.50225	My Island Channel	Lake	25	10	335	schist
29	09-13-14	54.64500	-101.50225	My Island Channel	Lake	40	10	335	schist
30	09-13-14	54.64500	-101.50225	My Island Channel	Lake	20	10	335	schist
31	09-13-14	54.64034	-101.50225	Redrock Bay - Waterfall	Lake	70	75	270	red granite
32	09-13-14	54.64034	-101.50225	Redrock Bay - Waterfall	Lake	30	75	270	red granite
33	09-13-14	54.64034	-101.50225	Redrock Bay - Waterfall	Lake	15	70	270	red granite
34	09-13-14	54.64127	-101.50225	Redrock Bay- Zen Island	Lake	35	70	130	red granite
35	09-13-14	54.64127	-101.50225	Redrock Bay- Zen Island	Lake	60	90	130	red granite
36	09-13-14	54.64127	-101.50225	Redrock Bay- Zen Island	Lake	100	45	120	red granite
37	09-13-14	54.64979	-101.50225	Mistik Ck Channel	Lake	30	45	175	green granite
38	09-13-14	54.64979	-101.50225	Mistik Ck Channel	Lake	60	50	155	green granite
39	09-13-14	54.64979	-101.50225	Mistik Ck Channel	Lake	50	90	185	green granite
40	09-13-14	54.65079	-101.50225	Umbilicaria Rock	Lake	50	90	105	green granite
41	09-13-14	54.65079	-101.50225	Umbilicaria Rock	Lake	60	90	180	green granite
42	09-13-14	54.65079	-101.50225	Umbilicaria Rock	Lake	60	90	180	green granite
43	06-27-15	54.64943	-101.50225	My Island	Lake	30	38	90	rhyolite
44	06-27-15	54.64943	-101.50225	My Island	Lake	30	38	90	rhyolite
45	06-27-15	54.64943	-101.50225	My Island	Lake	30	38	90	rhyolite
46	06-27-15	54.64827	-101.50225	Northwest Shore	Lake	40	45	90	rhyolite
47	06-27-15	54.64827	-101.50225	Northwest Shore	Lake	40	45	90	rhyolite
48	06-27-15	54.64827	-101.50225	Northwest Shore	Lake	40	45	90	rhyolite
49	06-27-15	54.64793	-101.50225	Small Island	Lake	submerged	0	45	rhyolite
50	06-27-15	54.64793	-101.50225	Small Island	Lake	submerged	0	45	rhyolite
51	06-27-15	54.64793	-101.50225	Small Island	Lake	submerged	0	45	rhyolite
52	06-27-15	54.64767	-101.50225	Northwest Shore	Lake	30	0	90	rhyolite
53	06-27-15	54.64767	-101.50225	Northwest Shore	Lake	submerged	0	90	rhyolite
54	06-27-15	54.64767	-101.50225	Northwest Shore	Lake	10	0	90	rhyolite

Table A1. Continued.

Sample Number	Date (m/d/y)	Latitude (°N)	Logitude (°W)	Colloquial Location	Lake Area	Height Above Water (cm)	Slope (0-90°)	Aspect (°)*	Geology
55	06-27-15	54.64512	-101.50225	Greenstone Bay	Lake	20	50	45	rhyolite
56	06-27-15	54.64512	-101.50225	Greenstone Bay	Lake	20	50	45	rhyolite
57	06-27-15	54.64512	-101.50225	Greenstone Bay	Lake	20	50	45	rhyolite
58	06-27-15	54.64618	-101.50225	Northwest Shore	Lake	50	30	225	rhyolite
59	06-27-15	54.64618	-101.50225	Northwest Shore	Lake	50	30	225	rhyolite
60	06-27-15	54.64618	-101.50225	Northwest Shore	Lake	50	30	225	rhyolite
61	06-27-15	54.64420	-101.50225	Greenstone Bay	Lake	submerged	0	340	rhyolite
62	06-27-15	54.64420	-101.50225	Greenstone Bay	Lake	submerged	0	340	rhyolite
63	06-27-15	54.64420	-101.50225	Greenstone Bay	Lake	5	0	340	rhyolite
64	06-27-15	54.64182	-101.50225	Greenstone Bay - Almost Lost Cove	Lake	15	50	0	rhyolite
65	06-27-15	54.64182	-101.50225	Greenstone Bay - Almost Lost Cove	Lake	submerged	50	0	rhyolite
66	06-27-15	54.64182	-101.50225	Greenstone Bay - Almost Lost Cove	Lake	submerged	50	0	rhyolite
67	06-27-15	54.64216	-101.50225	Greenstone Bay Point	Lake	20	25	90	rhyolite
68	06-27-15	54.64216	-101.50225	Greenstone Bay Point	Lake	20	25	90	rhyolite
69	06-27-15	54.64216	-101.50225	Greenstone Bay Point	Lake	20	25	90	rhyolite
70	06-27-15	54.63785	-101.50225	West Shore	Lake	10	26	0	rhyolite
71	06-27-15	54.63785	-101.50225	West Shore	Lake	50	26	0	rhyolite
72	06-27-15	54.63785	-101.50225	West Shore	Lake	10	26	0	rhyolite
73	06-27-15	54.63142	-101.50225	West Shore	Lake	surface	42	90	red granite
74	06-27-15	54.63142	-101.50225	West Shore	Lake	surface	42	90	red granite
75	06-27-15	54.63142	-101.50225	West Shore	Lake	surface	42	90	red granite
76	06-27-15	54.63201	-101.50225	East Shore -Island	Lake	10	40	90	rhyolite
77	06-27-15	54.63201	-101.50225	East Shore -Island	Lake	10	40	90	rhyolite
78	06-27-15	54.63201	-101.50225	East Shore -Island	Lake	10	40	90	rhyolite
79	06-27-15	54.63604	-101.50225	East Shore - Large Island	Lake	5	16	90	rhyolite
80	06-27-15	54.63604	-101.50225	East Shore - Large Island	Lake	5	16	90	rhyolite
81	06-27-15	54.63604	-101.50225	East Shore - Large Island	Lake	10	16	90	rhyolite
82	06-27-15	54.63720	-101.50225	East Shore -Island	Lake	20	22.5	90	rhyolite

Table A1. Continued.

Sample Number	Date (m/d/y)	Latitude (°N)	Logitude (°W)	Colloquial Location	Lake Area	Height Above Water (cm)	Slope (0-90°)	Aspect (°)*	Geology
83	06-27-15	54.63720	-101.50225	East Shore -Island	Lake	20	22.5	90	rhyolite
84	06-27-15	54.63720	-101.50225	East Shore -Island	Lake	20	22.5	90	rhyolite
85	06-28-15	54.65269	-101.50225	Mistik Creek	Creek	5	45	270	basalt/rhyolite mix
86	06-28-15	54.65269	-101.50225	Mistik Creek	Creek	5	45	270	basalt/rhyolite mix
87	06-28-15	54.65269	-101.50225	Mistik Creek	Creek	5	45	270	basalt/rhyolite mix
88	06-28-15	54.65498	-101.50225	Mistik Creek	Creek	surface	38	90	rhyolite
89	06-28-15	54.65498	-101.50225	Mistik Creek	Creek	surface	38	90	rhyolite
90	06-28-15	54.65498	-101.50225	Mistik Creek	Creek	submerged	38	90	rhyolite
91	06-28-15	54.63926	-101.50225	Hope Island	Lake	5	8	45	basalt
92	06-28-15	54.63926	-101.50225	Hope Island	Lake	5	8	45	basalt
93	06-28-15	54.63926	-101.50225	Hope Island	Lake	5	8	45	basalt
94	06-28-15	54.63809	-101.50225	East Shore - Hope Island Point	Lake	5	10	0	basalt
95	06-28-15	54.63809	-101.50225	East Shore - Hope Island Point	Lake	5	10	0	basalt
96	06-28-15	54.63809	-101.50225	East Shore - Hope Island Point	Lake	5	10	0	basalt
97	06-27-15	54.62942	-101.50225	Mistik Outflow	Bay/Creek	submerged	45	90	red granite
98	06-27-15	54.62942	-101.50225	Mistik Outflow	Bay/Creek	submerged	45	90	red granite
99	06-27-15	54.62942	-101.50225	Mistik Outflow	Bay/Creek	submerged	45	90	red granite
100	06-27-15	54.62958	-101.50225	Mistik Outflow	Bay/Creek	5	45	270	rhyolite
101	06-27-15	54.62958	-101.50225	Mistik Outflow	Bay/Creek	5	45	270	rhyolite
102	06-27-15	54.62958	-101.50225	Mistik Outflow	Bay/Creek	submerged	45	270	rhyolite

* Aspect: N=0°, 360°; E=90°; S=180°; W=270°

Table A2. Topography and surrounding vegetation around 102 *Dermatocarpon luridum* thalli collected from Payuk Lake, Manitoba.

Collection Number	Topography	Overhang or Shade	Surrounding Vegetation	Notes
1	Small rocks	Shrubs	Sweet fern, willow, alder	
2	Small rocks	none	Grasses, *Betula* sp., alder, wildrose, mint, sweet fern	
3	Large boulders	none	Birch	
4	Small rocks	none	dead brich, willow, grasses	
5	Large boulders	none	Fallen logs, grasses, mint, willow (dead and alive)	
6	Cliff face	none	Grasses, mosses in cracks, juniper	Very low water
7	Small rocks	Birch	Spruce, grasses, *Dicranum* sp.	
8	Large boulders	none	Grasses, *Dicranum* sp., *Equisetum* sp.	Surrounded by *Equisetum*
9	Large boulders	Black Spruce	Big spruce overhang	6ft cliff
10	Steep cliff	none	*C. uncialis* , birch, black spruce, wild rice	Steep cliff
11	Steep cliff	none	Black spruce, mint, moss	Steep cliff with layered/striated rock
12	Small rocks	none	Willow, *Equisetum* sp., moss	
13	Small rocks	Grasses	Grasses, willow	Growing in cracks
14	Pebbles	none	Dead alder, mosses, grasses, willow	Striated rock along shore
15	Steep cliff	Mosses and Alder	Mosses, alder	Growing in cracks
16	Large boulders	Shaded by rocks	Red osier dogwood, rose, willow, alder	Growing in cracks
17	Large boulders	none	Dead willow, rose, red osier dogwood	
18	Shallow bedroc	none	Willow, alder, grasses	Spider present, rock was striated
19	Small rocks	Black Spruce	Alder, rose, willow, dead black spruce	Striated rock along shore, wave-action affected
20	Medium rocks	none	Willow, rose, alder, grass	Striated rock along shore, wave-action affected
21	Large boulders	Willow	Willow, Bullrushes, dead branches	Rocks smooth
22	Large boulders	none	Willow, dead black spruce, sweet fern	Growing in cracks
23	Large boulders	none	Dead jack pine, grasses, mint	Rocks very loose
24	Large boulders	none	Grass, mint, birch, black spruce	Growing on loose rocks and in cracks
25	Large boulders	none	Grasses, mosses	Growing in cracks, marled rock. Windswept
26	Steep cliff	Dead birch	Birch	Growing in cracks, marled rock. Windswept
27	Large boulders	Birch	Birch, grasses	Staurothele present
28	Medium rocks	Dead branches	Birch, willow, grasses in cracks	
29	Large boulders	none	Birch, willow, grasses in cracks	Growing in cracks
30	Large boulders	Willow	Rose, willow, grasses	Striated, porous rock, growing in cracks, basalt maybe?
31	Large boulders	none	Birch, willow, grasses, Jack pine	*Staurothele* present, growing in cracks
32	Large boulders	none	Birch, willow, grasses, Jack pine	Sheltered, wet crevice
33	Large boulders	Dead birch	Birch	Large visible algal bloom, adjacent to waterfall

Table A2. Continued.

Collection Number	Topography	Overhang or Shade	Surrounding Vegetation	Notes
34	Steep cliff	Dead branches	Dead branches, sweet fern	Growing in crevice
35	Steep cliff	Granite rock	Bare	Staurothele present on shear 3ft face
36	Bedrock	Jack Pine	Jack pine, grasses	Staurothele present
37	Steep cliff	none	Grasses	Growing in crack, *Staurothele* present but not beside *D. l*
38	Steep cliff	none	Black spruce, rose, birch	Growing in cracks
39	Steep cliff	Grasses	Grasses	No other lichens present
40	Steep cliff	none	none	Staurothele present but could not get sample
41	Steep cliff	none	Birch, grasses	Growing in crevice of large boulders
42	Steep cliff	none	Jack pine, mint, ferns, *Umbilicaria*	Growing in crevice of large boulders
43	Large boulders	none	Ferns, white spruce, grasses, *Hedwigia* sp., Moss spp., *Physcia* sp	
44	Large boulders	none	Ferns, white spruce, grasses, *Hedwigia* sp., Moss spp., *Physcia* sp	
45	Large boulders	none	Ferns, white spruce, grasses, *Hedwigia* sp., Moss spp., *Physcia* sp	
46	Large boulders	downed branches	Yarrow, juniper, bearberry, grasses, white spruce, Myrica, *Solidago*	
47	Large boulders	downed branches	Yarrow, juniper, bearberry, grasses, white spruce, Myrica, *Solidago*	
48	Large boulders	downed branches	Yarrow, juniper, bearberry, grasses, white spruce, Myrica, *Solidago*	
49	Steep cliff	none	Myrica, willow, birch, *Mnium* sp., *Rhodobryum* sp.	Very steep rise, about 3ft
50	Steep cliff	none	Myrica, willow, birch, *Mnium* sp., *Rhodobryum* sp.	Very steep rise, about 3ft
51	Steep cliff	none	Myrica, willow, birch, *Mnium* sp., *Rhodobryum* sp.	Very steep rise, about 3ft
52	Large boulders	none	Myrica, willow, grasses, white spruce, wild rose, alder	
53	Large boulders	none	Myrica, willow, grasses, white spruce, wild rose, alder	
54	Large boulders	none	Myrica, willow, grasses, white spruce, wild rose, alder	
55	Large boulders	none	Grasses, *Umbilicaria* , *Ceratodon* , white spruce, *C. stellaris* , willow	
56	Large boulders	none	Grasses, *Umbilicaria* , *Ceratodon* , white spruce, *C. stellaris* , willow	
57	Large boulders	none	Grasses, *Umbilicaria* , *Ceratodon* , white spruce, *C. stellaris* , willow	
58	Large boulders	none	White spruce, yarrow, juniper, ferns, buttercups, grasses, saxifrage	
59	Large boulders	none	White spruce, yarrow, juniper, ferns, buttercups, grasses, saxifrage	
60	Large boulders	none	White spruce, yarrow, juniper, ferns, buttercups, grasses, saxifrage	
61	Large boulders	none	Grasses. Willow, mint, alder, sedges, white spruce, moss spp., *Betula nana*	
62	Large boulders	none	Grasses. Willow, mint, alder, sedges, white spruce, moss spp., *Betula nana*	
63	Large boulders	none	Grasses. Willow, mint, alder, sedges, white spruce, moss spp., *Betula nana*	
64	Large boulders	none	White spruce, birch, grasses, *Climaceum* sp. (moss), sweet fern	Quartz granite diorite intrusion
65	Large boulders	none	White spruce, birch, grasses, *Climaceum* sp. (moss), sweet fern	Quartz granite diorite intrusion
66	Large boulders	none	White spruce, birch, grasses, *Climaceum* sp. (moss), sweet fern	Quartz granite diorite intrusion

Table A2. Continued.

Collection Number	Topography	Overhang or Shade	Surrounding Vegetation	Notes
67	Large boulders	none	White spruce, grasses, moss spp., birch, willow, *Epilobium aungustifolium*	
68	Large boulders	none	White spruce, grasses, moss spp., birch, willow, *Epilobium aungustifolium*	
69	Large boulders	none	White spruce, grasses, moss spp., birch, willow, *Epilobium aungustifolium*	
70	Large boulders	none	White spruce, alder, *Cladina*, *Cladonia*, *Parmelia* spp.	
71	Large boulders	none	White spruce, alder, *Cladina*, *Cladonia*, *Parmelia* spp.	
72	Large boulders	none	White spruce, alder, *Cladina*, *Cladonia*, *Parmelia* spp.	
73	Steep cliff	none	White spruce, saxifrage, birch	Cliff about 4m high
74	Steep cliff	none	White spruce, saxifrage, birch	Cliff about 4m high
75	Steep cliff	none	White spruce, saxifrage, birch	Cliff about 4m high
76	Large boulders	none	Willow, jack pine, *Betula nana* , bearberry, bullrush	
77	Large boulders	none	Willow, jack pine, *Betula nana* , bearberry, bullrush	
78	Large boulders	none	Willow, jack pine, *Betula nana* , bearberry, bullrush	
79	Large boulders	none	White spruce, jumiper, mint, grasses, bearberry	
80	Large boulders	none	White spruce, jumiper, mint, grasses, bearberry	
81	Large boulders	none	White spruce, jumiper, mint, grasses, bearberry	
82	Bluff	juniper	juniper	Bluff
83	Bluff	juniper	juniper	Bluff
84	Bluff	juniper	juniper	Bluff
85	Large boulders	dead spruce	Myrica, white spruce, grasses, sweet fern, sweet gale, *Betula nana*	
86	Large boulders	dead spruce	Myrica, white spruce, grasses, sweet fern, sweet gale, *Betula nana*	
87	Large boulders	dead spruce	Myrica, white spruce, grasses, sweet fern, sweet gale, *Betula nana*	
88	Bluff	none	Grasses, white spruce, jack pine, Monkeyflower (legume)	
89	Bluff	none	Grasses, white spruce, jack pine, Monkeyflower (legume)	
90	Bluff	none	Grasses, white spruce, jack pine, Monkeyflower (legume)	
91	Large boulders	none	Willow, sweet fern, myrica, birch, white spruce, juniper, *Stereocaulon*	
92	Large boulders	none	Willow, sweet fern, myrica, birch, white spruce, juniper, *Stereocaulon*	
93	Large boulders	none	Willow, sweet fern, myrica, birch, white spruce, juniper, *Stereocaulon*	
94	Steep cliff	none	Myrica, Willow, white spruce, grasses, mint, dandilion	Steep cliff by highway beside rapids
95	Steep cliff	none	Myrica, Willow, white spruce, grasses, mint, dandilion	Steep cliff by highway beside rapids
96	Steep cliff	none	Myrica, Willow, white spruce, grasses, mint, dandilion	Steep cliff by highway beside rapids
97	Medium rocks	none	none	Open faced rocks with moving water
98	Medium rocks	none	none	Open faced rocks with moving water
99	Medium rocks	none	none	Open faced rocks with moving water
100	Large boulders	none	Jack pine, grasses, raspberry, juniper	On southwest side of bridge
101	Large boulders	none	Jack pine, grasses, raspberry, juniper	On southwest side of bridge
102	Large boulders	none	Jack pine, grasses, raspberry, juniper	On southwest side of bridge

APPENDIX B: RECIPE FOR BOLD'S BASAL MEDIUM (BBM) FOR GREEN ALGAE

This is recipe follows that of Bischoff and Bold (1963). Each nutrient must be prepared individually into a stock solution and autoclaved. For a volume of 1L, in a large beaker and mixing with a magnetic stirrer, add the following nutrients:

Chemical Elements	Stock Solution	Nutrient Solution (mL)
$NaNO_3$	2.5 g /100 ml	10
$MgSO_4 \cdot 7H_2O$	0.75 g /100 ml	10
NaCl	0.25 g /100 ml	10
K_2HPO_4	0.75 g /100 ml	10
KH_2PO_4	1.75 g /100 ml	10
$CaCl_2 \cdot 2H_2O$	0.25 g /100 ml	10
H_3BO_3	1.142 g /100 ml	1
Trace elements solution*	-	1
EDTA Stock**	-	1
Fe Solution***	-	1
Distilled water to 1.0 L	-	-

*Trace element solution preparation:

$ZnSO_4 \cdot 7H_2O$	8.82 g/L
$MnCl_2 \cdot 4H_2O$	1.44 g/L
MoO_3	0.71 g/L
$CuSO_4 \cdot 5H_2O$	1.57 g/L
$Co(NO_3)_2 \cdot 6H_2O$	0.49 g/L
Distilled water to 1.0 L	

** EDTA Stock solution preparation:

EDTA-Na_2	5.0 g/100 mL
KOH	3.1 g/100 mL
Distilled water to 100 mL	

***Fe Solution preparation:

FeSO4·7H2O	0.498 g/100 mL
Conc. H2SO4	0.1 mL
Distilled water to 100 mL	

In the combined solution, adjust the pH value to 7.0 using 1N NaOH. Add 2% of the final volume of agar (for 1 L, add 20 g agar). Autoclave the BBM solution at 121 °C for 20 minutes exposure. Let cool and pour plates or slants right away. Leftovers can be stored in the refrigerator.

APPENDIX C: WORKFLOW OF HYDROLOGICAL MODELLING AND SPATIAL ANALYSES IN THE LESA LAB DURING A TRAVEL STUDY TO ST. JOHN'S, NEWFOUNDLAND (APRIL 2015)

This appendix outlines the step-by-step methods used to obtain three main geographic distance measures using ArcGIS 10.2 (ArcMap, ArcCatalog; ESRI 2013), rather than in QGIS that was outlined in the main methods of the thesis. The analyses were performed during a two-week travel study to the Landscape Ecology and Spatial Analyses (LESA) lab at the Memorial University of Newfoundland (MUN) in St. John's, Newfoundland, under the mentorship of Dr. Yolanda Wiersma, in April 2015.

The geographic distances that were calculated were:
1) Euclidean distance of the collection sites (and therefore thalli sampled) around Payuk Lake to produce a distance matrix to be used in Mantel Test.
2) Shoreline (path) analysis to determine the distance between sites travelling only along the shoreline and produce a distance matrix for use in Mantel Test.
3) To create a "hydrological" stream network to determine the distance between sites, taking into account flow direction and accumulation within the lake, to produce a distance matrix for use in Mantel Test.

The files were located in the "C:\.....\MSc Studies\Data\Data Files\GIS\Newfoundland 2015\Hydrology" directory. All shapefiles used were processed to the Payuk Lake study extent and were downloaded from CanVec (GeoGratis; available at http://geogratis.gc.ca/api/en/nrcan-rncan/ess-sst/23387971-b6d3-4ded-a40b-c8e832b4ea08.html). Subdirectories within the Hydrology folder included:

\Cranberry Portage Topo 63K11	Contains topographic maps for Payuk Lake
\Schist Lake Topo 63K12	Contains topographic maps for Payuk Lake
\Hydrology Toolset Info	Contains information on the Hydrology Toolset
\Surface Toolset Info	Contains information on the Surface Toolset
\Metadata	Contains information on FRI codes, CanVec codes
\Shapefiles	Contains the shapefiles used in the analyses
\Raster Files	Contains the raster files used in the analyses

Prior to starting any analyses, the projection for all of the files used was checked in ArcMap and ArcCatalog. The projection used was **NAD_1983_UTM_Zone_14N**. The following outlines the raw steps taken, as well as the file names and file paths used. In ArcMap, the "All site coordinates.csv" file (containing the geographic coordinates of all of the collected lichen thalli) was added and converted to a point feature. The file was renamed as "NewSites.shp" and saved for use in calculating Euclidean distance (1). The file was duplicated for use in the other distance calculations (NewSites-Copy.shp for Shoreline distance (2) and NewSites-Copy2.shp for Stream network distance (3)).

Distance 1: Calculate the Euclidean distance between all sites around Payuk Lake

1) Create a new file geodatabase (Euclidean.gdb) in ArcCatalog:
    Create New Feature Dataset "Sites"
        Projection: NAD_1983_UTM_Zone_14N
        Accept other defaults
            Add features (import) ("Sites")
                C:\...\Hydrology\Shapefiles\NewSites.shp
    Create New Feature Dataset "Hydrology"
        Projection: NAD_1983_UTM_Zone_14N
        Accept other defaults
            Add features (import) ("Streams")
                C:\...\Hydrology\Shapefiles\TopoStreams_Prj.shp
            Add features (import) ("Islands")
                C:\...\Hydrology\Shapefiles\TopoIslands_Prj.shp
            Add features (import) ("Lakes")
                C:\...\Hydrology\Shapefiles\TopoLakes_Prj.shp

2) Open ArcMap.

3) Add data, select Euclidean.gdb and choose all feature datasets.

4) Calculate the Euclidean distances between the sites using the following Python code:

```
>>> arcpy.env.workspace = "C:\...\Hydrology\Euclidean.gdb"
>>> in_features = "Sites"
>>> near_features = "Sites"
>>> out_table = "Sites_EuclideanDistances"
>>> arcpy.PointDistance_analysis(in_features, near_features, out_table)
<Result 'C:\\...\\Hydrology\\Euclidean.gdb\\Sites_EuclideanDistances'>
```

5) Leaving ArcMap open for reference, open Excel.

6) Open the Sites_EuclideanDistances.dbf table in Excel and add two columns at the end; one for “Site” and “Near Site”.

7) Save the Excel file as .xls.

8) In ArcMap, select each site to see the ObjectID and near ID number. Input the site names into "Site" and "Near Site" columns in the excel sheet, in the corresponding polyline OBID row. This will just help to clarify which OBID and NEAR_ID correspond to each site in the distance table.

9) Save and close Excel.

Distance 2: Calculate the distance between the sites along the shoreline around Payuk Lake

1) Create a new file geodatabase (call it something like Lakeshore.gdb) in ArcCatalog:
    Create New Feature Dataset "Sites"
        Projection: NAD_1983_UTM_Zone_14N
        Accept other defaults
            Add features (import) ("Sites")
                C:\...\Hydrology\Shapefiles\NewSites-Copy.shp
    Create New Feature Dataset "Hydrology"
        Projection: NAD_1983_UTM_Zone_14N
        Accept other defaults
            Add features (import) ("Lake")
                C:\...\Hydrology\Shapefiles\Lake_polygon.shp

2) Open ArcMap.

3) Add data, select Lakeshore.gdb, add all features datasets.

4) Convert the lake polygon into polylines:
    ArcToolbox->Data Management Tools->Features->Polygon to Polyline
        input: Lake_polygon.shp
        output: Lake_shore.shp

5) Using the Editor tool, merge all the polylines making up the main shoreline into a single polyline.

6) Snap sites along the shoreline:
    ArcToolbox->Editing Tools->Snap
        input: NewSites-Copy.shp
        snap environment: Lake_shore.shp
            Type: EDGE
            Distance: 10000m

7) Using the Editor tool on Lake_shore.shp, split the shoreline polylines (including islands) at the places where the sites are snapped. Save edits, then Stop Editing.

8) Open the attribute table for Lake_shore.shp and add field called "Distance":
    Type: Double
    Scale: 0
    Precision: 0

9) Right click the newly created Distance field and select "Calculate geometry":
    property: length
    coordinate system: as data source (NAD_1983_UTM_Zone_14N)
    units: meters

10) Export attribute table to "Shore_distance.dbf"; save outside of the geodatabase.

11) Leaving ArcMap open for reference, open Excel.

12) Open the Shore_distance.dbf table in Excel and add two columns at the end; one for “Site at end1” and “Site at end2”.

13) Save the Excel file as .xls.

14) In ArcMap select each polyline segment to see the ObjectID number. See which sites are at the ends of that polyline and input the site names into "Site at End1" and "Site at end2" columns in the excel sheet, in the corresponding polyline OBID row

15) Save and close Excel.

Distance 3: Creation of Hydrological Network and flow length distance between sites using Spatial Analyst

1) Create a new file geodatabase (FlowNetwork.gdb) in ArcCatalog:
    Create New Feature Dataset "Sites"
        Projection: NAD_1983_UTM_Zone_14N
        Accept other defaults
            New Feature Class ("Sites")
                C:\...\Hydrology\Shapefiles\NewSites-Copy2.shp
    Create Raster dataset
        Projection: NAD-1983_UTM_Zone_14N
        Follow the rest of the prompts, accept defaults
        Select C:\...\Hydrology\Raster files\Cranberry_SRTM.tif

2) Open ArcMap.

3) Add data, select FlowNetwork.gdb, add all features/rasters.

4) Create Flow Direction:
    ArcToolbox->Spatial Analyst->Hydrology->Flow Direction
        input surface raster: Cranberry_SRTM.tif
        output flow direciton raster: FlowDirection (can be saved in FlowNetwork.gdb)
        Check the "force all edges to flow outward" box

5) Identify Sinks:
    ArcToolBox->Spatial Analyst->Hydrology->Sink
        input flow direction raster: FlowDirection
        output raster: Sink (can be saved in FlowNetwork.gdb)

6) Fill sinks to create depressionless DEM:

ArcToolbox-> Spatial Analyst->Hydrology->Fill

input raster: Cranberry_SRTM.tif

output raster: FilledDEM (can be saved in FlowNetwork.gdb)

z limit: none

7) Create new flow direction based on depressionless DEM:

ArcToolbox->Spatial Analyst->Hydrology->Flow Direction

input surface raster: FilledDEM

output raster: FlowDirection2 (can be saved in FlowNetwork.gdb)

Check the "force all edges to flow outward" box

8) Double check there are no new sinks:

ArcToolbox-> Spatial Analyst->Hydrology->Sink

input flow direction: FlowDirection2

output raster: Sink2

9) Repeat steps 6-8 as needed until all sinks are gone. Use the newly "filled" raster always for the input raster for flow direction.

10) Create a flow accumulation linear raster network:

ArcToolBox->Spatial Analyst->Hydrology->Flow Accumulation

input flow direction raster: FlowDirection2

output accumulation raster: FlowAcc

input weights: 1 (default)

output data type: FLOAT (default)

11) Create a stream order raster:

ArcToolbox->Spatial Analyst->Hydrology->Stream Order

input stream raster: FlowAcc

input flow direction: FlowDirection2

output raster: StreamOrder

method of stream order: Strahler

12) Convert the stream order to a feature:

ArcToolbox->Spatial Analyst->Hydrology->Stream to Feature

input stream raster: StreamOrder

input flow direction raster: FlowDirection2

output polyline feature: Payuk_streams.shp

simplify polygons: yes

13) Create stream links to assign values to sections of a raster linear:

ArcToolbox->Spatial Analyst->Hydrology->Stream Link

input stream raster: StreamOrder (or can use FlowAcc....gets the same result)

input flow direction: FlowDirection2 (or the latest flow direction)

output raster: StreamLinks (can be saved in FlowNetwork.gdb)

14) Create flow length raster downstream:
ArcToolbox->Spatial Analyst->Hydrology->Flow Length
input flow direction: FlowDirection2
direction measurement: downstream
weight: 1 (default)
output raster: FlowLength

15) Create flow length raster upstream:
ArcToolbox->Spatial Analyst->Hydrology->Flow Length
input flow direction: FlowDirection2
direction measurement: upstream
weight: 1 (default)
output raster: FlowLength2

16) Create drainage basins:
ArcToolbox->Spatial Analyst->Hydrology->Basin
input flow direction: FlowDirection2
output raster: DrainageBasin

To get the distances along the stream network, a few small steps are required.
17) Extract the raster values from the Flow Length layer on the sites:
ArcToolbox->Spatial Analyst->Extraction->Extract values to points
input features: NewSites-Copy2.shp
input flow length: FlowLength2 (upstream one)
output feature: Sites_FlowDistance.shp
interpolate values at point locations: no
append all input raster fields to output: yes

18) Export the attribute table to "FlowLength_rastervalues.dbf"; save outside of the geodatabase.

Assuming water within Payuk Lake all flows equally throughout along the flow accumulation network, snap the NewSites to the closest part of the main "network" they are near and calculate the Euclidean distance and path distance of the sites along the flow network.

19) Copy Payuk_streams.shp layer in ArcCatalog and add it to ArcMap. Call it Payuk_streams-Copy.shp.

20) Using the Editor tool extension on Payuk_streams-Copy.shp, merge the polylines that make up the main Mistik Creek/Twin Creek/Payuk Lake flow accumulation path.
Turn on FlowAcc and trace over the main network linear raster line, including Mistik Creek and Twin Creek.
Save edits and stop editing.

21) Select the newly merged polyline and export it to its own shapefile. (C:\...\Hydrology\Shapefiles\MistikCk.shp).

22) Snap the NewSites-Copy.shp to the main stream polyline:
ArcToolBox->Editing Tools->Snap
input: NewSites-Copy2.shp
snap environment: MistikCk.shp
Select EDGE and use a distance of 10000m

23Determine the raster values (distance in the main network) at each point:
ArcToolboox->Spatial Analyst->Extraction->Extract values by points
input features: NewSites-Copy2.shp
input flow length: FlowLength2 (upstream one)
output feature: Sites_Flow2.shp
interpolate values at point locations: no
append all input raster fields to output: yes

24) Calculate the Euclidean distance of all the sites along the network:
ArcToolbox->Analysis Tools->Proximity->Point Distance
Use the Python Code:

```
>>> arcpy.env.workspace = "C:\...\Hydrology\FlowNetwork.gdb"
>>> in_features = "NewSites-Copy2"
>>> near_features = "NewSites-Copy2"
>>> out_table = "Sites_FlowEuclidean"
>>> arcpy.PointDistance_analysis(in_features, near_features, out_table)
<Result'C:\\...\\Hydrology\\FlowNetwork.gdb\\Sites_FlowEuclidean'>
```

25) Leaving ArcMap open for reference, open Excel.

26) Open the Sites_FlowEuclidean.dbf table in Excel and add two columns at the end; one for “Site” and “Near Site”

27) Save the Excel file as .xls.

28) In ArcMap, select each site to see the ObjectID and near ID number. Input the site names into the "Site" and "Near Site" columns in the excel sheet, in the corresponding OBID row. This will clarify which OBID and NEAR_ID correspond to each site in the distance table.

29) Save and close Excel.

30) To get the path distance between the sites along the flow network, use the Editor Tool and split the polyline of MistikCk.shp at each of the sites (vertices), save the edits, and stop editing.

31) Open the attribute table to MistikCk.shp and add a new field "Distance":
Type: double
Scale: 0
precision: 0

32) Right click the newly created distance field and "Calculate geometry":
property: length
coordinate system: data source (NAD_1983_UTM_Zone_14N)
units: meters

33) Export the attribute table to "Flow_pathdistance.dbf"; save outside of the geodatabase.

34) Leaving ArcMap open for reference, open Excel.

35) Open the Flow_pathdistance.dbf table in Excel and add two columns at the end; one for “Site at end1” and “Site at end2”.

13) Save the Excel file as .xls.

14) In ArcMap, select each polyline segment to see the ObjectID number. See which sites are at the ends of that polyline and input the site names into the "Site at End1" and "Site at end2" columns in the excel sheet, in the corresponding polyline OBID row.

15) Save and close Excel.

To determine if there were patterns in the flow accumulation and direction of flow of potential runoff sources outside of the main flow network, the creation of “watersheds” was attempted in ArcGIS 10.2. However, due to the small scale of the data and study extent, this was unsuccessful. The following steps outlines how this would have been done if successful.

1) Create pour points (where water would flow) and snap to network:
ArcToolbox->Spatial Analyst->Hydrology->Snap Pour Points
input raster or point feature: StreamLinks (raster) or Payuk_streams (feature)
pour point field: VALUE (raster) or arcid (feature)
input flow accumulation raster: FlowAcc
output: PourPoints (as raster) or PourPoints2 (as feature)
snap distance: 5

2) Create watershed
ArcToolbox->Spatial Analyst->Hydrology->Watershed
input flow direction: FlowDirection2
input pour points: PourPoints (from raster) or PourPoints2 (from feature)
pour point field: VALUE
output: Watershed (as raster) or Watershed2 (as feature)